

A CMS Energy Company

Palisades Nuclear Plant
27780 Blue Star Memorial Highway
Covert, MI 49043

Tel: 616 764 2276
Fax: 616 764 3265

April 21, 2000

Nathan L. Haskell
Director, Licensing and
Performance Assessment

U.S. Nuclear Regulatory Commission
ATTN: Document Control Desk
Washington, DC 20555-0001

DOCKET 50-255 - LICENSE DPR-20 - PALISADES PLANT
REQUEST FOR APPROVAL OF REVISION TO INCORE MONITORING CODE
(PIDAL-3)

In accordance with the Palisades Technical Specifications and FSAR, in-core monitoring of neutron flux is currently performed using the PIDAL-3 computer code. Use of the PIDAL code was originally approved by the NRC in Amendment 144 to the Palisades Operating License dated April 3, 1992. Use of PIDAL-3, with the CASMO-3/SIMULATE-3 methodology, was approved via NRC Safety Evaluation Report (SER) dated May 6, 1997.

The attached report, "The PIDAL-3 Full Core System, February 2000," describes the latest code revisions, reviews the methodology used, describes analyses which have been completed to benchmark the revised code, and provides a sample output computer report. The report also discusses changes in the NRC SER approving the use of PIDAL that will be needed to permit use of the code revision. The analysis shows that the previously approved uncertainties on power distribution limits stated in the Technical Specifications bound the uncertainties of the revised PIDAL-3 calculations, such that no changes to either the Current Technical Specifications or the Improved Technical Specifications (to be implemented in October 2000) are required at this time.

The NRC review and approval to use the revised PIDAL-3 code is requested prior to the next refueling outage, currently scheduled to begin March 31, 2001. This will provide for more efficient use of plant resources by avoiding the need to run both old and new revisions of PIDAL during cycle 16. Approval of the change in the number of detectors required to be operable would also support Palisades' intended re-use of incore detector strings, scheduled to begin with the 2001 refueling outage. Incore detector re-use will provide significant cost and personnel radiation dose savings.

ADD

In addition, at the staff's earliest convenience, an opportunity is requested for our technical staff to meet with NRC technical reviewers to discuss the report and establish a dialogue to facilitate the staff's future activities. This meeting will be coordinated through the Palisades NRR Project Manager.

Consumers Energy looks forward to working with the NRC to support staff review of this information.

SUMMARY OF COMMITMENTS

This letter contains no new commitments and no revisions to existing commitments.



Nathan L. Haskell
Director, Licensing and
Performance Assessment

CC Administrator, Region III, USNRC
Project Manager, NRR, USNRC
NRC Resident Inspector - Palisades

Attachment

ATTACHMENT

**CONSUMERS ENERGY COMPANY
PALISADES PLANT
DOCKET 50-255**

April 21, 2000

**THE PIDAL-3 FULL CORE SYSTEM,
February 2000**

68 Pages

CONSUMERS ENERGY

Palisades Nuclear Plant

THE PIDAL-3 FULL CORE SYSTEM

February 2000

By

TC Altenau
TA Meyers
RC Harvill

TABLE OF CONTENTS

TABLE OF CONTENTS	1
1.0 INTRODUCTION	1
1.1 PIDAL METHODOLOGY EVOLUTION.....	5
1.2 PIDAL-3 CHANGES.....	5
2.0 SYSTEM DESCRIPTION	6
2.1 DATA COLLECTION	6
2.2 PIDAL-3 CALCULATION TRAIN	8
2.2.1 <i>INTERPIN-CS</i>	8
2.2.2 <i>CASMO-4</i>	8
2.2.3 <i>CMSLINK</i>	8
2.2.4 <i>SIMULATE-3</i>	8
3.0 PIDAL-3 METHODOLOGY	10
3.1 INPUT COLLECTION.....	10
3.2 THEORETICAL CALCULATIONS.....	10
3.3 DETECTOR POWER CALCULATIONS	11
3.4 RADIAL POWER DISTRIBUTION CALCULATIONS	13
3.5 AXIAL POWER DISTRIBUTION CALCULATIONS	15
3.6 TECHNICAL SPECIFICATION SURVEILLANCE CALCULATIONS	17
3.7 PIDAL-3 OUTPUT	19
4.0 PIDAL-3 VALIDATION	20
4.1 CALCULATIONS.....	20
4.2 COMPARISONS	20
4.3 UNCERTAINTY ANALYSIS	25
4.4 EFFECTS ON UNCERTAINTIES.....	25
4.4.1 <i>LOW LEAKAGE CORES</i>	25
4.4.2 <i>POOLABILITY AND NORMALITY OF DATA</i>	25
4.4.3 <i>FAILING LARGE NUMBERS OF INCORE INSTRUMENTS</i>	26
4.4.4 <i>RADIAL POWER TILTS</i>	27
4.4.5 <i>LARGE AXIAL OFFSETS</i>	27
4.5 RESULTS	32
5.0 CONCLUSION	32
6.0 REFERENCES	33
7.0 GLOSSARY	34
APPENDIX A	35
APPENDIX B	63

1.0 INTRODUCTION

The PIDAL-3 Incore Monitoring System is the third generation of the Palisades Incore Detector Algorithm capable of determining the reactor core power distribution, peaking factors, and local LHGR on a full core basis. PIDAL-3 was the [SER97] revision to the PIDAL methodology originally issued by the US NRC in [SER92] on April 3, 1992. Modifications encompassed the replacement of the Siemens Power Corporation methods PDQ and XTG for determination of theoretical assembly powers, detector conversion constants, and local peaking factors with SIMULATE-3, an advanced three-dimensional two-group reactor analysis code. This latest revision of PIDAL-3 encompasses the replacement of CASMO-3 with CASMO-4 for fuel cross-section generation, the elimination of 7 unnecessary detector strings, and the decrease in minimum detector operability from 75% to 50%.

The current Technical Specification limits were developed using the original PIDAL comparisons from cycles 5, 6, and 7, [TS323]. These were very similar eighth core symmetric high leakage core designs that transitioned from 330 to 390 EFPD. The latest PIDAL-3 analysis is based on cycles 12, 13, and 14 with quarter core symmetric ultra low leakage core designs that transition from 400 to 450 EFPD. Core loading maps for cycles 12 through 14 are provided in Figures 1.1 to 1.3. (Throughout this discussion the term "Technical Specifications" or [TS] refers to the Current Palisades Technical Specifications, unless preceded by "Improved.")

The movement to ultra low leakage core designs made it increasingly difficult for Palisades to adequately predict core power distributions with the PDQ/XTG methodology. Furthermore, previous PDQ/XTG quarter core modeling limited our ability to accurately deal with asymmetric power anomalies such as misaligned control rods. Expansion of the PIDAL methodology to include a full core SIMULATE-3 model both improved modeling accuracy and provided a tool for monitoring large quadrant power tilts.

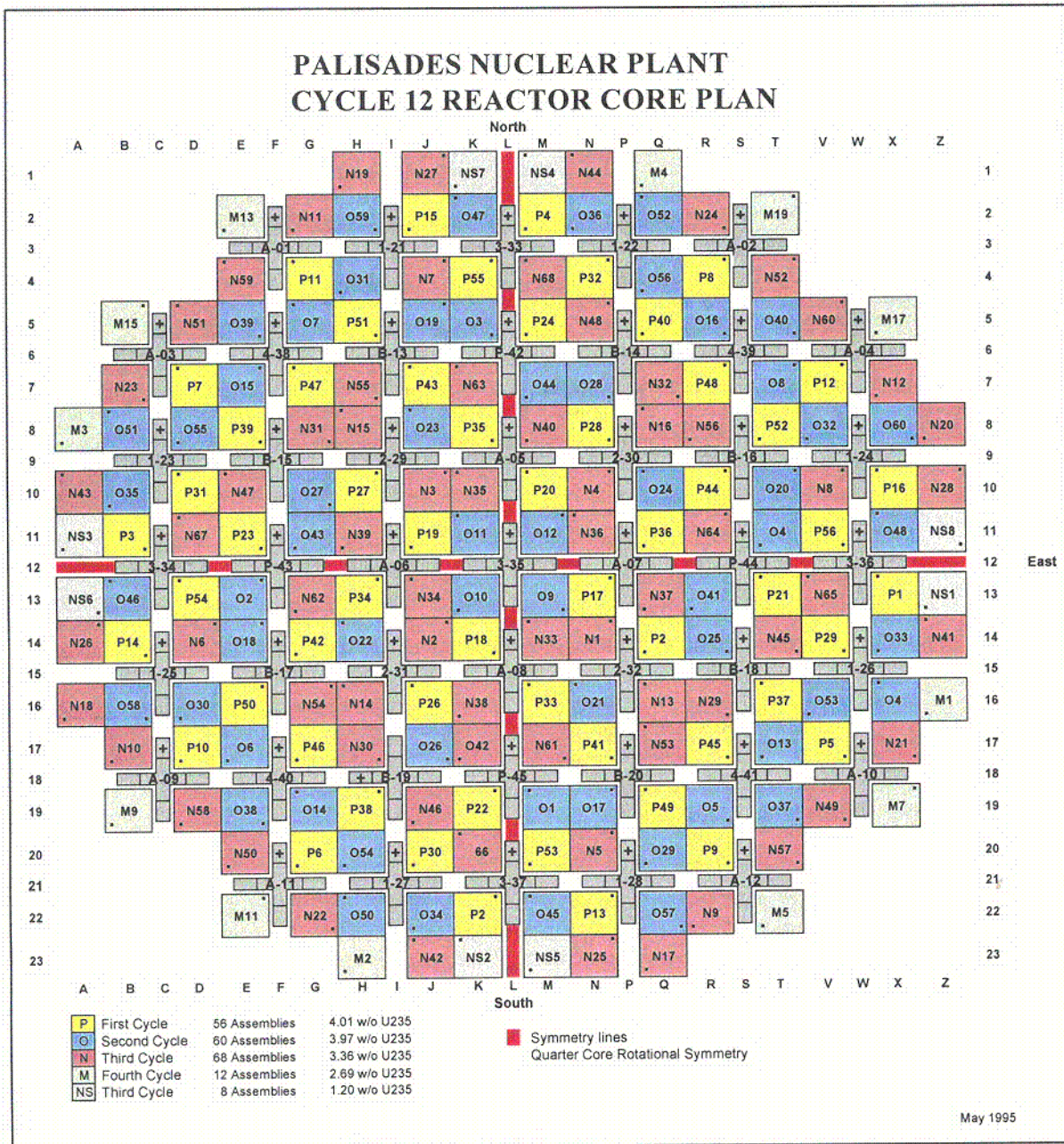
Incorporation of the CASMO-4/SIMULATE-3 model further reduced measurement uncertainties. However, Consumers Energy again has chosen to simply show that the uncertainties currently stated in [TS323] bound the present PIDAL-3 uncertainties. This is a conservative approach, but there are still significant core design and operating flexibility gains introduced by the improved accuracy of the SIMULATE-3 methodology. Therefore, no changes to [TS323] are required at this time.

With the approval of PIDAL-3 in [SER97] all assemblies with relative power fractions less than 1.0 have been eliminated from the measurement uncertainty analysis. Their relatively low absolute deviations between measured and predicted correspond to relatively high percent deviations. With this in mind, in an effort to reduce costs, dose, and outage duration, Palisades decided to eliminate 7 detectors starting in cycle 15. The 6 peripheral detectors were chosen because they are non-qualified, have no symmetric partners, and no longer provide us with any pertinent benchmark data in such low flux regions of the core. They deplete less than 10% of their rhodium per cycle. In addition, detector number 4 was eliminated since it also is non-qualified with no symmetric partners. This brings our total number of operable detectors from 43 to 36 strings, or 9 strings per quadrant (180 total detectors).

Our present [TS311] limit is 160. Therefore, in order to regain some operating margin this submittal is requesting a change from 75% operability of 43 strings to 50% operability of 36 strings. The 2 detectors per level per quadrant will still be a Technical Specification requirement. The present limit of 160 operable detectors will not be lowered to 90 until approval of this submittal and issuance an implementation of the Improved Technical Specifications, [ITSB321], where the operable limit is stated in the Bases, thus avoiding any changes to [TS311].

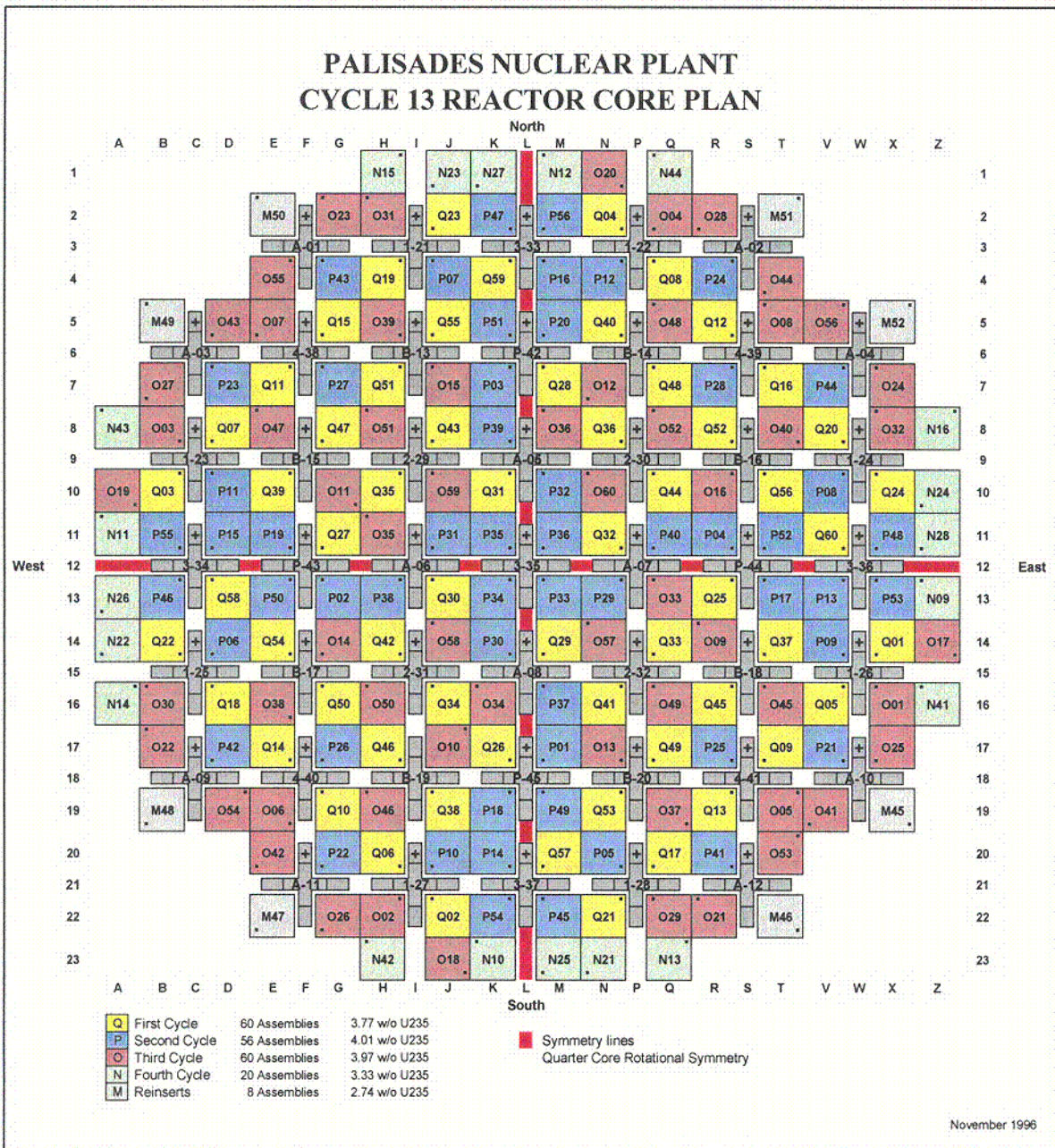
The following is a brief summary of the Palisades Incore Monitoring System methodology. Changes from previous PIDAL versions are highlighted in the discussion. Comparisons between measurement and predicted are made for key parameters such as Assembly Radial Power RMS Deviations, Assembly Radial Peaking Factors (F_R^A), Total Radial Peaking Factors (F_R^T), and Total Peaking Factors (F_Q). Finally, an analysis of cycles 12 through 14 shows that the uncertainties currently stated in the Palisades Technical Specifications bound the PIDAL-3 uncertainties.

Figure 1.1 Cycle 12 Core Loading Pattern



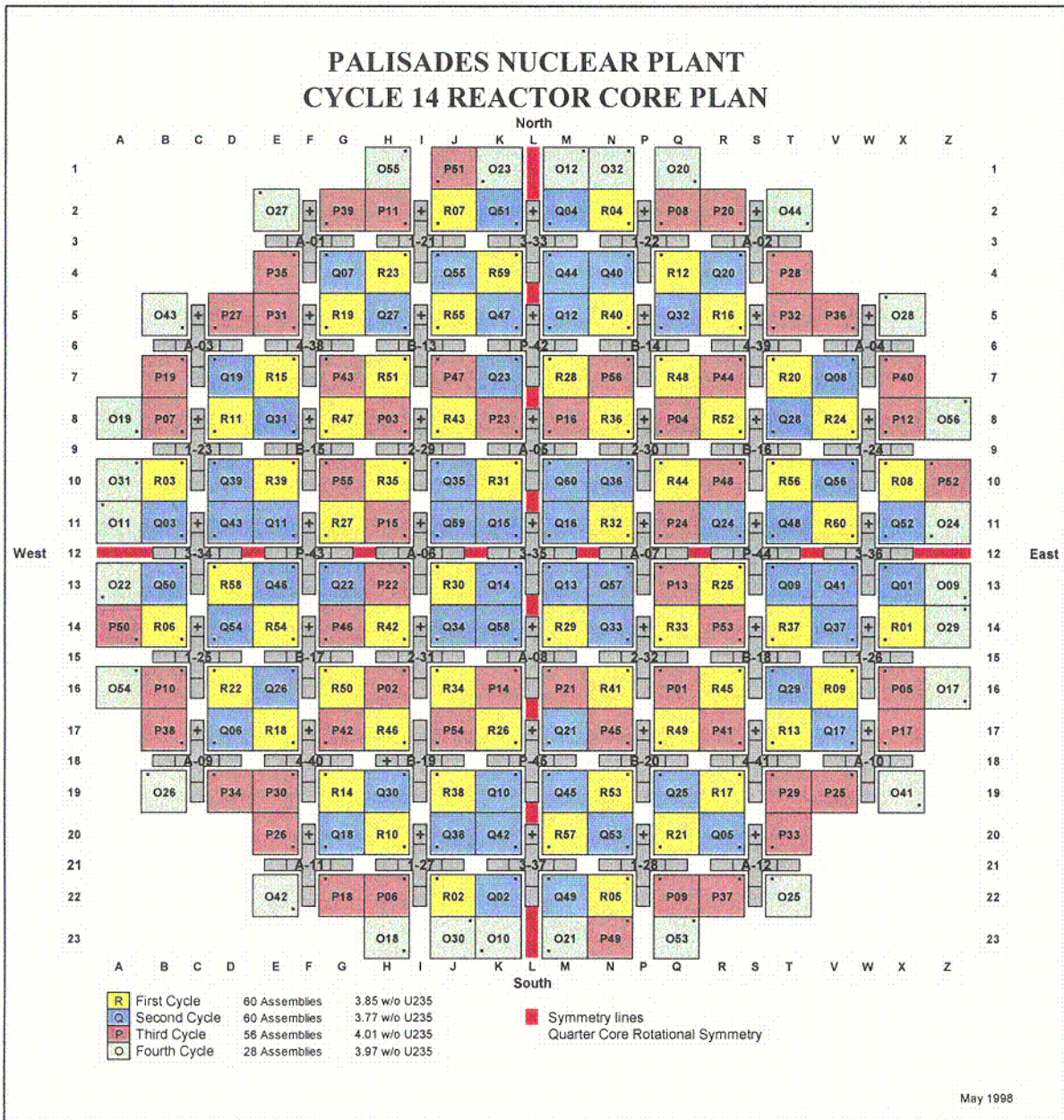
C-3

Figure 1.2 Cycle 13 Core Loading Pattern



C-1

Figure 1.3 Cycle 14 Core Loading Pattern



C-2

1.1 PIDAL METHODOLOGY EVOLUTION

The full core PIDAL code was first approved by the US NRC in [SER92] to replace the eighth core INCA code. There were two driving forces behind the change from INCA to PIDAL. First, there was a need for quarter core geometry capabilities in order to design cores, which met goals established for vessel fluence reduction, and increased cycle length. The movement to low leakage core designs in response to reactor vessel fluence caused radial peaking to increase and reduced the margin to the INCA based Technical Specification limits. Margin gained by switching to PIDAL translated directly into greater flexibility in core design and operation. Secondly, it was expected that the PIDAL system would eventually allow for full detection and measurement capabilities in the event of an asymmetric power anomaly; i.e. misaligned control rods. Unfortunately, this functionality was limited by both quarter core XTG models and SPC supplied quarter core PDQ W-prime and local peaking factor libraries.

In 1995 a new Palisades Plant Computer was installed at Palisades. Modifications were made to the PIDAL code to allow it to run on the DEC VAX 4000 workstations using the VMS platform. Concurrently, the XTG axial resolution was increased from 12 to 25 axial nodes over the active fuel height to accommodate axial blankets. [PID952] includes all the changes made to the program and the corresponding 50.59 Safety Review. No overall methodology changes were made. The PIDAL source code was updated and renamed PIDAL-2.

With the introduction of ultra low leakage cores at Palisades, the limits of the coarse mesh nodal code, XTG, had been approached. As a result of these modeling difficulties with XTG, Consumers Energy evaluated SIMULATE-3 and a subsequent effort to incorporate CASMO-3/SIMULATE-3 as the theoretical model in PIDAL was completed in [PID961] and approved in [SER97]. Upon completion, the new core monitoring code incorporating SIMULATE-3 had been renamed PIDAL-3. Finally, the minimum number of operable detectors, and the replacement of CASMO-3 with CASMO-4 for fuel cross-section generation was analyzed in [PID991] and [PID992].

1.2 PIDAL-3 CHANGES

The changes required to the PIDAL system to incorporate the SIMULATE-3 nodal code were grouped into four general categories:

- 1) Integration of SIMULATE-3 nodal powers.
- 2) Integration of SIMULATE-3 reaction rates.
- 3) Integration of SIMULATE-3 pin powers.
- 4) Expansion of PIDAL to full core theoretical coupling calculations.

PIDAL-3 uses nodal powers calculated by SIMULATE-3. Exposure dependent W-primes, which convert the measured detector fluxes to assembly powers, utilize full core non-depleting rhodium reaction rates provided by SIMULATE-3 using an explicit or implicit detector model. Rhodium depletion effects are accounted for by a 5th order polynomial curve fit describing a depletion dependent self-shielding factor in [PID992]. If employing an implicit detector model, the geometry effects are accounted for by a 5th order polynomial curve fit describing a fuel type and exposure dependent geometry factor also in [PID992]. Section 3.3 provides a detailed discussion on this conversion process. Likewise, SIMULATE-3 provides PIDAL-3 with full core local peaking factors (LPF) or pin-to-box (PTB) factors. Finally, the PIDAL-3 radial coupling is exclusively full core as opposed to previous quarter core coupling expanded to full core. The SIMULATE-3 full core nodal powers, rhodium reaction rates, and LPFs allow PIDAL-3 to effectively measure large quadrant power tilts.

2.0 SYSTEM DESCRIPTION

The Palisades reactor is a first generation ABB Combustion Engineering (ABBCE) two loop PWR. The core contains 204 fuel assemblies and 45 cruciform control blades. The reactor is currently rated at 2530 MWth and the power distribution within the core is measured via self-powered rhodium detectors or incore instruments (ICI). There are 45 possible instrumented fuel assemblies. Two of these locations are utilized for reactor coolant level monitoring, and 7 additional locations have been eliminated in [PID991] for reasons previously stated. Each of the remaining 36 locations contain five rhodium detectors equally spaced at 10, 30, 50, 70, and 90 percent of the original active fuel height. Figure 2.1 shows a layout of the Palisades reactor including control blade and incore detector locations.

The principle of operation involves the conversion of the incident neutron radiation on the emitter material (rhodium) to energize electrons which migrate through the solid insulation to the collector. The deficiency of electrons in the emitter results in a positive charge on the center conductor of the attached coaxial cable. The rate of charge production produces a low level current which is directly proportional to the rate of absorption at the emitter. This current is monitored by the PPC which performs sensitivity and background corrections while converting the input current to flux. A software interface between the PPC and PIDAL-3 generates the SIMULATE-3 and PIDAL-3 input files, and initiates the calculations.

2.1 DATA COLLECTION

The PPC is responsible for conversion of the rhodium detector current (amps) to flux (nv). The conversion uses the sensitivity factors, K_s , provided for each detector by ABBCE. The PPC keeps track of the rhodium depletion and adjusts the K_s values accordingly. As is standard for ABBCE type incore monitoring systems, a linear rhodium detector depletion law is used by the PPC:

$$K_{si}(t) = K_{si}(0) \times \left(1 - \frac{\Delta Q_i}{Q_\infty} \right) \quad (2.1)$$

where:

- $K_{si}(t)$ - Sensitivity of detector i at time t (amp/nv)
- $K_{si}(0)$ - Initial sensitivity of detector i (amp/nv)
- ΔQ_i - Accumulated charge of detector i at time t (coulombs)
- Q_∞ - Total possible accumulated charge of detector i at end of life (coulombs)

Equation (2.1) is implemented by the PPC as:

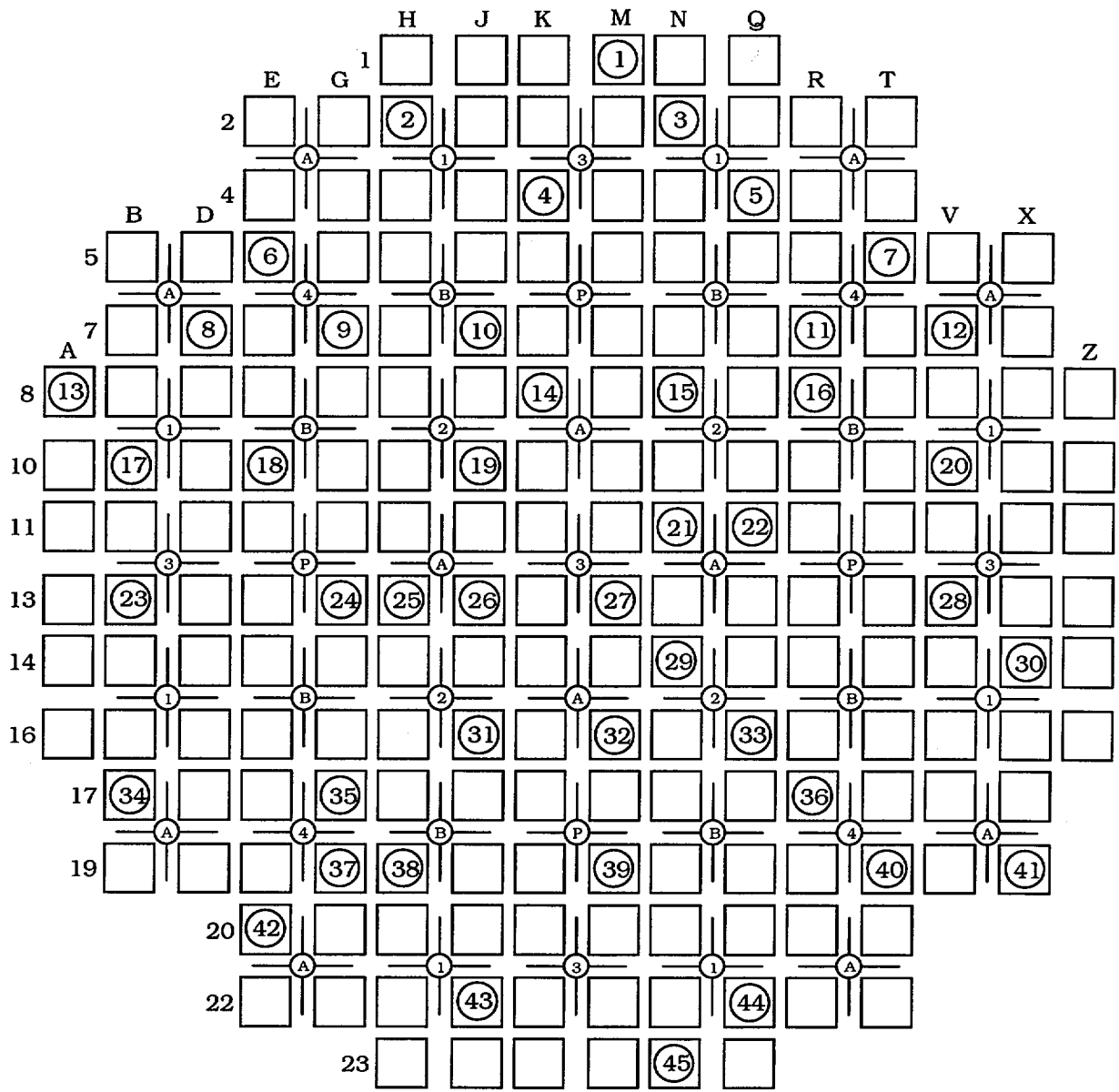
$$K_{si}(t) = K_{si}(0) - \gamma E_{mi} K_{si}(0) \quad (2.2)$$

where:

- $\gamma = \frac{1}{Q_\infty}$ - Detector Burnup Constant
- E_{mi} - Average daily background-corrected detector current for fixed detector i.

Rhodium detector currents (amps) are divided by K_s (amp/nv) yielding the detector flux (nv). These values along with core calorimetric power, control rod positions, and other various plant parameters describing the state of the PCS, are organized into input files for SIMULATE-3 and PIDAL-3 calculations.

Figure 2.1 Palisades Core Configuration



- Notes:
1. All instruments contain 5 rhodium detectors and 1 outlet thermocouple.
 2. ICIs 7 and 44 are used by the Reactor Vessel Level Monitoring System.
 3. ICIs 1, 4, 13, 34, 41, 42, and 45 have been eliminated in [PID991].

2.2 PIDAL-3 CALCULATION TRAIN

The Studsvik Core Management System (CMS) consists of INTERPIN-CS, CASMO-4, CMSLINK, and SIMULATE-3 to provide essential data to PIDAL-3. A SIMULATE-3 calculation is performed prior to every hourly PIDAL-3 calculation. SIMULATE-3 nodal powers, rhodium reaction rates, and LPFs are used by PIDAL-3. Figure 2.2 illustrates how these codes interact with PIDAL-3. The following sections briefly describe the CMS methodology, and a detailed discussion of the PIDAL-3 methodology is given in the following section.

2.2.1 INTERPIN-CS

INTERPIN-CS predicts the steady-state performance of UO₂ zircaloy-clad fuel operating in LWRs. The program is designed to produce fuel temperature input data for CASMO-4 and SIMULATE-3. Refer to [INTCS] for additional information.

2.2.2 CASMO-4

CASMO-4 is a multigroup two-dimensional transport theory code for burnup calculations on BWR and PWR assemblies or simple pin cells. The code handles a geometry consisting of cylindrical fuel rods of varying composition in a square pitch array with allowance for fuel rods loaded with gadolinium (Gd₂O₃), burnable absorber rods (B₄C), cluster control rods, incore instrument channels, water gaps, boron steel curtains, and cruciform control blades in the regions separating fuel assemblies. CASMO-4 generates fuel cross-sections for SIMULATE-3. Refer to [CAS4] for additional information.

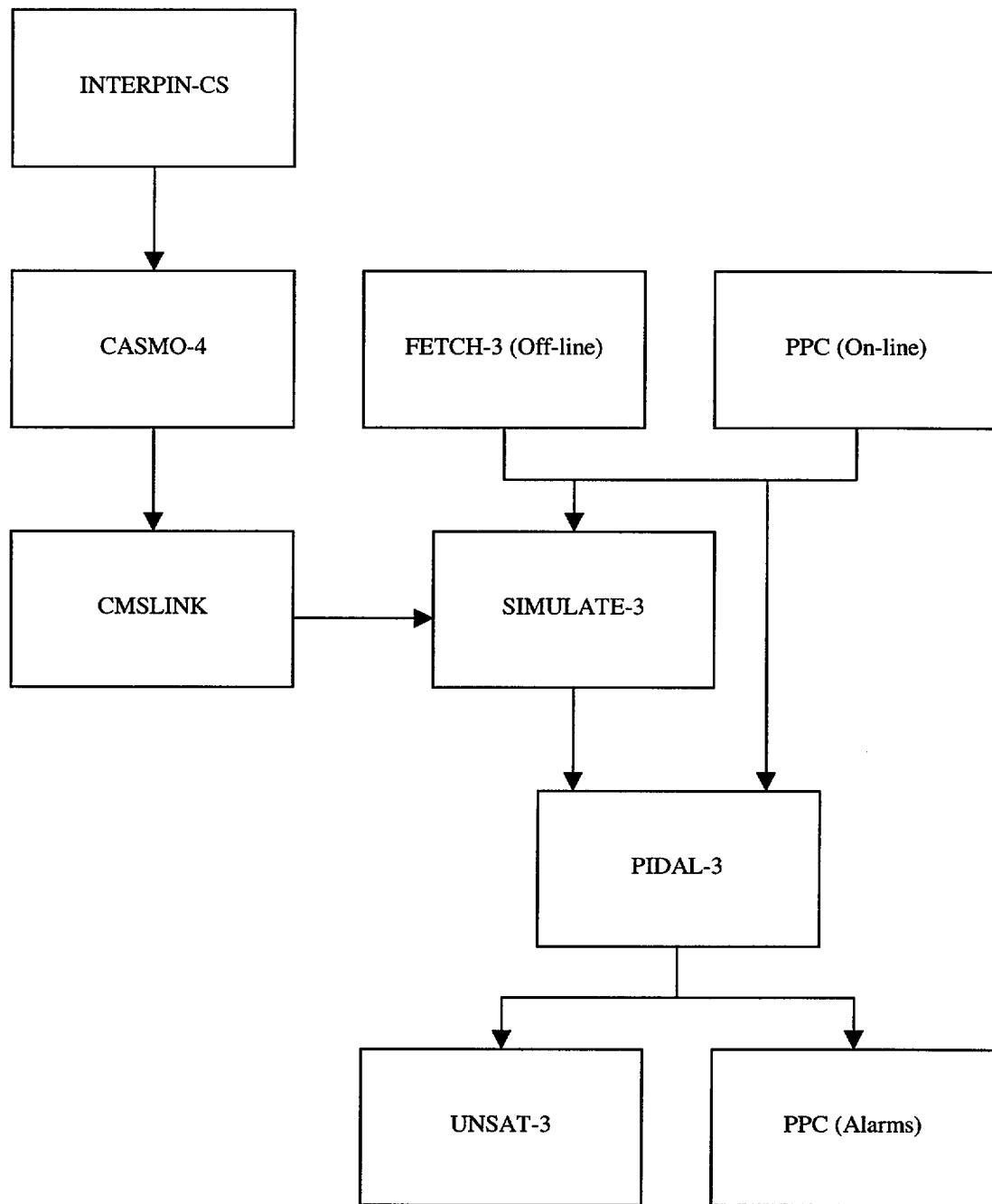
2.2.3 CMSLINK

CMSLINK is a linking code that processes CASMO-4 Card Image files into a binary data library use by SIMULATE-3. Refer to [CLINK] for additional information.

2.2.4 SIMULATE-3

SIMULATE-3 is an advanced three-dimensional two-group nodal code for the analysis of both PWRs and BWRs used by numerous utilities. The diffusion equation solution can be obtained in either two or three dimensions. SIMULATE-3 requires no adjustable parameters such as albedos or thermal leakage corrections. All cross-section information including discontinuity factors and pinwise assembly lattice data are provided by CASMO-4 assembly calculations via the CMSLINK binary library. SIMULATE-3 performs macroscopic depletion with microscopic depletion of particular fission products while modeling power operation coupled with thermal-hydraulic and Doppler feedback. The reconstruction of pin-by-pin power distributions is also included. Refer to [SIM3] and [S3MM] for additional information.

Figure 2.2 PIDAL-3 Calculation Flow



3.0 PIDAL-3 METHODOLOGY

The following sections summarize the PIDAL-3 methodology. The intent is to provide a complete overview of the PIDAL-3 functionality. No changes have been implemented with this latest version of PIDAL-3.

3.1 INPUT COLLECTION

PIDAL-3 receives its input data from four different files:

- 1) The Binary Input file, generated by the [PPC], supplies the primary input data. This file contains reactor power, pressure, flow, inlet temperature, and boron concentration. The NI excore powers fractions, CET temperatures, control rod positions, detector fluxes, sensitivities, and fractions of remaining rhodium are also included.
- 2) The ASCII TSSOR file supplies Technical Specification peaking limits information, number of fuel batches and sub-batches, and Startup & Operations Report data.
- 3) The Binary Restart file supplies cycle specific batchwise data and core loading in the first record, and fuel assembly exposures in each subsequent record. One record is added after each burnup case.
- 4) The ASCII Summary file, generated by SIMULATE-3, supplies all of the full core assembly powers, local peaking factors (pin-to-box), and rhodium reaction rate data. Axially collapsed peak pin and assembly exposure edits as well as linear heat generation rate edits are included for on-line comparisons by PIDAL-3. One file is created for each PIDAL-3 case.

3.2 THEORETICAL CALCULATIONS

PIDAL-3 performs a least squares axial curve fit of the SIMULATE-3 nodal powers (204×25) by solving for the boundary conditions with the lowest square sum error, PIDAL-3 then integrates over the 5 detector levels (204×5) to obtain the theoretical detector powers. These theoretical detector powers are used in the W-prime and coupling coefficient calculations (Sections 3.3 and 3.4), and the boundary conditions are used in the axial curve fit of the measured/inferred detector powers (Section 3.5).

The boundary conditions represent the top and bottom axial points where the flux goes to zero. We start at the end of the active fuel height, and iterate on increasing boundary conditions until we find the lowest square sum error.

This routine has been the same for all versions of PIDAL, including PIDAL-3. The only difference is PIDAL-3 uses SIMULATE-3 nodal powers.

3.3 DETECTOR POWER CALCULATIONS

The rhodium incore detectors deplete on average approximately 1% per full power month, so corrections are necessary to the detector signal to account for the effects of rhodium depletion. These corrections result from the change in detector self-shielding due to rhodium burnup, and the change in rhodium concentration itself. The sensitivity correction, described in Section 2.1, accounts for the change in rhodium concentration, but not for self-shielding. Since the detector signal is proportional to the rhodium reaction rate, given a constant flux, the rhodium reaction rate will decrease as the rhodium depletes but not at the same rate due to self-shielding as stated in [PID992] Appendix 7.1 or [SCE1] and [SCE2].

Correction of the detector signal for depletion of rhodium is accounted for by a multiplication factor, $N(t)/N_0$. $N(t)$ is the rhodium concentration at time t divided by N_0 , the initial (undepleted) rhodium concentration. From equation 2.1, we find the $K_S(t)/K_S(0)$ ratio is equivalent to $N(t)/N_0$. Therefore, the change in sensitivity corrects for the change in rhodium concentration and the $K_S(t)/K_S(0)$ ratio is equivalent to the fraction of remaining rhodium.

Since the SIMULATE-3 model does not account for rhodium depletion, we apply an external correction to the SIMULATE-3 rhodium reaction rates for self-shielding. This is slightly more complicated and requires an understanding of the physical phenomena known as self-shielding.

Self-Shielding occurs when a neutron absorbing material of finite thickness is bombarded by neutrons. Initially, if the neutron flux is approximately thermalized when it reaches the surface of the absorbing material, more neutrons will be absorbed at the surface of the material as compared to the center. For the rhodium detectors this means that more activation occurs on the surface compared to the center. However, as the surface of the rhodium detector is depleted the neutrons will begin to "see" more of the interior atoms. The effective diameter of the emitter material is thus decreasing and self-shielding is also. The overall result is an increase in the effective absorption cross-section of rhodium. This can be described by the following equation:

$$SSF = \frac{\int_V \int_E \sigma_{a \text{ depleted}}^{Rh} \phi dEdV}{\int_V \int_E \sigma_{a \text{ non-depleted}}^{Rh} \phi dEdV} \quad (3.1)$$

The numerator describes the rhodium reaction rate using depleting rhodium detector cross-sections, and the denominator uses non-depleting rhodium detector cross-sections. A function of self-shielding vs. fraction of remaining rhodium will emerge as the depleted to non-depleted reaction rates are plotted over exposure. If the SIMULATE-3 model incorporates an implicit ICI model instead of an explicit ICI model an additional geometry factor as a function of exposure must be applied to the SIMULATE-3 rhodium reaction rates.

CASMO-4 was used to generate the function of self-shielding factors (SSF) vs. fraction of remaining rhodium (DFRHO) and geometry factor (GMF) vs. assembly exposure by depleting each fuel type. A 5th order polynomial curve fit of the self-shielding factors vs. fraction of remaining rhodium and geometry factors vs. assembly exposure generate the essential coefficients (SCOEF) and (GCOEF) used to calculate the W-primes. These coefficients verify that the self-shielding factors are independent of fuel type but that geometry factors are not as stated in [PID992] Appendix 7.1 or [APS1] and [APS2].

To summarize, the detector signals (amps) are corrected for rhodium depletion by the depleting sensitivity values (amps/nv) and converted to flux (nv). The non-depleting SIMULATE-3 rhodium reaction rates are corrected for self-shielding by a self-shielding factor, and the depleting detector signal (nv) is converted to power (MWth) via the W-primes. The following equations demonstrate how the background and sensitivity corrected signal is converted to power from [PID992].

The average power over a detector is calculated using the following equation:

$$AVGPOW = \left(\frac{CALPOW}{RNAS} \right) \times \left(\frac{HAD}{HAX} \right) \quad (3.2)$$

where:

AVGPOW - Average power over a detector (MWth)
 CALPOW - Reactor core calorimetric power (MWth)
 RNAS - Number of assemblies in core
 HAD / HAX - Detector height / Active fuel height

The self-shielding and geometry factors are calculated using the following equations:

$$DSSF(i, j) = \left(\begin{array}{l} SCOEF(1) + SCOEF(2) \times DFRHO(i, j) + \\ SCOEF(3) \times DFRHO(i, j)^2 + SCOEF(4) \times DFRHO(i, j)^3 + \\ SCOEF(5) \times DFRHO(i, j)^4 + SCOEF(6) \times DFRHO(i, j)^5 \end{array} \right) \quad (3.3)$$

where:

DSSF(i,j) - Self shielding factor for detector string i level j
 DFRHO(i,j) - Remaining fraction of rhodium for detector string i level j
 SCOEF(6) - 6 curve fit self shielding coefficients

$$DGMF(i, j) = \left(\begin{array}{l} GCOEF(1) + GCOEF(2) \times S3DXP(DLOC(i), j) + \\ GCOEF(3) \times S3DXP(DLOC(i), j)^2 + GCOEF(4) \times S3DXP(DLOC(i), j)^3 + \\ GCOEF(5) \times S3DXP(DLOC(i), j)^4 + GCOEF(6) \times S3DXP(DLOC(i), j)^5 \end{array} \right) \quad (3.4)$$

where:

DGMF(i,j) - Geometry factor for detector string i level j
 S3DXP(DLOC(i),j) - SIMULATE-3 Detector Exposure for detector string i level j
 GCOEF(6) - 6 curve fit geometry coefficients
 DLOC(45) - 45 detector locations corresponding to 204 assembly numbers

The W-primes and detector powers are calculated using the following equations:

$$WPRIME(i, j) = \frac{S3DPF(DLOC(i), j) \times AVGPOW}{(S3RR2(DLOC(i), j) \times DSSF(i, j) \times DGMF(i, j))} \times CALIB \quad (3.5)$$

where:

WPRIME(i,j) - Detector signal to power conversion factor for detector string i level j
 S3DPF(DLOC(i),j) - SIMULATE-3 detector power fraction for detector string i level j
 S3RR2(DLOC(i),j) - SIMULATE-3 detector rhodium reaction rate for detector string i level j
 CALIB - Detector power to calorimetric power normalization constant

$$DPOWER(i, j) = WPRIME(i, j) \times DFLUX(i, j) \quad (3.6)$$

where:

DPOWER(i,j) - PIDAL-3 detector power for detector string i level j (MWth)
 DFLUX(i,j) - PIDAL-3 detector signal for detector string i level j (nv)

3.4 RADIAL POWER DISTRIBUTION CALCULATIONS

The original PIDAL methodology was based on the ABBCE method [CECOR]. Over the course of development, several enhancements were made to this methodology, and in general, PIDAL departs from [CECOR] in the way the inter-assembly coupling is generated.

The underlying assumption in the [CECOR] method is that the power in any assembly K can be given by the equation:

$$P(K, j) = \frac{\sum_m P(m, j)}{CC(K, j)} \quad (3.7)$$

where:

- P(K,j) - Power in assembly K, axial level j
- P(m,j) - Power in assembly m, axial level j. Assembly m is adjacent to assembly K.
- CC(K,j) - Assembly average coupling coefficient for assembly K, axial level j.

Using algebra, CC(K,j) is defined as:

$$CC(K, j) = \frac{\sum_m P(m, j)}{P(K, j)} \quad (3.8)$$

In the Palisades core, there are 204 assemblies (K = 204) and thus the dimension of CC is also 204. Obviously, P(K,j) is only known for assemblies which contain an operable incore detector. Therefore, a synthesis method is used to determine powers for each of the uninstrumented locations.

It is necessary for the CC(K,j)s to be defined or known for all core locations. The [CECOR] method precalculates the CC(K,j)s from planar depletion studies and fits these values based on burnup. This would be similar to calculating the CC(K,j)s based solely on the SIMULATE-3 predicted solution.

The problem with this method is that the CC(K,j)s are based solely on prediction and the final full core solution is greatly biased by the predicted solution. Therefore, it was determined that the preferred method would be to somehow infer the CC(K,j)s based on measurement as well.

Once the CC(K,j)s are known, the problem consists of determining the P(K,j)s for uninstrumented assemblies. Equation 3.7 can be rewritten as:

$$P(K, j) \times CC(K, j) = \sum_m P(m, j) \quad (3.9)$$

If equation 3.9 is written for each uninstrumented assembly K level j, then a set of equations on the order of 204 × 204 results for each detector level. If the unknown P(m,j)s are subtracted over to the left hand side of each equation and the known P(m,j)s remain on the right, then a very sparse banded matrix appears on the left, and a known vector appears on the right. Remember (or assume) that the CC(K,j)s are known.

Knowing that core locations 4, 9, and 13 are instrumented with detector strings 1, 2, and 3 (Figure 2.1), the first 5 equations are written for each detector level j in expanded matrix-vector notation as:

P_1CC_1	$-P_2$	0	0	0	0	0	0	0	0	0	0	$= P_9$
$-P_1$	P_2CC_2	$-P_3$	0	0	0	0	0	0	$-P_{10}$	0	0	$= 0$
0	$-P_2$	P_3CC_3	0	0	0	0	0	0	0	$-P_{11}$	0	$= P_4$
0	0	$-P_3$	P_4CC_4	$-P_5$	0	0	0	0	0	0	$-P_{12}$	$= 0$
0	0	0	0	P_5CC_5	$-P_6$	0	0	0	0	0	0	$= P_4+P_{13}$

The corresponding matrix equation for the above set of equations is written as:

$$\vec{A} \times \vec{P} = \vec{S} \quad (3.10)$$

where:

- \vec{A} - Coefficient matrix consisting of the CC(K,j)s and -1 multipliers to the P(m,j)s
- \vec{P} - Unknown P(K,j)s and P(m,j)s on the left hand side
- \vec{S} - Known P(m,j)s in a column of sums on the right hand side

What must be found is the vector \vec{P} solution. As alluded to by ABBCE in [CECOR], the matrix \vec{A} is a very sparse banded matrix. Therefore, an efficient way of solving the above set of simultaneous equations should be employed. ABBCE uses the conjugate gradient method. PIDAL employs a trustworthy Gaussian elimination routine for sparse matrices. The routine was part of the YALE Sparse Matrix Package available in the public domain.

After the vector \vec{P} has been determined, it is recombined with the known values of P(K,j) and the full core radial power solution for each detector level is obtained.

First, PIDAL-3 calculates the full core assembly average coupling coefficients based solely on the 204 SIMULATE-3 detector powers. Then the SIMULATE-3 coupling coefficients are integrated with the PIDAL-3 measured (known) detector powers to calculate the full core measured/inferred detector powers. The full core measured/inferred detector powers are then used to recalculate the full core assembly average coupling coefficients, which are used to recalculate the final full core measured/inferred detector powers.

As far as coupling is concerned, the PIDAL-3 methodology differs from the PIDAL-2 methodology only in that SIMULATE-3 detector powers are used to determine coupling coefficients for the full core as opposed to XTG powers used to determine coupling coefficients for the quarter core.

3.5 AXIAL POWER DISTRIBUTION CALCULATIONS

Up to this point, the core power distribution is given by a radial power distribution at each of five detector levels. Now, by curve fitting, a continuous function for axial power shape within each assembly is defined. This continuous function can then be used to infer the axial power distribution in the regions not covered by detectors. The general idea is to apply a five mode Fourier fit to the axial data for each assembly, resulting in a continuous function describing the axial distribution.

In order to do this, three assumptions are made:

- 1) It is assumed that the axial power distribution shape is adequately approximated by the Fourier sine function. Thus the function may be used for interpolating or extrapolating to compensate for the gross measurements.
- 2) It is assumed that the power goes to zero near the top and bottom of the active fuel height. This assumption allows the addition of points (boundary conditions) near the top and bottom to the five known points, effectively improving the curve fit.
- 3) It is assumed that the PIDAL-3 measured/inferred boundary conditions are adequately approximated by the SIMULATE-3 theoretical boundary conditions.

From the continuous function, a power distribution is generated for each assembly consisting of 51 axial nodes. This distribution is then collapsed to 25 axial nodes and even further to a two-dimensional radial and a one-dimensional axial power distribution.

The underlying assumption is that the axial power distribution within an assembly can be given by the sum of the first few Fourier modes. Written in equation form:

$$P(z) = \sum_{n=1}^N a_n \sin(n\pi Bz) \quad (3.11)$$

where:

P(z)	- Point power as a function of core fractional core height
N	- Number of Fourier modes (5 in our case)
a _n	- Unknown coefficients (5 in our case)
B	- Axial boundary condition, the real core height as a fraction of the apparent core height, H/(H + 2δ)
z	- Fractional core height, h/H (between 0 and 1)
δ	- Extrapolation distance, the extra distance past the core edge where the flux apparently goes to zero, (H/2)(1/B - 1)
h	- Axial position within core in inches
H	- Core height (131.8 inches)

Equation 3.11 assumes that the flux goes to zero at the edge of the active fuel region and therefore does not precisely describe the axial power distribution used by PIDAL. In reality, the flux actually extends beyond the active fuel region, therefore, we shall redefine P(z) to accommodate the actual point where the flux goes to zero:

$$P(z) = \sum_{n=1}^5 a_n \sin\left(n\pi\left(B(z - 0.5)\right) + \frac{n\pi}{2}\right) \quad (3.12)$$

Integrating equation 3.12 yields

$$POWER(i) = \sum_{n=1}^5 \frac{-a_n}{n\pi B} \cos\left(n\pi B(z - 0.5) + \frac{n\pi}{2}\right) \Bigg|_{Z_{lbot}}^{Z_{ltop}} \quad (3.13)$$

The unknowns in equation 3.12 and 3.13 are the five a_n coefficients. The axial boundary conditions (B) are determined from the SIMULATE-3 theoretical solution by solving equation 3.13 in reverse. The a_n coefficients are determined using the integrated detector powers.

If equation 3.13 is written in expanded form for each of the five known axial powers in an assembly, then a system of five equations and five unknowns emerge. The system of equations can then be solved simultaneously for the a_n coefficients. The resulting a_n coefficients are used in equation 3.12 to describe the axial power profile of the assembly.

To summarize:

- 1) A loop is performed over each assembly in the core. Within the loop, equation 3.13 is expanded to five terms for each of the five axial powers known for that assembly, resulting in a system of five equations and five unknowns. The system is solved simultaneously and the coefficients, a_n , are determined.
- 2) After the coefficients for all 204 assemblies are known, a second loop over the assemblies is performed. In this loop, the coefficients in Equation 3.12 are used to determine point powers at 51 equally spaced axial positions in each assembly. When this loop is complete, the full core three-dimensional power distribution consisting of 204×51 axial nodes is known.

PIDAL-3 axial power distribution methodology differs from previous PIDAL versions only in that the SIMULATE-3 theoretical nodal powers are used to determine the axial boundary conditions and inferred detector powers instead of XTG.

3.6 TECHNICAL SPECIFICATION SURVEILLANCE CALCULATIONS

Based on the data input to PIDAL-3 and the resultant measured core power distributions, the following Palisades Technical Specification (TS) surveillances are performed:

TS 3.1.1.e	Monitoring axial power shape within limits
TS 3.11.1.a	Incore detector operability
TS 3.11.1.b	Calculation of incore alarms for the incore monitoring system
TS 3.11.2.a	Calculation of target axial offset (AO) and allowable power level (APL)
TS 3.11.2.a-c	Excure system calibration for LHGR monitoring
TS 3.11.2.b	Excure system calibration for ASI monitoring
TS 3.11.2.c	Excure system calibration for quadrant power tilt (T_Q) monitoring
TS 3.23.1	Monitoring LHGR within limits
TS 3.23.2	Monitoring radial peaking factors within limits
TS 3.23.3	Monitoring T_Q within limits

The TS limits established for the core average axial power shape (AO or ASI) are designed to ensure that the assumed axial power profiles used in the development of the primary coolant inlet temperature LCO bound all measured axial power profiles. The excure detectors monitor ASI continuously and are calibrated to the PIDAL-3 measured core average AO.

The latest uncertainty analysis for Palisades from [PID992] requires that 50% of the incores are operable for PIDAL-3 to be valid for TS surveillance or incore alarm limit setpoints. In order to protect the core from abnormally high local power densities, the PPC continuously compares the incoming incore detector signals to the alarm setpoints. The alarm setpoint for each detector is simply an alarm factor added to the detector signal. The alarm factor is the minimum margin to the LHGR TS limit measured within the detector level.

Calculation of the target AO and APL, along with the verification that the excure monitoring system is calibrated for monitoring LHGR, ASI, and T_Q is performed as part of a single surveillance. The excure ASI monitoring function is calibrated based on the PIDAL-3 target AO. The excure T_Q monitoring function is also calibrated based on the PIDAL-3 target T_Q . The PIDAL-3 APL is based on the limiting LHGR and ensures that the LHGR limits are bounding for a given band of AO.

Verification that the excure monitoring system is calibrated consists of comparing PIDAL-3 T_Q and AO with corresponding excure T_Q and ASI values. If any of the 4 excure channels diverge from PIDAL-3 by more than the allowable margin, the excure channel is declared inoperable and recalibrated.

LHGR limits exist to ensure the peak cladding temperature will not exceed 2200 °F in the event of a LOCA. LHGR is monitored continuously by the incore monitoring system alarm setpoints or by the excure monitoring system T_Q and ASI alarms if the PPC fails. PIDAL-3 must calculate the LHGRs in order to generate alarm setpoints or calibrate excure channels. PIDAL-3 calculates the peak pin powers by applying SIMULATE-3 LPFs to the assembly nodal powers. The peak pin powers are converted to LHGRs and compared to TS limits.

PIDAL-3 performs a verification of two different radial peaking factors:

F_R^A - Assembly Radial Peaking Factor

Maximum ratio of individual fuel assembly power to core average assembly power integrated over the total core height, including tilt.

F_R^T - Total Radial Peaking Factor

Maximum ratio of the individual fuel pin power to the core average pin power integrated over the total core height, including tilt.

The assembly radial peaking factor is determined from the axially collapsed nodal power distribution. The total radial peaking factor is determined from the axially collapsed nodal power distribution multiplied by the LPFs and a ratio of average fuel pins/assembly to the number of fuel pins in each assembly as follows:

$$FRT = RPD \times LPF$$

$$FRT = FRA \times \frac{\text{Avg Number of pins in assembly}}{\text{Number of pins in assembly}} \times LPF$$

$$FRT = \frac{\text{Assembly Power}}{\text{Avg Assembly Power}} \times \frac{\text{Avg Number of pins in assembly}}{\text{Number of pins in assembly}} \times LPF \quad (3.14)$$

$$FRT = \frac{\text{Avg Pin Power in assembly}}{\text{Avg Pin Power in core}} \times \frac{\text{Peak Pin Power}}{\text{Avg Pin Power in assembly}}$$

$$FRT = \frac{\text{Peak Pin Power}}{\text{Avg Pin Power in core}}$$

The relationship of RPD to RPF is as follows:

$$RPD = RPF \times \frac{\text{Avg Number of pins in assembly}}{\text{Number of pins in assembly}}$$

$$RPD = \frac{\text{Assembly Power}}{\text{Avg Assembly Power}} \times \frac{\text{Avg Number of pins in assembly}}{\text{Number of pins in assembly}}$$

$$RPD = \frac{\text{Avg Pin Power in assembly}}{\text{Avg Pin Power in core}}$$

PIDAL-3 incorporates an innovative method of calculating T_Q from the incore detectors. A system of equations is used which defines all the possible combinations of tilt between two-way symmetric detectors for each level. PIDAL-3 also has the ability of calculating integral T_Q based on quadrant assembly powers if there are not enough symmetric operable incore combinations. The T_Q calculation based on two-way symmetric combinations is preferable since the quadrant assembly powers are a combination of measured and inferred powers and are, therefore, influenced by SIMULATE-3.

3.7 PIDAL-3 OUTPUT

PIDAL-3 calculates the accumulated assembly exposure distribution based on the total thermal power output over a given time period (MWhrs) and a nodal power distribution representative of the time period.

PIDAL-3 produces a variety of default summary edits:

Edit	Subroutine	Description
First Page	PAGONE	Summary of File Trail Data (FTD)
	GETRES	Exposure Step Mating Identification
	PAGONE	Plant Input Parameters
	PAGONE	Control Rod Locations and Positions
	PAGONE	Axial Locations of each ICI within each String
P3X FMAP	CORMAP	Full Core Assembly Ids, Pins/Assembly, ICI Locations
P3X QICI	DETSIG	ICI Signals (nv) and Powers (MWth) by 1/4 Core Symmetry
P3X 2DPF	SOLVES	P3 vs S3 2D Measured/Inferred (M/I) Detector Power Fractions for each ICI level and failed ICIs by PDEV
P3X 2RPF	RADIAL	P3 vs S3 Axially Collapsed Assembly Relative Power Fractions
P3X DRPF	PERDEV	P3 vs S3 ICI Detector Power Fractions and Percent Deviations
P3X 3DDV	HISTOG	P3 vs S3 ICI Detector Power Distribution of Deviations
P3X FCAL	EDSOME	Total ICI Core Power to Calorimetric Power Ratio
P3X 3TPF	GETTPF	P3 F_Q (Total) Peaking Factor with Assembly and Axial Location
S3X 3TPF	GETTPF	S3 F_Q (Total) Peaking Factor with Assembly and Axial Location
P3X 3QPT	TILT	ICI Quadrant Power Tilt based on 2-way Symmetric ICIs by level
	TLTERR	Possible Symmetric Sets of Operable ICIs for 6 Quadrant Combinations
	INTTLT	ICI Quadrant Power Tilt based on Integral Quadrant Powers
	EDTILT	Incore and Excore Quadrant Power Tilts and Comparisons
P3X ZRPF	EDSOME	P3 vs S3 Radially Collapsed Assembly Relative Power Fractions
P3X TSPF		TS Peaking Factor Verification
P3X BFRA	EDPEAK	Sub-batch F_R^A (Assembly) Peaking Factors with TS Uncertainties
P3X BFRT	EDPEAK	Sub-batch F_R^T (Pin) Peaking Factors with TS Uncertainties
P3X BKWF	EDLHGR	Sub-batch LHR (kw/ft) with TS Uncertainties
P3X FALM	CLIMIT	ICI Alarm Factors for most limiting LHR by ICI level
P3X 3APL	GETAPL	Allowable Power Level for Monitoring LHR using only Excores
P3X 2PIN	EDKWFT	P3 vs S3 F_R^T (Pin) Peaking Factors by Assembly
P3X PKWF		P3 vs S3 Peak Nodal LHR by Assembly (kw/ft) and Corresponding Axial Locations
P3X 2EXP	EXPOZF	Axial Collapsed Assembly Exposures (gwd/mtu)
P3X CEXP		Axial Collapsed Assembly Cycle Exposures (gwd/mtu)
P3X BRPF	POWMAX	Sub-batch Average and Maximum Relative Power Fractions
P3X BEXP	BRNMAX	Sub-batch Average and Maximum Exposures (gwd/mtu)
P3X 3ICI	CALARM	ICI Alarm Limits, Currents, and Sensitivities by each ICI
P3X FSUM	CORDAT	Summary of Core Information and Axial Offsets
P3X FASI	EXMON	Excore Monitoring System Operator Information
P3X TS06A	MT6BOR	MT-06 TS Surveillance Calculation Summary
P3X TS06B	MT6SUM	DWT-12 TS Surveillance Calculation Summary

An example PIDAL-3 output is provided as Appendix A.

4.0 PIDAL-3 VALIDATION

The PIDAL-3 comparisons are made between CASMO-4 and CASMO-3 data for cycles 12 through 14. Key parameters such as Assembly Radial Power RMS Deviations, F_R^A , F_R^T , and F_Q are considered. An analysis of the measurement uncertainty in the PIDAL-3 peaking factor calculations is also performed for these reference cycles. The derived uncertainties are compared to those currently approved in the Palisades Technical Specifications. Details of the calculations are documented in [PID991] and [PID992].

4.1 CALCULATIONS

Fifty PIDAL-3 cases for cycles 12 to 14 were run to generate the measurement uncertainties; all covering steady-state HFP operation from BOC to EOC. These 50 cases were rerun including only the 36 detector strings Palisades intends to load from cycle 15 to the end of life. These 50 cases were then rerun in 5 different scenarios involving failing 50% of the operable detectors for each cycle (18 total strings). Finally, 2 cases were run covering an end of cycle 11 xenon transient and middle of cycle 11 dropped control rods, both developed in [PID961].

4.2 COMPARISONS

The following cycle 12 to 14 comparisons were made between CASMO-4 and CASMO-3 PIDAL-3 models:

- Figures 4.1a-c Cycles 12-14 Assembly RMS Deviations
- Figures 4.2a-c Cycles 12-14 Assembly Radial Peaking vs. Exposure
- Figures 4.3a-c Cycles 12-14 Total Radial Peaking vs. Exposure
- Figures 4.4a-c Cycles 12-14 Total Peaking Factor vs. Exposure
- Figures 4.5a-c Cycles 9-14 Uncertainty Analysis Summaries
- Figure 4.5d Cycles 12-14 Poolability and Normality Study

The assembly power RMS deviations are comparable between CASMO-4 and CASMO-4 over the 3 cycles. CASMO-4 shows improvement for cycle 12, but no additional improvement for cycles 13 and 14. The absence of significant improvement is due to CASMO-4 using an implicit detector model with the additional geometry factor compared to CASMO-3 using an explicit detector model. The geometry factor adds additional uncertainty despite the accuracy simply by adding an additional correction. This comparison provides important verification that the implicit detector model is working correctly.

The assembly radial peaking factor, F_R^A , total radial peaking factor, F_R^T , and the total peaking factor, F_Q , show almost identical results between CASMO-3 and CASMO-4. Again, this validates the CASMO-4 code using the implicit detector model.

As Expected the Uncertainty Analysis for CASMO-4 showed significant improvement over CASMO-3 for cycles 9 to 11 as well as cycles 12 to 14. Each uncertainty component improved with CASMO-4 with the LPF or PTB factor improving the most per [CMS992]. This is due in large part to CASMO-4's ability to model gadolinia pins and the surrounding pins more accurately. With the improved accuracy comes more degrees of freedom, and overall lower uncertainties. The 50% incore operability study in [PID992] showed comparable results to the original 75% incore operability in [PID892].

The poolability study showed cycles 12 and 13 to be above the minimum value for 95% confidence, and cycle 14 to be well below. This was not unexpected due to the continuously improving trend in standard deviation between calculated and measured data from beginning to end of cycle. Refer to Section 4.4.2 for a detailed explanation of poolability and normality effects on the uncertainties.

Figure 4.1a Cycle 12 Assembly Power RMS Deviations

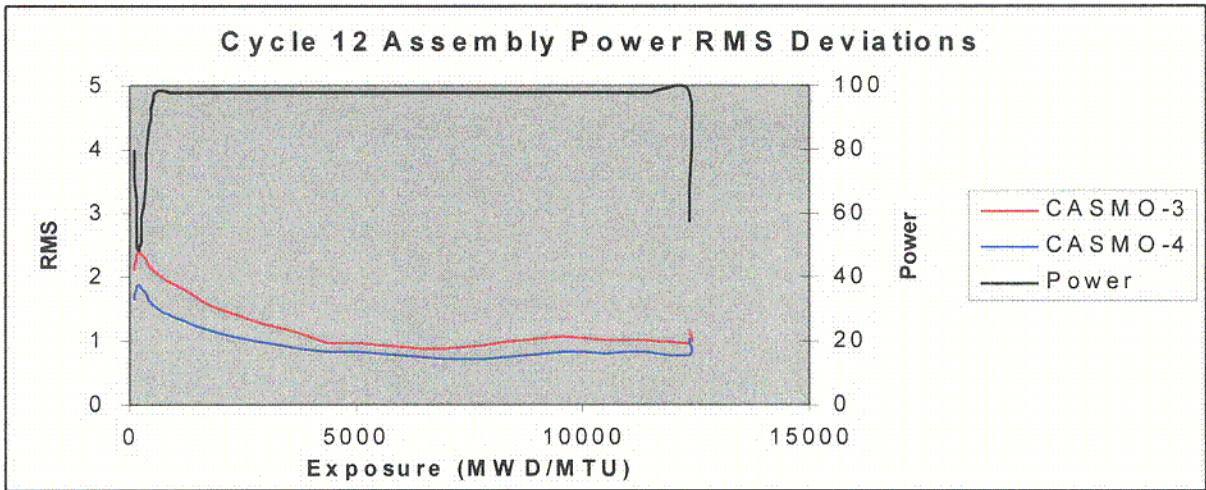


Figure 4.1b Cycle 13 Assembly Power RMS Deviations

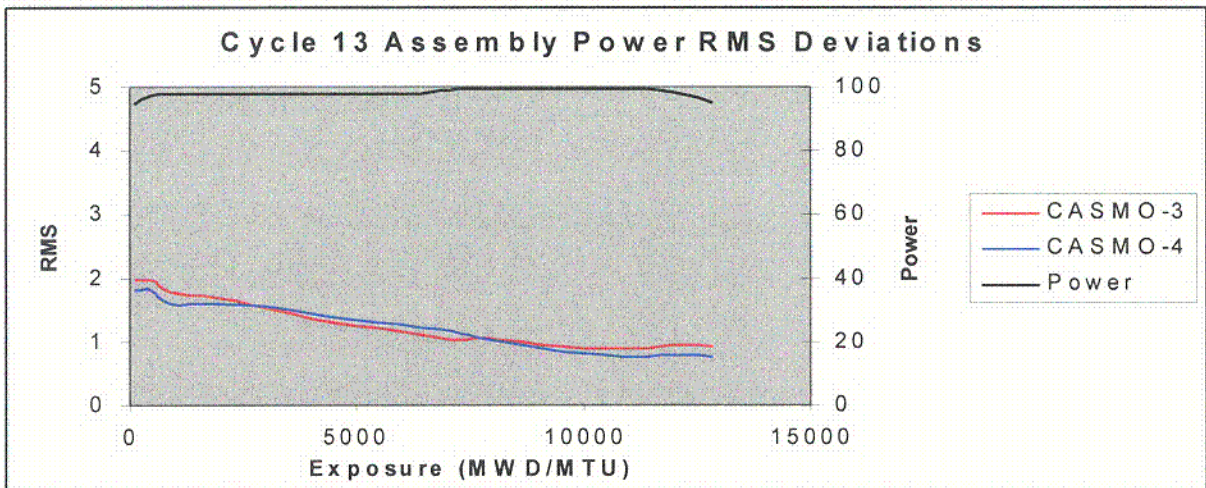
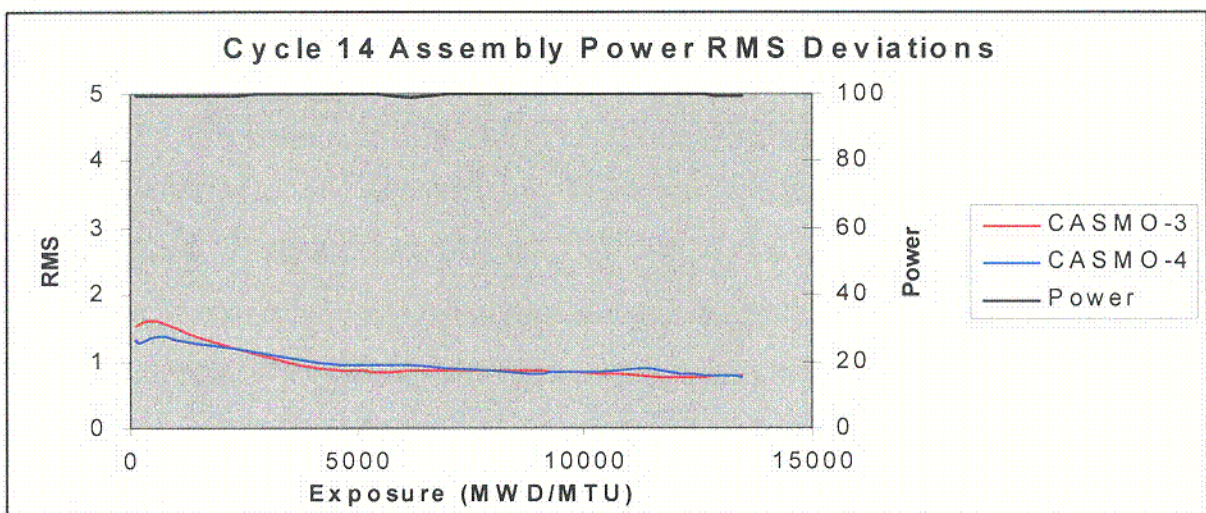


Figure 4.1c Cycle 14 Assembly Power RMS Deviations



C-4

Figure 4.2a Cycle 12 Assembly Radial Peaking Factor

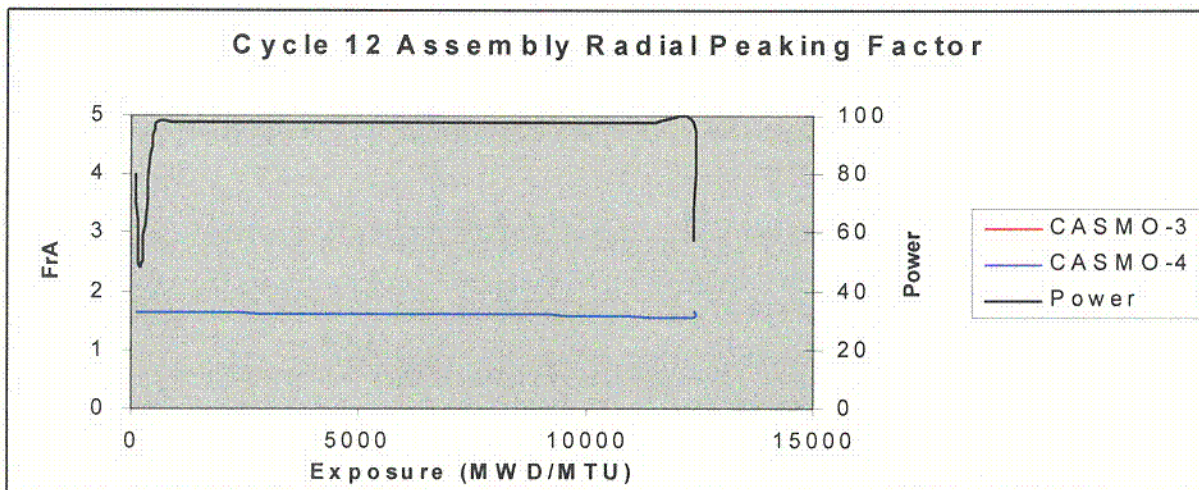


Figure 4.2b Cycle 13 Assembly Radial Peaking Factor

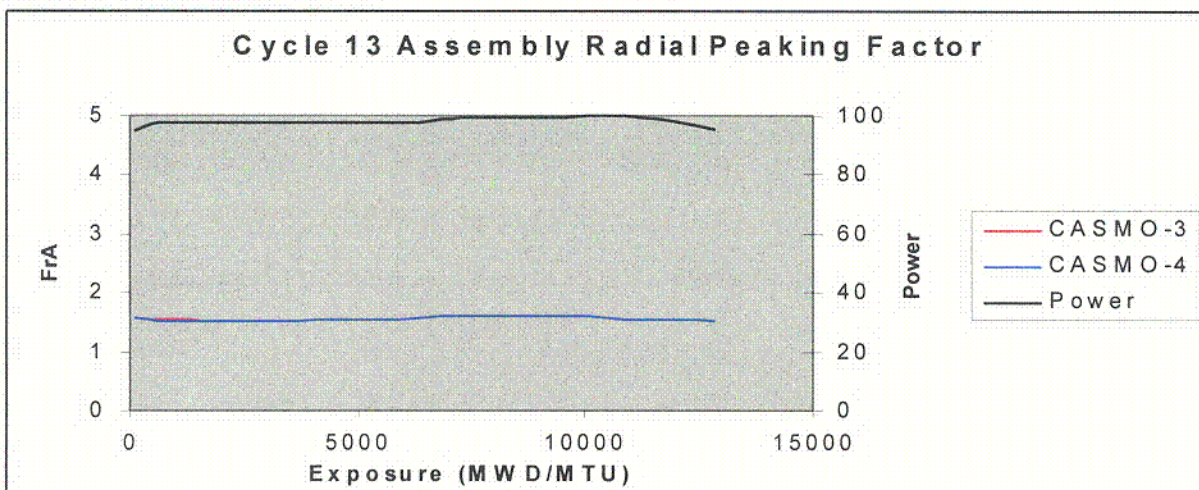
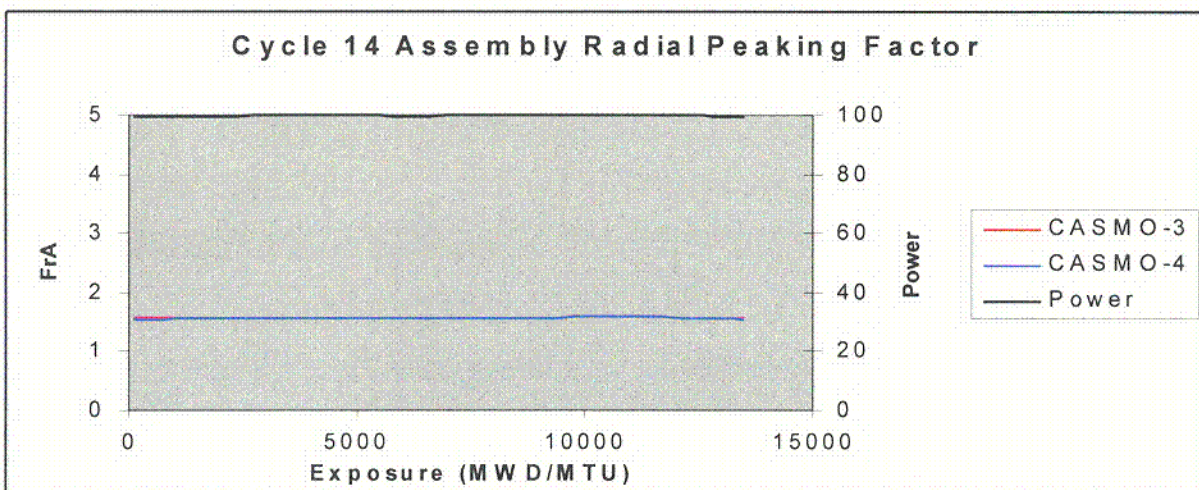


Figure 4.2c Cycle 14 Assembly Radial Peaking Factor



C-5

Figure 4.3a Cycle 12 Total Radial Peaking Factor

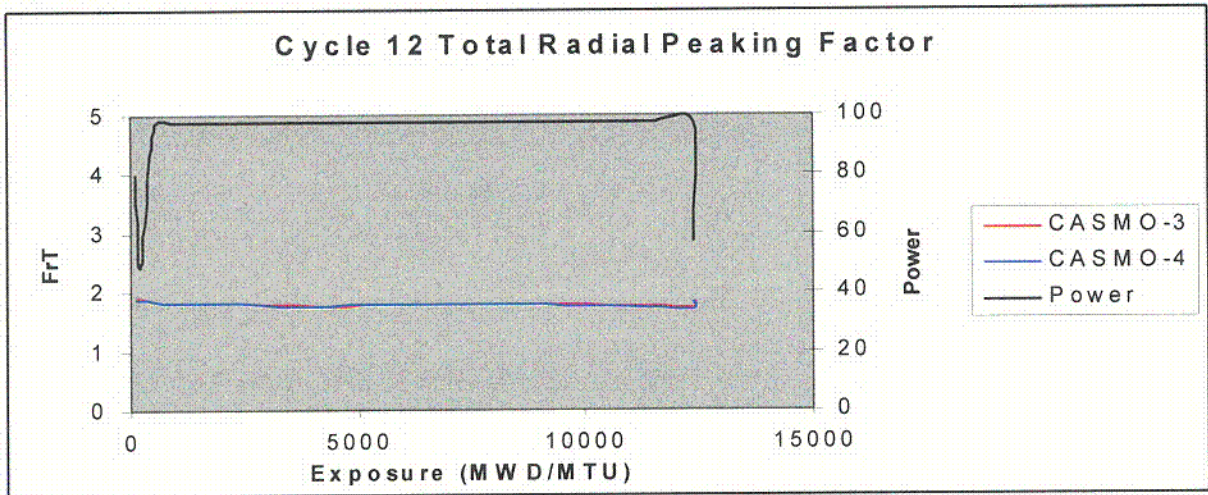


Figure 4.3b Cycle 13 Total Radial Peaking Factor

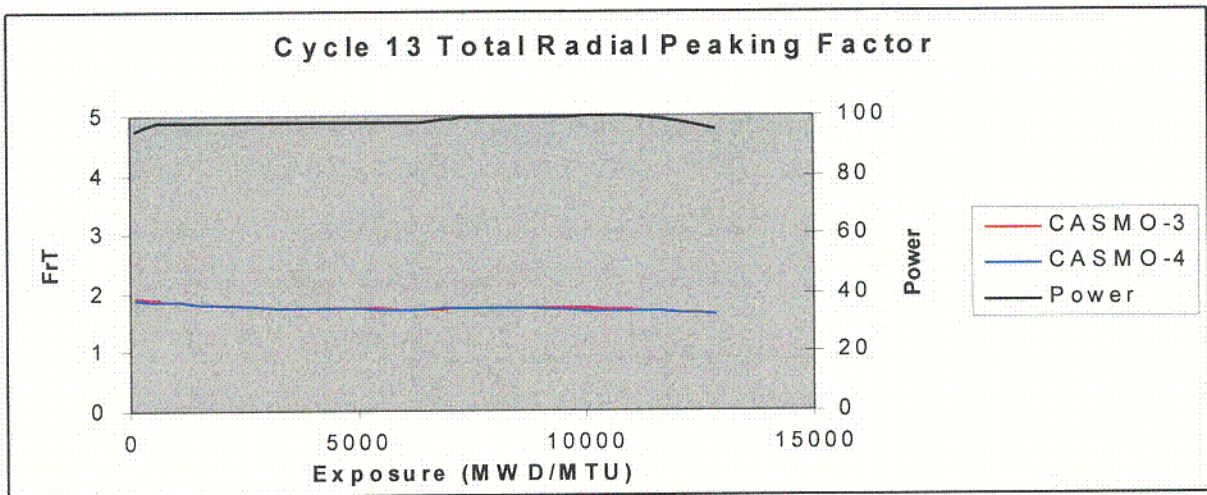
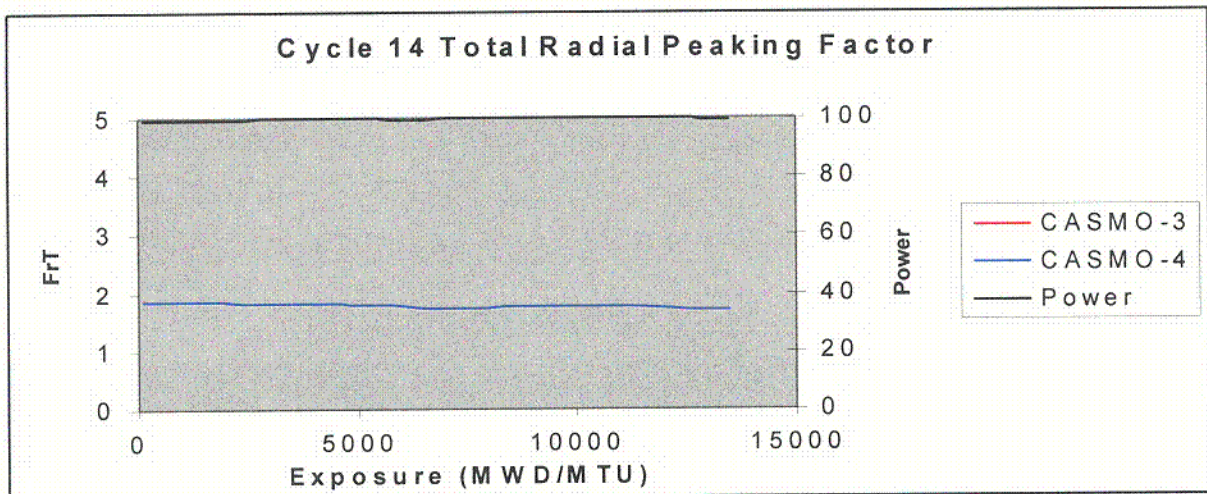


Figure 4.3c Cycle 14 Total Radial Peaking Factor



C-Ce

Figure 4.4a Cycle 12 Total Peaking Factor

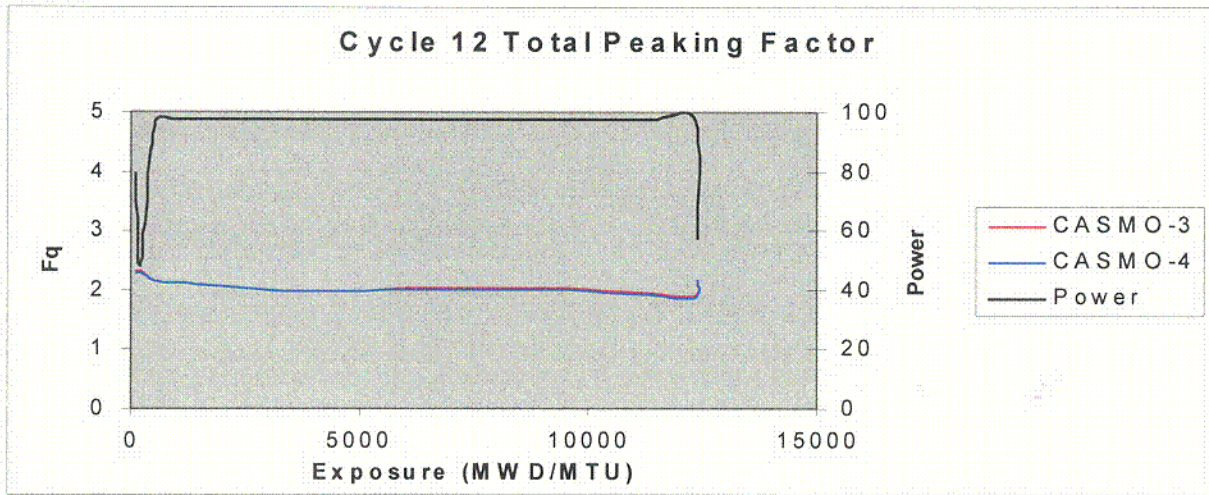


Figure 4.4b Cycle 13 Total Peaking Factor

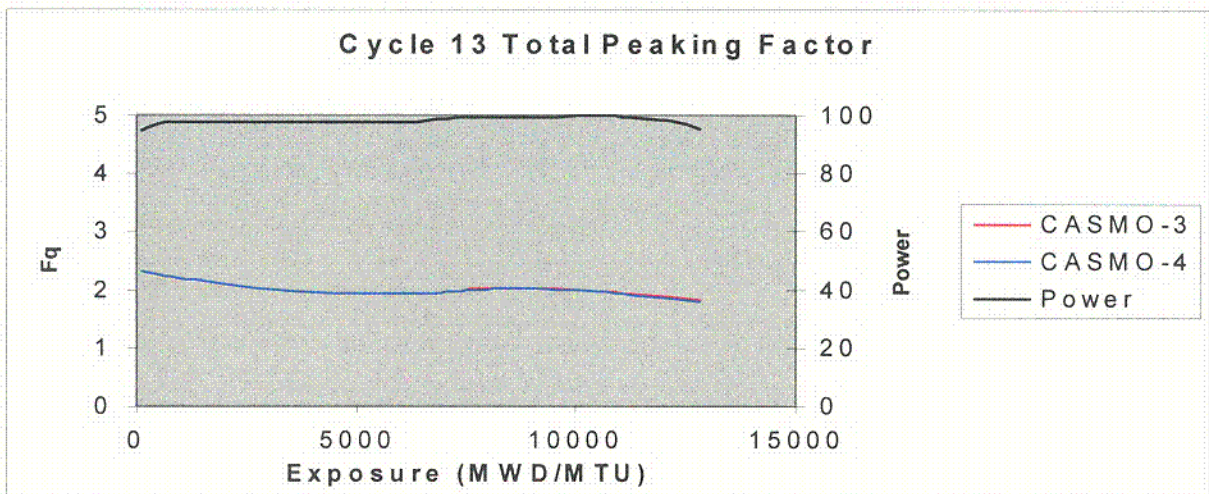
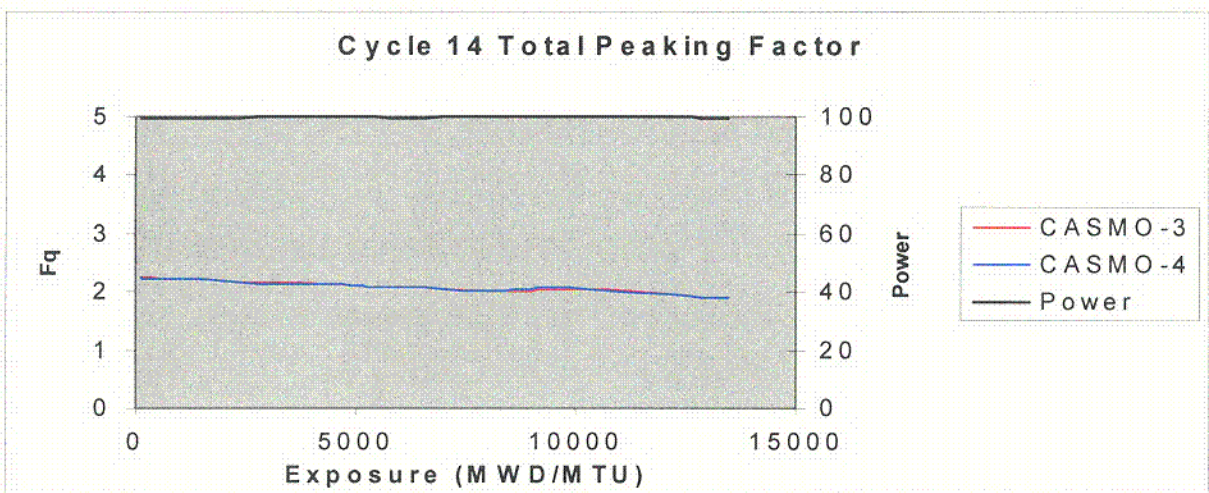


Figure 4.4c Cycle 14 Total Peaking Factor



4.3 UNCERTAINTY ANALYSIS

In order to determine the uncertainties associated with the PIDAL-3 full core monitoring model, it was necessary to employ the appropriate statistical model. As with all previous PIDAL uncertainty calculations, Siemens methodology in [EXXON] was chosen.

Two computer codes and EXCEL are used to generate the statistical analysis data:

The PIDAL-3 program is used to determine the measured and inferred full core detector powers and power distributions required. The PIDAL-3 program fails each detector string one at a time, and recalculates the power distribution based on inferred data. The uncertainty analysis data is written to the uncertainty file described in [PID3] Users Manual attachment 9.

The UNSAT-3 program is used to calculate the F(s), F(sa), F(r), and F(z) uncertainty components. The F(L) uncertainty component was calculated in [CMS992], and is based on the B&W critical experiments in [BAW1810]. UNSAT-3 reads the Uncertainty file generated by PIDAL-3 statistical analysis routines and calculates the deviations, means and standard deviations required by this analysis. UNSAT-3 also sets up histogram data files for plotting figures (See Figures 4.6-4.8). [PID3] Users Manual attachment 13 describes the input requirements to UNSAT-3.

The EXCEL spreadsheet (Figure 4.5a) was used in [PID992] to determine the overall uncertainties along with the various effects listed below. The results of the computer cases with the individual component uncertainties are combined in order to determine the overall uncertainties as defined by the statistical model in [PID3] Uncertainty Analysis Manual Section 3.

4.4 EFFECTS ON UNCERTAINTIES

Included in this analysis was a study of various effects on the final uncertainties such as:

- 1) Low Leakage Cores
- 2) Poolability and Normality of Data
- 3) Failing Large Numbers of Incore Instruments
- 4) Radial Power Tilts
- 5) Large Axial Offsets

4.4.1 LOW LEAKAGE CORES

Since the inception of low leakage core designs, one of the consequences is that the uncertainties for low power assemblies with relative power fractions (RPF) < 1.0 are inflated due to higher percent deviations given the same absolute deviation. One possible solution is to use absolute differences instead of percent differences, but the absolute differences in low power assemblies is small compared to average assemblies and would not be conservative. The uncertainty analysis methodology was not changed in order to comply with the NRC expectation that a previously approved methodology be used. The alternative is to eliminate all assemblies with a RPF < 1.0 . Since the assemblies of interest have RPFs > 1.0 , this produces a representative uncertainty that is conservative for peak assemblies, but not so conservative as to penalize the peak unnecessarily as stated in [OPPD].

4.4.2 POOLABILITY AND NORMALITY OF DATA

Before combining data in a statistical analysis, the data must be tested for poolability. Two questions must be answered: First, should the data be poolable? Second, does it make sense? The widely accepted Bartlett Test can be used to determine poolability of data within each cycle and across the cycles as described in [STEA].

In order for data to be poolable, it must be independent and devoid of trends. First, the data generated by the PPC is predictable at steady-state conditions regardless of how often the data is sampled. Therefore, we have

truly dependent data and one could significantly increase the degrees of freedom by sampling more data points. This is true of all nuclear plants and is also the case with the original PIDAL uncertainties generated by pooling cycles 5, 6, and 7. Second, since the inception of low leakage core designs, BOC uncertainties tend to be higher than EOC uncertainties since the cores are more heterogeneous at BOC and become more homogeneous at EOC after the peaks have burned out.

With this in mind, it appears that Palisades is unable to pool data within a cycle let alone between cycles. OPPD had a similar problem and they contacted Charles T. Rombough of CTR Technical Services Inc. for assistance. He advised OPPD to use fewer time points to reduce the degrees of freedom and produce more independent data. OPPD believed that a conservative estimate of 12 time points across the cycle produced independent data. Palisades has concluded that this approach is acceptable for use in the PIDAL-3 application. If we use fewer time points across the cycle, we produce more independent data and reduce the degrees of freedom. By sampling approximately every 1000 MWD/MTU (once a month), we believe the data is independent, and we have significantly reduced the degrees of freedom. The much lower degrees of freedom is also very conservative. The SIMULATE-3 model produced a much flatter assembly radial power RMS deviations across the cycles compared to XTG. Poolability across cycles 5, 6, and 7 was deemed possible given the similarity in core designs and cycle length.

For the normality test, as described in [ANSI], we used the W test and the D-prime test. The data for cycles 12 to 14 exhibit normal distributions across the cycles per [PID992] and Figures 4.6a-d through 4.8a-d. Figure 4.7c is the exception. Since the installation of axial blankets in cycle 13, PIDAL-3 does not accurately curve fit the measured/inferred data from Section 3.5 over the bottom and top nodes (Nodes 1 and 25) with only 5 detector levels. PIDAL-3 cannot reproduce the SIMULATE-3 data, due to the very large power gradient caused by the axial blankets (i.e. PIDAL-3 cannot bend the power distribution down far enough to satisfy SIMULATE-3). Thus the $F(r)$ and $F(z)$ components show higher than normal uncertainties, and $F(r)$ shows an abnormal distribution. Since the bias is negative, the PIDAL-3 model is over-predicting the SIMULATE-3 model and is therefore conservative. This is similar to the result obtained by Siemens in [EXXON]. As a footnote, cycle 14 shows considerable improvement over cycle 13 with the second batch of blanket fuel.

4.4.3 FAILING LARGE NUMBERS OF INCORE INSTRUMENTS

Current Palisades Technical Specifications require that 75% of all possible detector locations, with a minimum of two detectors per core level per quadrant be working in order to declare the incore monitoring system operable. The latest submittal per [PID991] and [PID992] requires 50% operability of the 36 remaining detector locations, and retains the requirement for at least two detectors per core level per quadrant. This is consistent with current ABBCE specifications.

[EXXON] came to the conclusion that the accuracy of an incore monitoring system or methodology depended more on which detectors were operable than on the total number operable. [EXXON] also concluded that it was best to use all available data points in determining the individual component uncertainties, and therefore, did not go into great detail investigating the effects of large numbers of incore failures on the measured/inferred power distribution. These conclusions are valid because, for random detector failures, there is an equal probability that the well behaved detectors and the non-well behaved detectors would fail.

In order to prove these conclusions, it would be necessary to test every possible combination of failed detectors for a large set of power distributions. From a computational standpoint, this is not practical. Therefore, a test was devised to verify that incore failures resulting in 50% detector operability would produce accurate measurements.

A base test case was chosen at the middle of cycles 12, 13, and 14, and the results for each of the component uncertainties were recorded. Five sets of 18 failed incore strings were then chosen using a random number generator in EXCEL. The statistical analysis was repeated for each of the 5 failed sets. The results of the 5 sets were compared to the base case. The maximum positive deviations were identified and bounding values were added to each of the uncertainties across all of the cycles. The effects of large radial power tilts with 50% of the detectors failed were not examined. The inception of the SIMULATE-3 full core coupling calculations in [PID961], and the elimination of assemblies with RPFs < 1.0 significantly reduced the consequences of losing 25-50% of the detectors from the original submittal with tilt.

The uncertainty analysis for cycles 9 to 14 already eliminates the operable detectors with RPFs less than 1.0, and no effect on uncertainties was observed for the [PID961] cases run examining tilted cores and 25% detector failures. In [PID992], penalties with 50% of detectors failed is comparable to [PID892] with 25% of detectors failed.

Based on these results, the uncertainties associated with the PIDAL-3 system documented by this report are valid for an incore monitoring system operable with up to 50% of its 180 remaining incore detectors failed.

4.4.4 RADIAL POWER TILTS

The original PIDAL methodology in [PID892] determined the F(s) uncertainty component for power distributions with quadrant power tilts up to 5%. The Palisades Technical Specifications allow for full power operation with quadrant power tilts of up to 5%.

The F(s) uncertainty component was recalculated for radial tilted cores in [GAB906]. The results showed that in all cases the F(s) value (0.0277) was bounding for quadrant power tilts up to 2.8%. It was also found that the F(s) value depended strongly on the direction and magnitude of the oscillation causing the power tilt. For cores oscillating about the diagonal core axis, the F(s) value was valid for tilts up to 5%. For oscillations about the major core axis, the F(s) value was valid for tilts up to 2.8%. Since the Palisades Technical Specifications allow for full power operation with quadrant power tilts of up to 5%, and it was clear that the overall PIDAL uncertainties were only valid for tilts up to 2.8%, it was necessary to derive a second set of uncertainties for tilts above 2.8%.

With the inception of SIMULATE-3 in [PID961], radial power tilts between 2.8% and 5.0% do not require additional uncertainties since SIMULATE-3 and PIDAL-3 can monitor the full core including dropped control rods. The major limitation of the original PIDAL submittal was a quarter core XTG model, and quarter core PDQ W-primes and LPFs. No effect on uncertainties was observed in the [PID961] and [PID992] cases, which examined tilted cores up to 5%.

4.4.5 LARGE AXIAL OFFSETS

The [PID961] and [PID992] uncertainty analyses both contain an actual power transient, which produced a xenon driven power oscillation. The movement of control rods and changes in boron concentration have the greatest effect on SIMULATE-3's ability to reproduce the transient. The major limitation is due to the frequency of snapshots from the PPC (1 per hour). Too many evolutions can occur within each hour for SIMULATE-3 to accommodate over the entire transient. For example, control rod movements 10 minutes passed the hour produce very different results than those 10 minutes to the hour. Therefore, as a transient continues PIDAL-3 and SIMULATE-3 begin to diverge. Fifteen minute time steps are currently available with the PPC and will improve the uncertainties.

Figure 4.5a Uncertainty Analysis Summary with CASMO-4

Cycle	Sample Variance Input for Uncertainty Components					Calculated Peaking Factor Variances			Degrees of Freedom Input for Uncertainty Components					Calculated Peaking Factor Degrees of Freedom			Tolerance Factor Input from [OWEN]			TS Tolerance Limits with 25 or 50% Failures		
	Sf(s)	Sf(sa)	Sf(r)	Sf(z)	Sf(L)	Sf(q)	Sf(rT)	Sf(rA)	Df(s)	Df(sa)	Df(r)	Df(z)	Df(L)	Df(q)	Df(rT)	Df(rA)	Kf(q)	Kf(rT)	Kf(rA)	F(q)	F(rT)	F(rA)
TS Limits																						
New	0.0277	0.0194	0.0022	0.0151	0.0135	0.0344	0.0237	0.0195	8768	1754	2754	1122	188	4826	1226	1790	1.692	1.727	1.712	0.0623	0.0455	0.0401
Used	0.0306	0.0241	0.0021	0.0151	0.0135	0.0368	0.0277	0.0242	3415	683	969	1122	188	3823	878	694	1.692	1.733	1.746	0.0664	0.0526	0.0490
Tilt	0.0393	0.0051	0.0026	0.0151	0.0135	0.0443	0.0377	0.0362	1800	360	408	1122	188	2487	460	364	1.703	1.770	1.785	0.0795	0.0713	0.0695
9	0.0140	0.0091	0.0009	0.0055	0.0100	0.0181	0.0136	0.0091	1530	306	1800	1800	96	827	270	306	1.736	1.809	1.798	0.0344	0.0301	0.0239
10	0.0142	0.0095	0.0010	0.0048	0.0100	0.0180	0.0138	0.0096	1380	276	2056	2056	96	784	271	288	1.739	1.809	1.804	0.0343	0.0305	0.0248
11	0.0172	0.0143	0.0009	0.0063	0.0100	0.0206	0.0175	0.0143	1700	340	1988	1988	96	1154	413	340	1.727	1.778	1.790	0.0386	0.0366	0.0331
12	0.0134	0.0113	0.0009	0.0054	0.0100	0.0176	0.0151	0.0113	1470	294	1896	1896	96	758	326	294	1.741	1.793	1.802	0.0336	0.0326	0.0279
13	0.0117	0.0099	0.0045	0.0076	0.0100	0.0177	0.0148	0.0109	1865	373	2184	2184	96	847	369	544	1.736	1.784	1.760	0.0337	0.0319	0.0267
14	0.0147	0.0062	0.0031	0.0083	0.0100	0.0199	0.0133	0.0088	2010	402	2432	2432	96	1212	271	531	1.727	1.809	1.760	0.0374	0.0296	0.0230
15																						
16																						
17																						
18																						
19																						
20																						
21																						
22																						
11 Xenon	0.0191	0.0160	0.0012	0.0060	0.0100	0.0224	0.0189	0.0160	1960	392	3028	3028	96	1460	470	392	1.727	1.770	1.780	0.0417	0.0390	0.0360

Cycle	Reference	Notes
New	[PID892] EA-P-PID-89002 Rev 0	1) Spreadsheet Equations from [PID892]
Used	[PID892] EA-P-PID-89002 Rev 0	2) CCLR Limits based on [PID892]
Tilt	[GB906] EA-GAB-90-06 Rev 0	Fq = 0.0425 FrT = 0.0400 FrA = 0.0375
9-14	[PID892] EA-PID-99-02 Rev 0	3) Penalty for Large Number of ICI failures: For [PID892] the penalty for 25% failure as applied Fq + 0.0041 FrT + 0.0046 FrA + 0.0067 For [PID892] the penalty for 50% failure as applied Fq + 0.0030 FrT + 0.0055 FrA + 0.0075
	[OWEN] Factors for One-sided Tolerance Limits, DB Owen, March 1963, Pages 46 to 51	4) All assembly powers < 1.0 have been eliminated

Figure 4.5b Uncertainty Analysis Summary with CASMO-3

Cycle	Sample Variance Input for Uncertainty Components					Calculated Peaking Factor Variances			Degrees of Freedom Input for Uncertainty Components					Calculated Peaking Factor Degrees of Freedom			Tolerance Factor Input from [OWEN]			TS Tolerance Limits with 25% Failures		
	Sf(s)	Sf(sa)	Sf(r)	Sf(z)	Sf(L)	Sf(q)	Sf(rT)	Sf(rA)	Df(s)	Df(sa)	Df(r)	Df(z)	Df(L)	Df(q)	Df(rT)	Df(rA)	Kf(q)	Kf(rT)	Kf(rA)	F(q)	F(rT)	F(rA)
TS Limit																						
9	0.0161	0.0112	0.0010	0.0078	0.0163	0.0242	0.0198	0.0112	1530	306	1800	1800	96	439	195	306	1.774	1.840	1.798	0.0429	0.0364	0.0201
10	0.0187	0.0148	0.0010	0.0075	0.0163	0.0259	0.0220	0.0148	1375	275	2068	2068	96	545	257	275	1.760	1.814	1.807	0.0456	0.0399	0.0267
11	0.0212	0.0176	0.0009	0.0068	0.0163	0.0276	0.0240	0.0176	1780	358	1980	1980	96	683	330	358	1.746	1.792	1.768	0.0482	0.0430	0.0314
12	0.0150	0.0125	0.0009	0.0064	0.0163	0.0231	0.0206	0.0125	1465	293	1884	1884	96	369	220	293	1.784	1.828	1.802	0.0412	0.0377	0.0225
13	0.0143	0.0120	0.0046	0.0091	0.0163	0.0240	0.0208	0.0129	1895	379	2176	2176	96	436	237	504	1.774	1.821	1.763	0.0426	0.0379	0.0227
14	0.0164	0.0099	0.0032	0.0095	0.0163	0.0252	0.0193	0.0104	2010	402	2432	2432	96	521	183	489	1.763	1.847	1.768	0.0444	0.0356	0.0184
15																						
16																						
17																						
18																						
19																						
20																						
21																						
22																						
11 Xenon	0.0273	0.0197	0.0013	0.0065	0.0163	0.0325	0.0258	0.0197	3015	603	3000	3000	96	1212	436	603	1.727	1.774	1.752	0.0561	0.0454	0.0345

Cycle	Reference	Notes
TS Limit	[PID892] EA-P-PID-89002 Rev 0	1) Spreadsheet Equations from [PID892]
9-14	[PID991] EA-PID-99-01 Rev 0	2) Penalty for Large Number of ICI failures: For [PID892] the penalty for 25% failure as applied Fq + 0.0041 FrT + 0.0048 FrA + 0.0067 For [PID991] the penalty for 25% failure as applied Fs + 0.0010 Fsa + 0.0005
11 Xenon	[PID961] EA-PID-96-01 Rev 0	3) All assembly powers < 1.0 have been eliminated
	[OWEN] Factors for One-sided Tolerance Limits, DB Owen, March 1963, Pages 46 to 51	

Figure 4.5c Uncertainty Analysis Summary with CASMO-4 and 50% ICI Operability

Cycle	Sample Variance Input for Uncertainty Components				Calculated Peaking Factor Variances			Degrees of Freedom Input for Uncertainty Components				Calculated Peaking Factor Degrees of Freedom			Tolerance Factor Input from [OWEN]			TS Tolerance Limits For 50% Failures				
	SI(s)	SI(sa)	SI(t)	SI(z)	SI(L)	SI(q)	SI(rT)	SI(rA)	DI(s)	DI(sa)	DI(t)	DI(z)	DI(L)	DI(q)	DI(rT)	DI(rA)	KI(q)	KI(rT)	KI(rA)	F(q)	F(rT)	F(rA)
12F0	0.0147	0.0105	0.0010	0.0065	0.0100	0.0188	0.0145	0.0105	2250	450	2858	2858	96	958	337	450	1.729	1.781	1.770	0.0322	0.0280	0.0188
12F1	0.0147	0.0104	0.0010	0.0055	0.0100	0.0188	0.0145	0.0104	990	198	2858	2858	96	789	271	198	1.739	1.809	1.838	0.0323	0.0282	0.0191
12F2	0.0143	0.0114	0.0010	0.0055	0.0100	0.0183	0.0152	0.0114	1105	221	2858	2858	96	788	296	221	1.739	1.801	1.828	0.0318	0.0274	0.0208
12F3	0.0125	0.0082	0.0010	0.0055	0.0100	0.0170	0.0130	0.0083	1075	215	2858	2858	96	657	228	228	1.748	1.825	1.825	0.0297	0.0237	0.0151
12F4	0.0147	0.0115	0.0010	0.0055	0.0100	0.0186	0.0153	0.0115	1130	226	2858	2858	96	821	302	228	1.737	1.800	1.825	0.0323	0.0275	0.0210
12F5	0.0139	0.0113	0.0010	0.0055	0.0100	0.0180	0.0151	0.0113	990	198	2858	2858	96	738	279	198	1.742	1.807	1.838	0.0314	0.0273	0.0208
13F0	0.0154	0.0110	0.0042	0.0072	0.0100	0.0202	0.0154	0.0118	2830	566	3488	3488	96	1339	432	747	1.728	1.774	1.742	0.0349	0.0273	0.0206
13F1	0.0171	0.0140	0.0042	0.0072	0.0100	0.0215	0.0177	0.0146	1985	277	3488	3488	96	1281	404	327	1.728	1.778	1.793	0.0372	0.0315	0.0262
13F2	0.0175	0.0143	0.0042	0.0072	0.0100	0.0218	0.0179	0.0149	1960	272	3488	3488	96	1298	398	320	1.728	1.779	1.794	0.0377	0.0318	0.0267
13F3	0.0172	0.0135	0.0042	0.0072	0.0100	0.0216	0.0173	0.0141	1375	275	3488	3488	96	1290	398	327	1.728	1.779	1.793	0.0373	0.0308	0.0253
13F4	0.0174	0.0139	0.0042	0.0072	0.0100	0.0217	0.0176	0.0145	1385	277	3488	3488	96	1295	401	328	1.728	1.778	1.793	0.0375	0.0313	0.0260
13F5	0.0158	0.0134	0.0042	0.0072	0.0100	0.0205	0.0172	0.0140	1300	260	3488	3488	96	1155	383	310	1.728	1.781	1.797	0.0354	0.0306	0.0252
14F0	0.0234	0.0118	0.0038	0.0081	0.0100	0.0270	0.0158	0.0122	3245	649	3876	3876	96	2888	472	793	1.703	1.770	1.739	0.0460	0.0280	0.0212
14F1	0.0225	0.0155	0.0038	0.0081	0.0100	0.0262	0.0188	0.0180	1630	328	3876	3876	96	1795	444	370	1.712	1.774	1.783	0.0449	0.0334	0.0285
14F2	0.0217	0.0131	0.0038	0.0081	0.0100	0.0255	0.0169	0.0136	1710	342	3876	3876	96	1799	429	397	1.712	1.774	1.779	0.0437	0.0300	0.0242
14F3	0.0213	0.0103	0.0038	0.0081	0.0100	0.0252	0.0149	0.0110	1630	328	3876	3876	96	1741	355	423	1.712	1.788	1.778	0.0431	0.0266	0.0196
14F4	0.0240	0.0108	0.0038	0.0081	0.0100	0.0275	0.0152	0.0114	1630	328	3876	3876	96	1852	386	404	1.712	1.784	1.778	0.0471	0.0271	0.0203
14F5	0.0184	0.0080	0.0038	0.0081	0.0100	0.0228	0.0134	0.0089	1630	328	3876	3876	96	1538	276	497	1.712	1.807	1.786	0.0390	0.0242	0.0157

Cycle	Reference	Notes
TS Limit	[PID892] EA-P-PID-89002 Rev 0	1) Spreadsheet Equations from [PID892] 2) Penalty for Large Number of ICI failures: For [PID892] the penalty for 25% failure as calculated Fq + 0.0041 FrT + 0.0048 FrA + 0.0067 For [PID992] the penalty for 50% failure as calculated Fq + 0.0028 FrT + 0.0054 FrA + 0.0073
12-14	[PID992] EA-PID-99-02 Rev 0	
	[OWEN] Factors for One-sided Tolerance Limits, DB Owen, March 1963, Pages 48 to 51	

Figure 4.5d Poolability and Normality Summary with CASMO-4

Cycle 12 Fs		Cycle 13 Fs		Cycle 14 Fs	
ST DEV	OBSERV	ST DEV	OBSERV	ST DEV	OBSERV
0.0120	105	0.0101	110	0.0141	105
0.0121	105	0.0103	110	0.0141	105
0.0123	105	0.0104	110	0.0142	110
0.0123	100	0.0104	110	0.0142	110
0.0124	105	0.0105	110	0.0142	105
0.0124	100	0.0106	110	0.0143	105
0.0126	105	0.0107	110	0.0143	105
0.0126	100	0.0109	110	0.0144	110
0.0130	105	0.0112	110	0.0144	105
0.0135	110	0.0114	110	0.0145	105
0.0142	110	0.0116	110	0.0145	105
0.0148	110	0.0128	110	0.0147	105
0.0155	105	0.0134	115	0.0147	105
0.0170	105	0.0135	105	0.0149	105
		0.0135	110	0.0152	105
		0.0138	105	0.0157	105
		0.0142	110	0.0158	105
				0.0161	105
				0.0161	105

[ANSI] Table 1			
	C12	C13	C14
An	0.5251	0.4968	0.4808
An-1	0.3318	0.3273	0.3232
An-2	0.2460	0.2540	0.2561
An-3	0.1802	0.1988	0.2059
An-4	0.1240	0.1524	0.1641
An-5	0.0727	0.1109	0.1271
An-6	0.0240	0.0725	0.0932
An-7		0.0359	0.0612
An-8			0.0303

Bartlett Test					
K	14	K	17	K	19
S ^z	1.80E-04	S ^z	1.39E-04	S ^z	2.18E-04
C	1.0032	C	1.0030	C	1.0032
X ^z	33.2169	X ^z	52.5869	X ^z	8.0031
X ^z (95)	22.4	X ^z (95)	26.3	X ^z (95)	28.9

W Test					
B	4.89E-03	B	5.36E-03	B	2.63E-03
S ^z	2.94E-05	S ^z	3.38E-05	S ^z	8.41E-06
W	0.8128	W	0.8492	W	0.8201
W (95)	0.8740	W (95)	0.8740	W (95)	0.8740

Reference	
[ANSI]	ANSI N15.15-1974 Assessment of the Assumption of Normality - Table 1 (Appendix 7.10)
W (95)	ANSI N15.15-1974 Assessment of the Assumption of Normality - Table 2 (Appendix 7.10)
X ^z (95)	Statistical Theory with Engineering Applications - Table 5 (Appendix 7.9)

Figure 4.6a

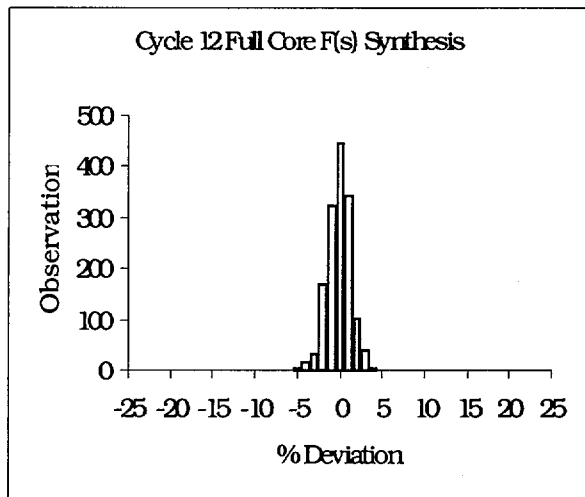


Figure 4.6b

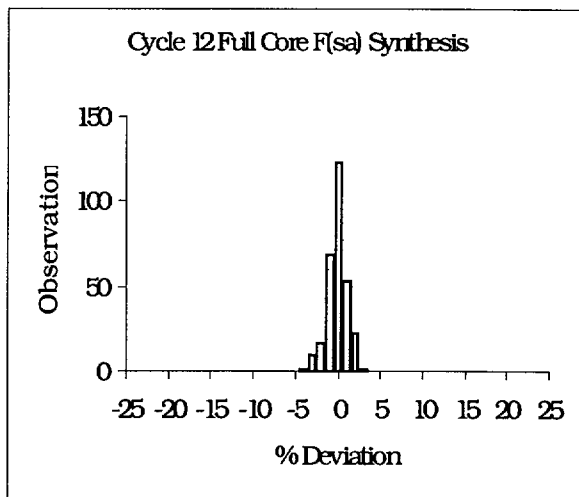


Figure 4.6c

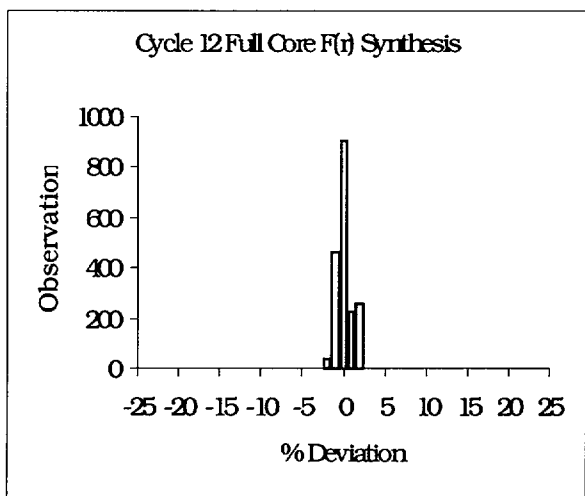


Figure 4.6d

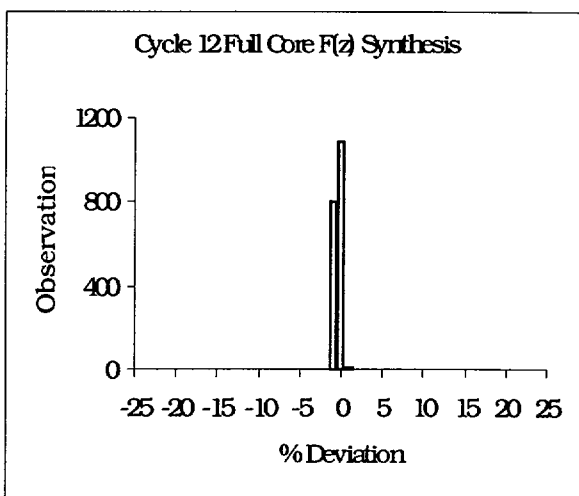


Figure 4.7a

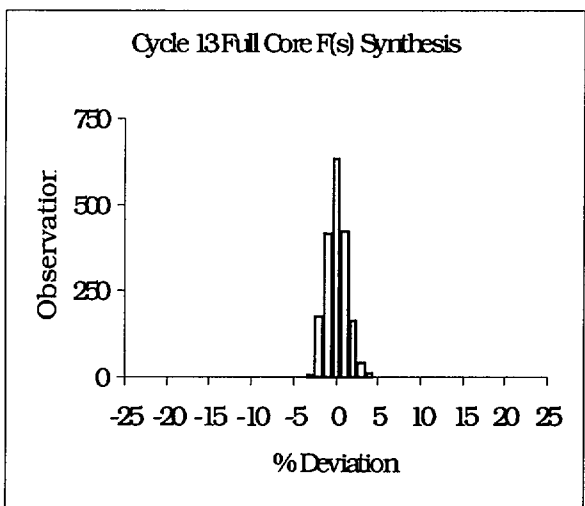


Figure 4.7b

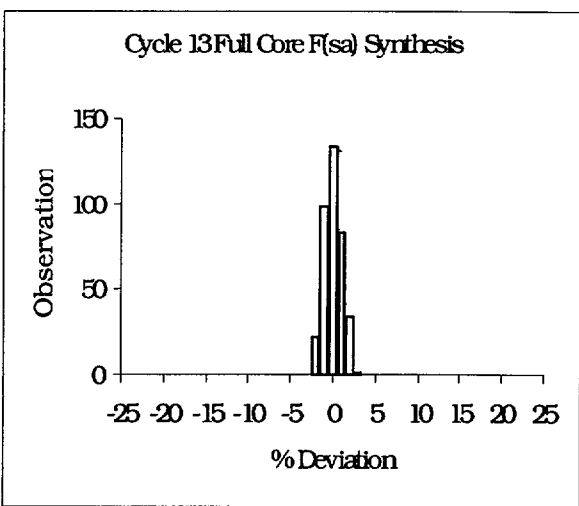


Figure 4.7c

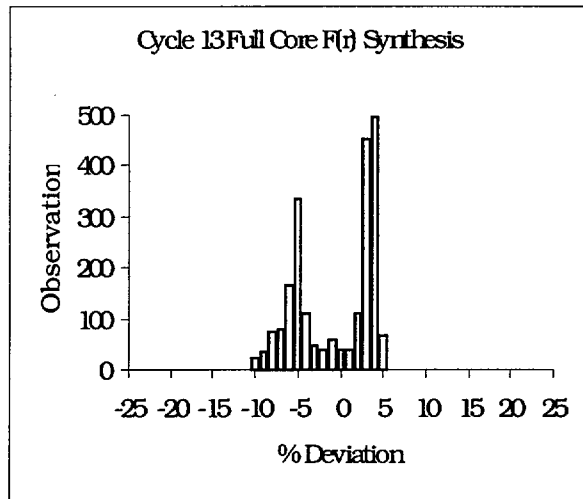


Figure 4.7d

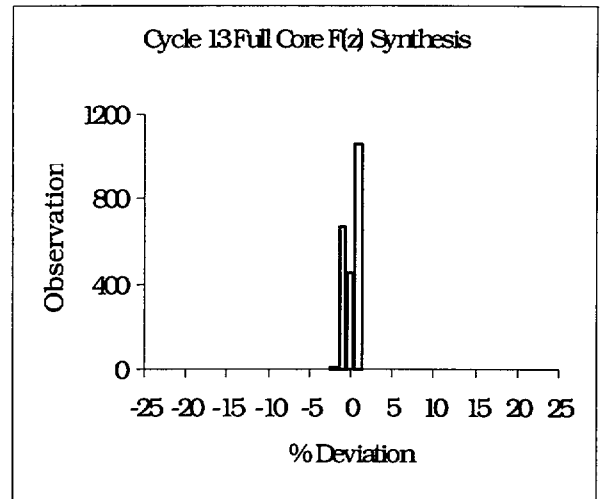


Figure 4.8a

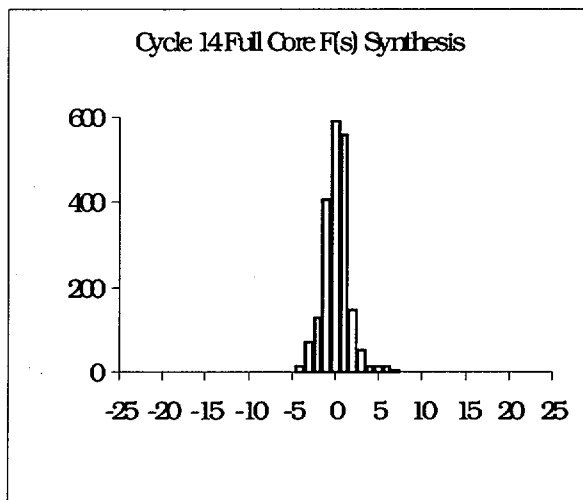


Figure 4.8b

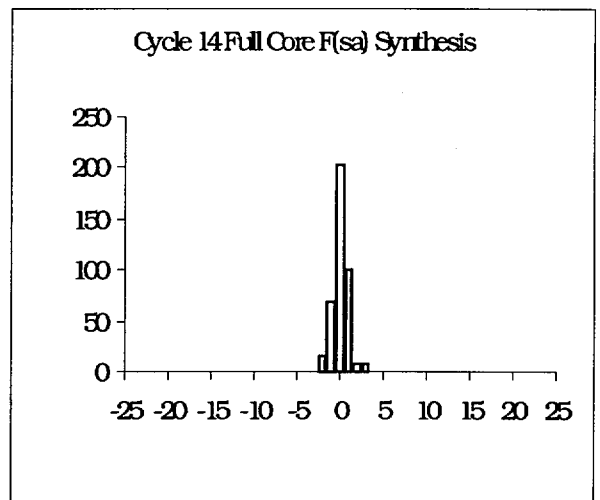


Figure 4.8c

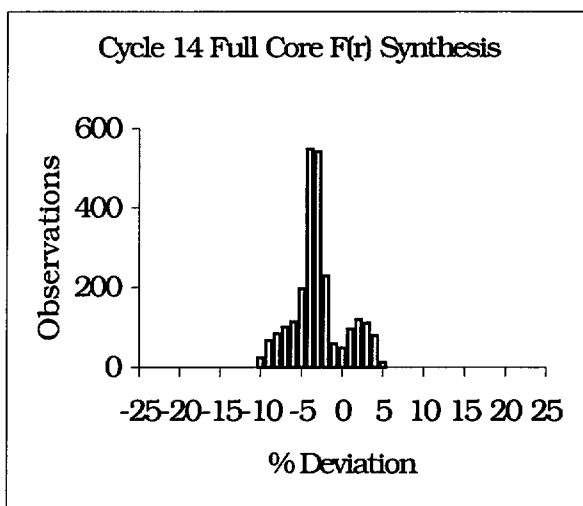
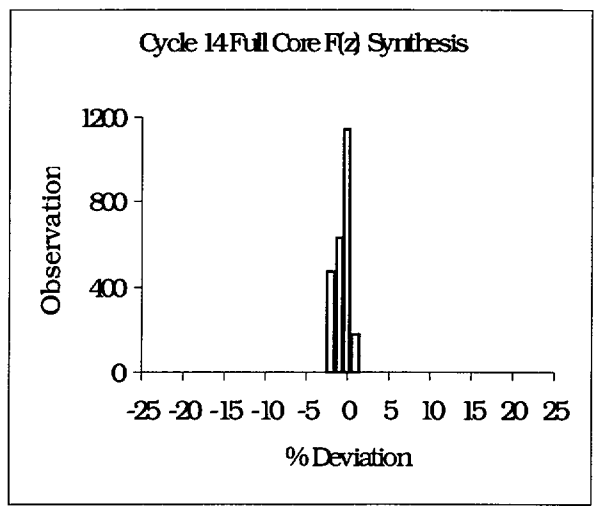


Figure 4.8d



4.5 RESULTS

The fundamental methods used in calculating the coupling coefficients, W-primes, and LPFs have not changed since [SER96]. Overall the changes made to the PIDAL-3 model incorporating CASMO-4 improved the overall comparisons between SIMULATE-3 and PIDAL-3 as expected per [PID992] Appendix 7.3.

The measurement uncertainties also reflect CASMO-4 enhancements over CASMO-3. The CASMO-4 model greatly reduced the component uncertainties. The mean also shifted closer to zero thus allowing for the continued use of a zero bias as assumed in the original uncertainty analysis, with the standard deviations normally distributed about the mean. The degrees of freedom were greatly reduced by limiting the time points to approximately 1000 MWD/MTU to improve the independence of the data and allow for pooling within the cycle. Cycles 12 to 14 were not pooled across the cycles, as were cycles 5 to 7 in the original uncertainty analysis.

Statistical analysis results can be seen in Figures 4.5a-c, and the corresponding histograms in Figures 4.6a-d to 4.8a-d show the standard deviation distributions about the mean. All of the 95/95 uncertainty components analyzed are lower than the original uncertainties for cycles 5 to 7. The degrees of freedom as discussed in Section 4.4.2 were significantly reduced, and PIDAL-3 is still bounded by the original measurement uncertainties.

5.0 CONCLUSION

The final CASMO-4 results produced significant improvements compared to CASMO-3 as expected. The ability of CASMO-4 to model gadolinia pins explicitly and the other changes discussed in [PID992] Appendix 7.3 greatly improved SIMULATE-3's ability to predict pin powers as discussed in [CMS992].

The PIDAL-3 program has been validated per [PID992], and the uncertainty analysis results are bounded by the present Palisades Technical Specification values (TS Table 3.23-3 or Figure 4.5a). This proposed update to the PIDAL SER will not require Technical Specification changes at this time, but the following changes will occur when this submittal is approved and the new Palisades Improved Technical Specifications (ITS) are implemented in the fourth quarter of 2000:

Palisades original TS Table 3.23-3 uncertainty values will be moved from the ITS bases to the COLR. After the ITS is issued it is our intent to remove the additional uncertainties for radial tilts above 2.8%. Sections 4.4.3 and 4.4.4 previously stated that the PIDAL-3 methodology, with the full core SIMULATE-3 model, has the ability to measure radial tilts (e.g. dropped control rods) without any additional penalty to the uncertainties for up to 5% quadrant power tilts.

In addition, it is Palisades intent to reinsert incore detectors starting with cycle 16, we intend to observe an additional penalty to the uncertainties until we obtain enough data to verify the effects of reused incore detectors on the PIDAL-3 uncertainty analysis. No effect is anticipated since ABBCE has shown that the linear depletion law in equation 2.2 holds for rhodium depletion up to a minimum 66% as stated in [ICILE].

The new uncertainties to be listed in the COLR:

	Fresh	Used
$F_{Q,T}$	0.0425	0.0500
$F_{R,T}$	0.0400	0.0475
$F_{R,A}$	0.0375	0.0450

6.0 REFERENCES

- [ANSI] American National Standards Institute Inc., 'Assessment of the Assumption of Normality (Employing Individual Observed Values)', ANSI N15.15-1974, Approved October 3, 1973
- [APS1] APS ANS ARP Paper 'Continuing Advancements in Incore Power Distribution Measurement Methods Using SIMULATE-3 and CECOR 3.0', Knoxville 04/94 ([PID992] App. 7.1).
- [APS2] APS ANS NSE Paper 'Continuing Advancements in Incore Power Distribution Measurement Methods Using SIMULATE-3 and CECOR 3.4', pgs. 57-66, 01/95 ([PID992] App. 7.1).
- [CAS3] 'CASMO-3; A Fuel Assembly Burnup Program, Users Manual', Studsvik/SOA-94/9 Rev. 0.
- [CAS4] 'CASMO-4; A Fuel Assembly Burnup Program, Users Manual', Studsvik/SOA-95/1 Rev. 0.
- [CECOR] 'Calculational Verification of the Combustion Engineering Full Core Instrumentation Analysis System CECOR', W.B. Terney et al, Combustion Engineering Inc, presented at International Conference On World Nuclear Power, Wash D.C., 11/19/76.
- [CLINK] CMS-LINK Users Manual, Studsvik/SOA-9704 Rev. 1.
- [CMS991] EA-CMS-99-01 Rev. 0, 'CMS Model Development for Cycles 1 to 15', 0599.
- [CMS992] EA-CMS-99-02 Rev. 0, 'CMS Calculation of the B&W Critical Experiments'.
- [EXXON] XN-NF-83-01(P), 'Exxon Nuclear Analysis of Power Distribution Measurement Uncertainty for St. Lucie Unit 1', January 1983.
- [GAB906] EA-GAB-90-06 'PIDAL Quadrant Power Tilt Uncertainty', August 1990.
- [ICILE] 'In-core Instrumentation (ICI) Life Extension', Final Report, Task 679, CEOG, March 1995.
- [INCA] INCA Users Manual, Nuclear Power Department, Combustion Engineering Ver. 1.0.
- [ITSB321] Palisades Improved Technical Specifications Bases, B3.2.1.
- [OPPD] CECORLIB 3.3, Omaha Public Power District, EA-FC-94-044 Rev. 0, 1994.
- [OWEN] 'Factors for One-Sided Tolerance Limits for Variable Sampling Plans', D.B. Owen, Sandia Corporation Monograph, SCR-607, March 1963.
- [P3MM] 'The PIDAL-3 Full Core System, Methodology Manual' Rev. 15, 10/1999.
- [P3UA] 'The PIDAL-3 Full Core System, Uncertainty Analysis Manual' Rev. 7, 10/1999.
- [PID3] 'The PIDAL-3 Full Core System, Users Manual' Rev. 8, 10/1999.
- [PID952] EA-PID-95-02 Rev 0, 'PIDAL/PMS Conversion', July 1995.
- [PID961] EA-PID-96-01 Rev 0, 'PIDAL-3 CODE', June 1996.
- [PID991] EA-PID-99-01 Rev. 0, 'PIDAL-3 Code Update with PPC Trending', October 1999.
- [PID992] EA-PID-99-02 Rev. 0, 'PIDAL-3 Model Enhancements using CASMO-4', December 1999.
- [S3MM] 'SIMULATE-3 Methodology Manual', Studsvik/SOA-95/18 Rev. 0.
- [SCE1] SCE ANS Paper 'Correction of Rhodium Detector Signals for Comparison to Design Calculations', 1989 Winter Meeting ([PID992] App. 7.1).
- [SCE2] SCE ANS Paper 'Benchmark Calcs. of Monitoring System Coefficients using C3/S3' ([PID992] App. 7.1).
- [SER92] Docket Number 50-255, 'Palisades Plant; Amendment to Facility Operating License', Amendment No. 144, License No. DPR-20, April 3, 1992.
- [SER97] 'SER by the Office of NRR Related to Revision of PIDAL In-core Monitoring Code, Consumers Power Company, Palisades Plant, Docket No. 50-255', May 6, 1997.
- [SIM3] 'SIMULATE-3 Advanced Three-Dimensional Two-Group Reactor Analysis Code, Users Manual', Studsvik/SOA-95/15 Rev 0.
- [STEA] 'Statistical Theory with Engineering Applications', A. Hald, Wiley & Sons 1952, pg. 290.
- [TS311] Palisades Technical Specifications, Section 3.11.1.
- [TS323] Palisades Technical Specifications, Section 3.23, Table 3.23-3.

7.0 GLOSSARY

95/95	Tolerance Limit - this limit ensures that there is a 95 percent probability that at least 95 percent of the true peaking values will be less than the PIDAL-3 measured/inferred peaking values plus the associated tolerance limit.
ABBCE	ABB Combustion Engineering.
APL	Allowable Power Level. See Palisades Tech Spec 3.11.2.
ARO	All Rods Out. All control rods pulled out of the active fuel region.
BOL / BOC	Beginning of Life / Beginning of Cycle.
CASMO-3	An advanced two-dimensional transport theory infinite lattice fuel assembly burnup code, developed by Studsvik of America, Inc., to generate the fuel cross sections for SIMULATE-3.
CASMO-4	An advanced two-dimensional transport theory infinite lattice fuel assembly burnup code, developed by Studsvik of America, Inc., to generate the fuel cross sections for SIMULATE-3.
CECOR	An incore analysis program developed by ABB Combustion Engineering to determine (measure) the power distribution on a full core basis.
CET	Core Exit Thermocouple at the top of each ICI string.
EOL / EOC	End of Life / End of Cycle.
EXPOSURE CASE	PIDAL-3 calculation where depletion of the core takes place according to PPC determined exposure increment.
HFP	Hot Full Power. Rated Power (2530 MWth).
INCA	An incore analysis program developed by ABB Combustion Engineering to determine (measure) the power distribution on an eighth core basis.
K_s	Incore Sensitivity, usually in amps/nv. Utilized by the PPC to account for rhodium depletion in each detector.
LPF	Local Peaking Factor. Ratio of peak pin in assembly to average pin in assembly.
LHGR	Linear heat generation rate, usually in kw/ft.
Normal	Refers to a statistically "normal" or Gaussian distribution of data.
PIDAL-3	An on-line incore analysis program, developed by Consumers Energy, to determine (measure) the power distribution on a full core basis.
POWER CASE	PIDAL-3 calculation where no depletion of the core takes place.
PPC	Palisades Plant Computer System: Network of DEC workstations used to monitor all plant data points (i.e. G2VXs, Host, PMS Database).
PTB	Pin-to-box factor (Same as LPF).
RE	Reactor Engineering.
RPD	Relative Power Density. Ratio of the average pin power in assembly to the average pin power in the core (Normalized to 1.0).
RPF	Relative Power Fraction. Ratio of the assembly power to the core average assembly power (Normalized to 1.0).
SIMULATE-3	An advanced three-dimensional two-group diffusion theory nodal code, developed by Studsvik of America, Inc., to determine the theoretical power distribution and core characteristics on a full core basis.
SPC	Siemens Power Corporation.
SSF	Self Shielding Factor. Applied to the SIMULATE-3 rhodium reaction rates to account for non-depleting detectors in the CASMO-3 or CASMO-4/SIMULATE-3 model.
T_Q	Quadrant Power Tilt.

APPENDIX A

EXAMPLE PIDAL-3 OUTPUT

PIDAL - PALISADES INCORE DETECTOR ALGORITHM

PIDAL-3

VERSION 4.00
DATE 01/01/99

CYCLE 12

PIDAL-3 FILE TRAIL DATA

P3 INPUT FILE	PIDINP
P3 TSSOR FILE	/nukef/program/cms/CYCLE/IMS/cycle12.sor
P3 RESTART FILE	cycle12.pre
S3 SUMMARY FILE	test.sum
P3 OUTPUT FILE	test.out
P3 ALARM FILE	test.alm
P3 ACCOUNTING FILE	test.acc
P3 TREND FILE	test.tnd
P3 UNCERTAINTY FILE	test.unc

USER COMMENTS CYCLE 12 PIDAL E-01 TO E-18 CASES

PLANT SNAPSHOT DATE 09/15/1995 19:30:03
MATING TO EXPOSURE STEP 2 DATE 09/01/1995 00:06:02

NOTE - CURRENT RESTART FILE NOT UPDATED

PIDAL-3 INPUT PARAMETERS	CORE THERMAL POWER	2462.3 MWT
	CORE PERCENT POWER	97.3 %
	BORON CONCENTRATION	1092.0 PPM
	CORE INLET TEMPERATURE	532.5 F
	PRIMARY COOLANT PRESSURE	2045.7 PSIA
	PRIMARY COOLANT FLOW	141.9 E+06 LBS/HR
	GROUP 4 AVERAGE POSITION	131.1 IN WITHDRAWN
	P3/S3 MAXIMUM DEVIATION	20.0 %
	P3 MINIMUM ICI POWER	0.0001 MWT

CONTROL ROD POSITIONS	A-01	1-21	3-33	1-22	A-02	
	130.1	130.8	131.0	131.2	131.0	
	A-03	4-38	B-13	P-42	B-14	4-39
	131.0	131.0	130.9	130.9	131.1	130.9
	1-23	B-15	2-29	A-05	2-30	B-16
	130.6	131.3	131.3	130.5	130.6	131.1
	3-34	P-43	A-06	3-35	A-07	P-44
	130.8	130.2	131.1	131.2	130.9	131.3
	1-25	B-17	2-31	A-08	2-32	B-18
	131.0	130.3	130.6	131.3	131.1	131.0
	A-09	4-40	B-19	P-45	B-20	4-41
	130.8	131.1	130.9	131.3	130.1	131.3
	A-11	1-27	3-37	1-28	A-12	INDEX NUMBER
	131.6	131.0	131.4	131.0	131.3	IN WITHDRAWN

INCORE INSTRUMENT POSITIONS	TOP OF ACTIVE FUEL	334.800 CM	131.811 IN
	322.736 CM	127.061 IN
	5	282.736 CM	111.313 IN
	255.680 CM	100.661 IN
	4	215.680 CM	84.913 IN
	188.624 CM	74.261 IN
	3	148.624 CM	58.513 IN
	121.568 CM	47.861 IN
	2	81.568 CM	32.113 IN
	54.512 CM	21.461 IN
	1	14.512 CM	5.713 IN
		

BOTTOM OF ACTIVE FUEL

PRI.P3X FMAP - CYCLE 12 1/4 CORE ROTATIONAL LOADING PATTERN

	A	B	D	E	G	H	J	K	M	N	Q	R	T	V	X	Z
1						1 N219 209 0	2 N227 216 0	3 NS07 160 0	4 NS04 160 1	5 N244 216 0	6 M104 209 0					
2				7 M113 209 0	8 N211 216 0	9 O359 216 2	10 P115 216 0	11 O247 216 0	12 P104 216 0	13 O236 216 3	14 O252 216 0	15 N224 216 0	16 M119 209 0			
4				17 N459 216 0	18 P111 216 0	19 O231 216 0	20 N107 216 0	21 P255 216 4	22 N568 216 0	23 P232 216 0	24 O256 216 5	25 P108 216 0	26 N352 216 0			
5		27 M115 209 0	28 N351 216 0	29 O239 216 6	30 O107 216 0	31 P251 216 0	32 O219 216 0	33 O103 216 0	34 P224 216 0	35 N348 216 0	36 P240 216 0	37 O116 216 0	38 O240 216 7	39 N460 216 0	40 M117 209 0	
7		41 N223 216 0	42 P107 216 8	43 O115 216 0	44 P247 216 9	45 N455 216 0	46 P243 216 10	47 N463 216 0	48 O244 216 0	49 O228 216 0	50 N232 216 0	51 P248 216 11	52 O108 216 0	53 P112 216 12	54 N212 216 0	
8	55 M103 209 13	56 O251 216 0	57 O255 216 0	58 P239 216 0	59 N231 216 0	60 N215 216 0	61 O223 216 0	62 P235 216 14	63 N240 216 0	64 P228 216 15	65 N216 216 0	66 N456 216 16	67 P252 216 0	68 O232 216 0	69 O360 216 0	70 N220 209 0
10	71 N243 216 0	72 O235 216 17	73 P231 216 0	74 N347 216 18	75 O227 216 0	76 P227 216 0	77 N103 216 19	78 N235 216 0	79 P220 216 0	80 N104 216 0	81 O224 216 0	82 P244 216 0	83 O220 216 0	84 N108 216 20	85 P116 216 0	86 N228 216 0
11	87 NS03 160 0	88 P103 216 0	89 N567 216 0	90 P223 216 0	91 O243 216 0	92 N239 216 0	93 P219 216 0	94 O111 216 0	95 O112 216 0	96 N236 216 21	97 P236 216 22	98 N464 216 0	99 O104 216 0	100 P256 216 0	101 O248 216 0	102 NS08 160 0
13	103 NS06 160 0	104 O246 216 23	105 P254 216 0	106 O102 216 0	107 N462 216 24	108 P234 216 25	109 N234 216 26	110 O110 216 0	111 O109 216 27	112 P217 216 0	113 N237 216 0	114 O241 216 0	115 P221 216 0	116 N565 216 28	117 P101 216 0	118 NS01 160 0
14	119 N226 216 0	120 P114 216 0	121 N106 216 0	122 O218 216 0	123 P242 216 0	124 O222 216 0	125 N102 216 0	126 P218 216 0	127 N233 216 0	128 N101 216 29	129 P225 216 0	130 O225 216 0	131 N345 216 0	132 P229 216 0	133 O233 216 30	134 N241 216 0
16	135 N218 209 0	136 O358 216 0	137 O230 216 0	138 P250 216 0	139 N454 216 0	140 N214 216 0	141 P226 216 31	142 N238 216 0	143 P233 216 32	144 O221 216 0	145 N213 216 33	146 N229 216 0	147 P237 216 0	148 O253 216 0	149 O249 216 0	150 M101 209 0
17		151 N210 216 34	152 P110 216 0	153 O106 216 0	154 P246 216 35	155 N230 216 0	156 O226 216 0	157 O242 216 0	158 N461 216 0	159 P241 216 0	160 N453 216 0	161 P245 216 36	162 O113 216 0	163 P105 216 0	164 N221 216 0	
19		165 M109 209 0	166 N458 216 0	167 O238 216 0	168 O114 216 37	169 P238 216 38	170 N346 216 0	171 P222 216 0	172 O101 216 39	173 O217 216 0	174 P249 216 0	175 O105 216 0	176 O237 216 40	177 N349 216 0	178 M107 209 41	
20				179 N350 216 42	180 P106 216 0	181 O254 216 0	182 P230 216 0	183 N566 216 0	184 P253 216 0	185 N105 216 0	186 O229 216 0	187 P109 216 0	188 N457 216 0			
22				189 M111 209 0	190 N222 216 0	191 O250 216 0	192 O234 216 43	193 P102 216 0	194 O245 216 0	195 P113 216 0	196 O357 216 44	197 N209 216 0	198 M105 209 0			
23						199 M102 209 0	200 N242 216 0	201 NS02 160 0	202 NS05 160 0	203 N225 216 45	204 N217 209 0					

ASSEMBLY NUMBER
 ASSEMBLY LABEL
 PINS/ASSEMBLY
 ICI (7 & 44 LEVEL INDICATIONS)

PRI.P3X QICI - INCORE INSTRUMENT SIGNALS BY 1/4 CORE ROTATIONAL SYMMETRY

ICI	BOTTOM		LOWER MIDDLE		MIDDLE		UPPER MIDDLE		TOP	
	FLUX (NV)	(MWT)	FLUX (NV)	(MWT)	FLUX (NV)	(MWT)	FLUX (NV)	(MWT)	FLUX (NV)	(MWT)
1	1.298E+13	0.1771	1.756E+13	0.2418	1.856E+13	0.2564	1.862E+13	0.2568	1.320E+13	0.1799
2	2.299E+13	0.8164	3.073E+13	1.0712	3.281E+13	1.1536	3.239E+13	1.1418	2.425E+13	0.8794
3	2.535E+13	0.9004	3.444E+13	1.1941	3.660E+13	1.2824	3.574E+13	1.2570	2.623E+13	0.9549
17	2.593E+13	0.9210	3.492E+13	1.2104	3.661E+13	1.2828	3.557E+13	1.2509	2.597E+13	0.9455
30	2.603E+13	0.9245	3.473E+13	1.2041	3.651E+13	1.2793	3.534E+13	1.2429	2.588E+13	0.9425
43	2.615E+13	0.9290	3.510E+13	1.2170	3.647E+13	1.2779	3.566E+13	1.2541	2.686E+13	0.9780
4	4.551E+13	1.5975	6.286E+13	2.2048	6.576E+13	2.3173	6.278E+13	2.2135	4.635E+13	1.6435
5	4.003E+13	1.4064	5.120E+13	1.7583	5.351E+13	1.8577	5.095E+13	1.7790	3.594E+13	1.3006
6	3.168E+13	1.1206	4.259E+13	1.4696	4.379E+13	1.5273	4.277E+13	1.4973	3.255E+13	1.1826
40	3.221E+13	1.1392	4.309E+13	1.4869	4.457E+13	1.5545	4.296E+13	1.5038	3.239E+13	1.1766
8	4.025E+13	1.4860	5.528E+13	2.0339	5.690E+13	2.1037	5.493E+13	2.0312	4.004E+13	1.4899
9	5.281E+13	1.8614	7.110E+13	2.5015	7.335E+13	2.5939	7.019E+13	2.4828	5.133E+13	1.8273
11	5.442E+13	1.9182	7.008E+13	2.4657	7.369E+13	2.6058	6.905E+13	2.4427	4.891E+13	1.7399
35	5.279E+13	1.8605	7.040E+13	2.4769	7.360E+13	2.6029	7.032E+13	2.4875	5.085E+13	1.8086
36	5.352E+13	1.8863	7.087E+13	2.4933	7.315E+13	2.5870	7.002E+13	2.4769	5.055E+13	1.7995
10	5.104E+13	1.7986	6.869E+13	2.4181	7.204E+13	2.5496	6.970E+13	2.4669	5.127E+13	1.8248
12	4.198E+13	1.5500	5.518E+13	2.0316	5.702E+13	2.1086	5.444E+13	2.0136	3.829E+13	1.4253
13	6.603E+12	0.1528	9.071E+12	0.2031	9.403E+12	0.2126	9.368E+12	0.2129	7.415E+12	0.1772
14	4.847E+13	1.7110	0.000E+00	0.0000	6.581E+13	2.3321	6.438E+13	2.2819	4.795E+13	1.7108
22	5.223E+13	1.8431	6.486E+13	2.2844	6.860E+13	2.4304	6.634E+13	2.3507	4.722E+13	1.6848
25	4.145E+13	1.4631	6.586E+13	2.3199	6.941E+13	2.4589	6.729E+13	2.3842	5.034E+13	1.7958
32	5.108E+13	1.8029	6.615E+13	2.3300	6.847E+13	2.4258	6.632E+13	2.3501	5.020E+13	1.7907
15	4.803E+13	1.6955	6.280E+13	2.2120	6.586E+13	2.3332	6.397E+13	2.2648	4.814E+13	1.7163
31	4.810E+13	1.6981	6.370E+13	2.2434	6.632E+13	2.3494	6.455E+13	2.2852	4.857E+13	1.7317
16	4.148E+13	1.2516	5.542E+13	1.6127	5.838E+13	1.7207	5.639E+13	1.6727	4.353E+13	1.3604
18	4.345E+13	1.3245	5.573E+13	1.6372	5.818E+13	1.7263	5.685E+13	1.6969	4.322E+13	1.3570
19	4.109E+13	1.2585	5.291E+13	1.5672	5.618E+13	1.6838	5.493E+13	1.6549	4.310E+13	1.3628
29	4.122E+13	1.2625	5.283E+13	1.5647	5.555E+13	1.6650	5.470E+13	1.6480	4.241E+13	1.3410
20	3.911E+13	1.1885	5.147E+13	1.5162	0.000E+00	0.0000	5.209E+13	1.5612	3.835E+13	1.2030
21	4.333E+13	1.3105	5.555E+13	1.6207	5.880E+13	1.7330	5.728E+13	1.6940	4.470E+13	1.3877
26	4.388E+13	1.3270	5.553E+13	1.6201	5.888E+13	1.7353	5.732E+13	1.6954	4.432E+13	1.3761
23	2.889E+13	1.0437	3.983E+13	1.4051	4.213E+13	1.5002	3.985E+13	1.4267	2.895E+13	1.0740
24	4.438E+13	1.3348	5.684E+13	1.6503	6.036E+13	1.7719	5.843E+13	1.7276	4.445E+13	1.3813
27	4.968E+13	1.8069	6.426E+13	2.3029	6.775E+13	2.4522	6.543E+13	2.3740	4.994E+13	1.8578
28	3.999E+13	1.1718	5.190E+13	1.4636	5.366E+13	1.5291	5.148E+13	1.4748	3.788E+13	1.1436
33	3.894E+13	1.1975	4.991E+13	1.4882	5.230E+13	1.5743	5.154E+13	1.5535	3.983E+13	1.2522
34	1.494E+13	0.4433	2.053E+13	0.5859	2.267E+13	0.6544	2.167E+13	0.6292	1.621E+13	0.4965
37	4.669E+13	1.6781	6.047E+13	2.1358	6.295E+13	2.2425	5.934E+13	2.1232	4.406E+13	1.6241
38	5.405E+13	1.9023	7.038E+13	2.4739	7.206E+13	2.5456	6.849E+13	2.4223	4.938E+13	1.7572
39	4.747E+13	1.7204	6.128E+13	2.1891	6.359E+13	2.2919	6.132E+13	2.2180	4.539E+13	1.6836
41	6.787E+12	0.1661	8.306E+12	0.1947	9.228E+12	0.2198	8.786E+12	0.2107	6.801E+12	0.1730
42	1.805E+13	0.5411	2.335E+13	0.6729	2.448E+13	0.7147	2.387E+13	0.7012	1.852E+13	0.5741
45	1.132E+13	0.3244	1.570E+13	0.4358	1.616E+13	0.4523	1.621E+13	0.4564	1.196E+13	0.3526

CYCLE 12 E 3 97.3% POWER - DATE/TIME 09/15/1995 19:30:03

PRI.P3X 2DPF - NORMALIZED P3/S3 POWER MAP FOR LEVEL 3

THERE WERE 1 FAILED DETECTORS PRIOR TO SOLUTION FOR THIS LEVEL

RMS DEVIATION FOR THIS MAP = 1.61 %

	A	B	D	E	G	H	J	K	M	N	Q	R	T	V	X	Z
1						0.192	0.279	0.166	0.160	0.237	0.134					
						0.191	0.281	0.169	0.163	0.236	0.133					
						0.601	-0.569	-1.364	-2.031	0.517	0.808					
2				0.129	0.378	0.720	1.108	0.878	1.110	0.800	0.651	0.365	0.128			
				0.129	0.378	0.712	1.115	0.891	1.118	0.793	0.645	0.362	0.127			
				-0.183	0.199	1.054	-0.653	-1.495	-0.717	0.978	0.914	0.835	0.866			
4				0.444	1.276	1.144	0.997	1.446	0.966	1.382	1.160	1.276	0.443			
				0.446	1.279	1.147	1.009	1.486	0.978	1.381	1.149	1.266	0.439			
				-0.508	-0.245	-0.271	-1.169	-2.752	-1.196	0.067	0.908	0.792	0.892			
5		0.130	0.447	0.953	1.401	1.635	1.350	1.416	1.560	1.077	1.580	1.378	0.972	0.456	0.132	
		0.127	0.439	0.962	1.405	1.641	1.359	1.439	1.579	1.081	1.575	1.369	0.962	0.446	0.129	
		2.252	1.737	-0.903	-0.261	-0.327	-0.656	-1.625	-1.213	-0.383	0.325	0.650	1.028	2.068	2.061	
7		0.373	1.313	1.382	1.619	1.083	1.591	1.077	1.257	1.238	1.071	1.626	1.421	1.316	0.385	
		0.362	1.266	1.369	1.616	1.083	1.588	1.098	1.275	1.247	1.071	1.616	1.405	1.279	0.378	
		2.870	3.602	0.946	0.173	-0.063	0.189	-1.925	-1.472	-0.745	-0.012	0.629	1.103	2.837	2.051	
8	0.133	0.655	1.168	1.586	1.073	1.015	1.233	1.456	1.031	1.456	1.013	1.074	1.645	1.158	0.717	0.192
	0.133	0.645	1.149	1.575	1.071	1.020	1.252	1.527	1.054	1.470	1.020	1.083	1.641	1.147	0.712	0.191
	-0.182	1.524	1.644	0.647	0.167	-0.410	-1.494	-4.918	-2.263	-0.923	-0.672	-0.853	0.229	0.917	0.607	0.394
10	0.238	0.801	1.395	1.078	1.247	1.467	1.051	1.073	1.547	1.042	1.242	1.577	1.353	1.006	1.113	0.280
	0.236	0.793	1.381	1.081	1.247	1.470	1.055	1.096	1.573	1.055	1.252	1.588	1.359	1.009	1.115	0.281
	1.098	1.006	0.991	-0.341	0.020	-0.178	-0.346	-2.143	-1.670	-1.192	-0.791	-0.718	-0.417	-0.251	-0.178	-0.152
11	0.168	1.147	0.994	1.592	1.281	1.054	1.562	1.525	1.524	1.082	1.517	1.088	1.425	1.470	0.884	0.168
	0.163	1.118	0.978	1.579	1.275	1.054	1.573	1.544	1.544	1.096	1.527	1.098	1.439	1.486	0.891	0.169
	2.551	2.573	1.657	0.813	0.428	-0.021	-0.750	-1.214	-1.263	-1.332	-0.671	-0.874	-0.948	-1.072	-0.741	-0.605
13	0.176	0.936	1.524	1.460	1.106	1.535	1.083	1.529	1.531	1.555	1.041	1.260	1.558	0.954	1.108	0.162
	0.169	0.891	1.486	1.439	1.098	1.527	1.096	1.544	1.544	1.573	1.054	1.275	1.579	0.978	1.118	0.163
	4.371	4.890	2.457	1.429	0.763	0.494	-1.197	-0.988	-0.850	-1.188	-1.244	-1.231	-1.345	-2.427	-0.888	-0.644
14	0.292	1.157	1.035	1.380	1.603	1.257	1.050	1.561	1.086	1.039	1.442	1.230	1.070	1.370	0.799	0.237
	0.281	1.115	1.009	1.359	1.588	1.252	1.055	1.573	1.096	1.055	1.470	1.247	1.081	1.381	0.793	0.236
	3.749	3.659	2.476	1.536	0.926	0.412	-0.428	-0.758	-0.945	-1.481	-1.919	-1.392	-1.042	-0.841	0.738	0.470
16	0.198	0.740	1.176	1.668	1.093	1.023	1.466	1.048	1.514	1.232	0.983	1.058	1.565	1.144	0.646	0.133
	0.191	0.712	1.147	1.641	1.083	1.020	1.470	1.054	1.527	1.252	1.020	1.071	1.575	1.149	0.645	0.133
	3.726	3.717	2.439	1.633	0.913	0.345	-0.228	-0.561	-0.864	-1.589	-3.756	-1.217	-0.643	-0.431	0.131	0.222
17		0.408	1.314	1.428	1.625	1.076	1.247	1.271	1.090	1.573	1.072	1.615	1.368	1.266	0.364	
		0.378	1.279	1.405	1.616	1.071	1.247	1.275	1.098	1.588	1.083	1.616	1.369	1.266	0.362	
		7.556	2.713	1.616	0.517	0.469	0.012	-0.340	-0.725	-1.004	-1.072	-0.096	-0.063	-0.013	0.530	
19		0.136	0.458	0.981	1.400	1.589	1.084	1.576	1.431	1.350	1.633	1.404	0.970	0.443	0.137	
		0.129	0.446	0.962	1.369	1.575	1.081	1.579	1.439	1.359	1.641	1.405	0.962	0.439	0.127	
		4.895	2.521	1.935	2.193	0.858	0.297	-0.205	-0.613	-0.641	-0.488	-0.043	0.862	0.775	7.422	
20				0.446	1.286	1.160	1.388	0.978	1.482	1.005	1.144	1.278	0.448			
				0.439	1.266	1.149	1.381	0.978	1.486	1.009	1.147	1.279	0.446			
				1.547	1.589	0.948	0.481	0.011	-0.309	-0.362	-0.307	-0.094	0.307			
22				0.129	0.367	0.651	0.798	1.119	0.890	1.113	0.711	0.377	0.129			
				0.127	0.362	0.645	0.793	1.117	0.891	1.115	0.712	0.378	0.129			
				1.464	1.364	0.898	0.625	0.157	-0.112	-0.151	-0.197	-0.116	0.114			
23						0.134	0.237	0.164	0.169	0.282	0.191					PIDAL-3
						0.133	0.236	0.163	0.169	0.281	0.191					SIMULATE-3
						0.815	0.587	0.215	0.078	0.598	0.029					(P3-S3)/P3*100%

RMS DEVIATION FOR THIS MAP = 1.55 %

	A	B	D	E	G	H	J	K	M	N	Q	R	T	V	X	Z
1						0.194	0.279	0.163	0.158	0.238	0.135					
						0.192	0.280	0.165	0.159	0.235	0.133					
						1.249	-0.251	-1.125	-0.732	1.006	1.036					
2				0.132	0.383	0.720	1.088	0.866	1.086	0.795	0.648	0.368	0.130			
				0.131	0.380	0.707	1.094	0.879	1.093	0.785	0.641	0.365	0.129			
				0.766	0.848	1.779	-0.541	-1.463	-0.684	1.283	1.019	0.665	0.643			
4				0.453	1.261	1.140	1.001	1.419	0.968	1.362	1.153	1.254	0.447			
				0.450	1.260	1.140	1.012	1.465	0.981	1.365	1.142	1.249	0.444			
				0.483	0.102	-0.001	-1.096	-3.229	-1.257	-0.197	0.877	0.339	0.530			
5		0.133	0.457	0.967	1.399	1.614	1.342	1.414	1.544	1.089	1.559	1.367	0.966	0.460	0.134	
		0.129	0.444	0.960	1.398	1.622	1.353	1.439	1.568	1.095	1.564	1.368	0.960	0.450	0.131	
		3.126	2.705	0.657	0.055	-0.475	-0.788	-1.758	-1.539	-0.570	-0.307	-0.087	0.538	2.008	2.185	
7		0.379	1.300	1.388	1.603	1.096	1.574	1.095	1.265	1.243	1.082	1.590	1.405	1.298	0.389	
		0.365	1.249	1.368	1.606	1.098	1.582	1.115	1.283	1.255	1.089	1.606	1.398	1.260	0.380	
		3.464	3.921	1.416	-0.135	-0.183	-0.497	-1.800	-1.464	-0.966	-0.590	-0.975	0.527	2.975	2.234	
8	0.136	0.656	1.168	1.579	1.094	1.033	1.246	1.472	1.057	1.454	1.026	1.085	1.617	1.149	0.712	0.193
	0.133	0.641	1.142	1.564	1.089	1.036	1.263	1.532	1.079	1.474	1.036	1.098	1.622	1.140	0.707	0.192
	2.314	2.247	2.151	0.951	0.457	-0.313	-1.386	-4.070	-2.036	-1.359	-0.990	-1.169	-0.287	0.854	0.663	0.464
10	0.240	0.798	1.383	1.103	1.259	1.467	1.072	1.099	1.551	1.064	1.248	1.563	1.345	1.009	1.092	0.280
	0.235	0.785	1.365	1.095	1.255	1.474	1.079	1.121	1.582	1.079	1.263	1.582	1.353	1.012	1.094	0.280
	1.918	1.671	1.305	0.679	0.318	-0.456	-0.676	-1.981	-1.998	-1.402	-1.191	-1.220	-0.587	-0.328	-0.204	-0.053
11	0.163	1.120	0.998	1.580	1.290	1.078	1.562	1.539	1.537	1.104	1.508	1.103	1.426	1.450	0.875	0.164
	0.159	1.093	0.981	1.568	1.283	1.079	1.582	1.562	1.562	1.121	1.532	1.115	1.438	1.465	0.879	0.165
	2.512	2.427	1.745	0.770	0.491	-0.123	-1.249	-1.485	-1.641	-1.581	-1.590	-1.087	-0.889	-1.042	-0.444	-0.351
13	0.171	0.917	1.493	1.456	1.121	1.531	1.105	1.540	1.537	1.555	1.064	1.269	1.549	0.966	1.089	0.159
	0.165	0.879	1.465	1.438	1.115	1.532	1.121	1.562	1.562	1.582	1.079	1.283	1.568	0.981	1.093	0.159
	3.735	4.196	1.886	1.201	0.485	-0.076	-1.473	-1.384	-1.637	-1.743	-1.392	-1.126	-1.248	-1.472	-0.394	-0.145
14	0.288	1.126	1.032	1.368	1.587	1.265	1.073	1.564	1.110	1.066	1.446	1.241	1.088	1.358	0.795	0.238
	0.280	1.094	1.012	1.353	1.582	1.263	1.079	1.582	1.121	1.079	1.474	1.255	1.095	1.365	0.785	0.235
	3.035	2.846	1.984	1.108	0.320	0.123	-0.592	-1.130	-0.983	-1.285	-1.928	-1.129	-0.668	-0.526	1.358	1.109
16	0.197	0.727	1.159	1.635	1.102	1.038	1.467	1.075	1.522	1.249	1.006	1.080	1.555	1.142	0.645	0.134
	0.192	0.707	1.140	1.622	1.098	1.036	1.474	1.079	1.532	1.263	1.036	1.089	1.564	1.142	0.641	0.133
	2.847	2.756	1.721	0.822	0.406	0.184	-0.506	-0.354	-0.617	-1.121	-2.953	-0.864	-0.548	-0.034	0.637	0.789
17		0.400	1.282	1.411	1.599	1.094	1.258	1.284	1.113	1.570	1.090	1.600	1.371	1.252	0.369	
		0.380	1.260	1.398	1.606	1.089	1.255	1.283	1.115	1.582	1.098	1.606	1.368	1.249	0.365	
		5.005	1.736	0.928	-0.401	0.456	0.220	0.065	-0.209	-0.768	-0.724	-0.345	0.213	0.246	0.863	
19		0.136	0.459	0.977	1.395	1.580	1.104	1.570	1.438	1.351	1.617	1.402	0.976	0.450	0.137	
		0.131	0.450	0.960	1.368	1.564	1.095	1.568	1.439	1.353	1.622	1.398	0.960	0.444	0.129	
		3.443	1.907	1.700	1.961	1.005	0.803	0.130	-0.011	-0.107	-0.281	0.268	1.586	1.254	5.883	
20				0.456	1.272	1.160	1.380	0.988	1.468	1.016	1.142	1.264	0.455			
				0.444	1.249	1.142	1.365	0.981	1.465	1.012	1.140	1.260	0.450			
				2.600	1.799	1.496	1.069	0.800	0.178	0.366	0.254	0.317	0.965			
22				0.132	0.373	0.654	0.804	1.106	0.886	1.102	0.712	0.382	0.133			
				0.129	0.365	0.641	0.785	1.093	0.879	1.094	0.707	0.380	0.131			
				2.403	2.004	1.943	2.426	1.178	0.800	0.676	0.590	0.551	0.875			
23						0.136	0.241	0.161	0.167	0.288	0.194					
						0.133	0.235	0.159	0.165	0.280	0.192					
						2.069	2.283	1.363	1.286	2.843	1.253					

PIDAL-3
SIMULATE-3
(P3-S3)/P3*100x

PRI.P3X DRPF - P3 VS S3 DETECTOR POWERS

ICI	LEVEL 1			LEVEL 2			LEVEL 3			LEVEL 4			LEVEL 5			2 RPF		
	P-3	S-3	DEV	P-3	S-3	DEV	P-3	S-3	DEV	P-3	S-3	DEV	P-3	S-3	DEV	P-3	S-3	DEV
1	0.151	0.149	1.2	0.159	0.161	-1.0	0.160	0.163	-2.0	0.166	0.165	0.6	0.153	0.156	-2.1	0.158	0.159	-0.7
2	0.695	0.691	0.6	0.705	0.704	0.1	0.720	0.712	1.1	0.737	0.716	2.8	0.745	0.715	4.1	0.720	0.707	1.8
3	0.767	0.764	0.4	0.786	0.782	0.4	0.800	0.793	1.0	0.811	0.797	1.7	0.809	0.785	3.0	0.795	0.785	1.3
4	1.361	1.452	-6.7*	1.451	1.502	-3.5	1.446	1.486	-2.8	1.428	1.465	-2.6	1.393	1.388	0.3	1.419	1.465	-3.2
5	1.198	1.137	5.1*	1.157	1.147	0.9	1.160	1.149	0.9	1.148	1.148	0.0	1.102	1.132	-2.7	1.153	1.142	0.9
6	0.954	0.958	-0.3	0.967	0.958	0.9	0.953	0.962	-0.9	0.966	0.964	0.2	1.002	0.969	3.3	0.967	0.960	0.7
7	0.983	0.958	0.0	0.962	0.958	0.0	0.972	0.962	0.0	0.965	0.964	0.0	0.949	0.969	0.0	0.966	0.960	0.5
8	1.266	1.239	2.1	1.338	1.278	4.5	1.313	1.266	3.6	1.310	1.255	4.3	1.263	1.199	5.1*	1.300	1.249	3.9
9	1.586	1.614	-1.8	1.646	1.640	0.4	1.619	1.616	0.2	1.602	1.594	0.5	1.549	1.539	0.6	1.603	1.606	-0.1
10	1.532	1.581	-3.2	1.591	1.601	-0.6	1.591	1.588	0.2	1.591	1.579	0.8	1.547	1.538	0.6	1.574	1.582	-0.5
11	1.634	1.614	1.2	1.622	1.640	-1.1	1.626	1.616	0.6	1.576	1.594	-1.2	1.475	1.539	-4.4	1.590	1.606	-1.0
12	1.320	1.249	5.4*	1.337	1.292	3.3	1.316	1.279	2.8	1.299	1.264	2.7	1.208	1.203	0.4	1.298	1.260	3.0
13	0.130	0.128	1.7	0.134	0.129	3.6	0.133	0.133	-0.2	0.137	0.136	1.0	0.150	0.142	5.5*	0.136	0.133	2.3
14	1.457	1.537	-5.4*	1.516	1.534	0.0	1.456	1.527	-4.9	1.472	1.530	-3.9	1.450	1.522	-5.0	1.472	1.532	-4.1
15	1.444	1.476	-2.2	1.455	1.474	-1.3	1.456	1.470	-0.9	1.461	1.474	-0.9	1.455	1.470	-1.1	1.454	1.474	-1.4
16	1.066	1.106	-3.8	1.061	1.075	-1.3	1.074	1.083	-0.9	1.079	1.092	-1.2	1.153	1.143	0.8	1.085	1.098	-1.2
17	0.785	0.764	2.6	0.796	0.782	1.7	0.801	0.793	1.0	0.807	0.797	1.2	0.801	0.785	2.0	0.798	0.785	1.7
18	1.128	1.108	1.8	1.077	1.074	0.3	1.078	1.081	-0.3	1.095	1.090	0.4	1.150	1.135	1.3	1.103	1.095	0.7
19	1.072	1.094	-2.0	1.031	1.042	-1.0	1.051	1.055	-0.3	1.067	1.075	-0.7	1.155	1.156	-0.1	1.072	1.079	-0.7
20	1.012	1.010	0.3	0.997	1.002	-0.4	1.006	1.009	0.0	1.007	1.013	-0.5	1.020	1.032	-1.2	1.009	1.012	-0.3
21	1.116	1.145	-2.6	1.066	1.089	-2.1	1.082	1.096	-1.3	1.093	1.111	-1.7	1.176	1.188	-1.0	1.104	1.121	-1.6
22	1.570	1.537	2.1	1.503	1.534	-2.1	1.517	1.527	-0.7	1.516	1.530	-0.9	1.428	1.522	-6.6*	1.508	1.532	-1.6
23	0.889	0.858	3.5	0.924	0.884	4.3	0.936	0.891	4.9	0.920	0.891	3.2	0.910	0.866	4.9	0.917	0.879	4.2
24	1.137	1.125	1.1	1.086	1.086	0.0	1.106	1.098	0.8	1.114	1.112	0.2	1.171	1.172	-0.1	1.121	1.115	0.5
25	1.531	1.537	0.0	1.526	1.534	-0.5	1.535	1.527	0.5	1.538	1.530	0.5	1.522	1.522	0.0	1.531	1.532	-0.1
26	1.130	1.145	-1.3	1.066	1.089	-2.1	1.083	1.096	-1.2	1.094	1.111	-1.6	1.166	1.188	-1.9	1.105	1.121	-1.5
27	1.539	1.610	-4.6	1.515	1.555	-2.6	1.531	1.544	-0.9	1.531	1.540	-0.6	1.575	1.582	-0.5	1.537	1.562	-1.6
28	0.998	0.982	1.6	0.963	0.973	-1.0	0.954	0.978	-2.4	0.951	0.977	-2.7	0.969	0.994	-2.5	0.966	0.981	-1.5
29	1.075	1.094	-1.7	1.029	1.042	-1.2	1.039	1.055	-1.5	1.063	1.075	-1.1	1.137	1.156	-1.7	1.066	1.079	-1.3
30	0.788	0.764	3.0	0.792	0.782	1.2	0.799	0.793	0.7	0.802	0.797	0.6	0.799	0.785	1.7	0.795	0.785	1.4
31	1.446	1.476	-2.0	1.476	1.474	0.1	1.466	1.470	-0.2	1.474	1.474	0.0	1.468	1.470	-0.2	1.467	1.474	-0.5
32	1.536	1.537	-0.1	1.533	1.534	-0.1	1.514	1.527	-0.9	1.516	1.530	-0.9	1.518	1.522	-0.3	1.522	1.532	-0.6
33	1.020	1.047	-2.6	0.979	1.010	-3.1	0.983	1.020	-3.8	1.002	1.032	-3.0	1.061	1.091	-2.8	1.006	1.036	-3.0
34	0.378	0.373	1.1	0.385	0.370	3.9	0.408	0.378	7.6*	0.406	0.383	5.5*	0.421	0.400	4.9	0.400	0.380	5.0*
35	1.585	1.614	-1.8	1.630	1.640	-0.6	1.625	1.616	0.5	1.605	1.594	0.6	1.533	1.539	-0.4	1.599	1.606	-0.4
36	1.607	1.614	-0.4	1.640	1.640	0.0	1.615	1.616	-0.1	1.598	1.594	0.2	1.525	1.539	-0.9	1.600	1.606	-0.3
37	1.429	1.384	3.2	1.405	1.380	1.8	1.400	1.369	2.2	1.370	1.358	0.9	1.376	1.350	2.0	1.395	1.368	2.0
38	1.620	1.568	3.2	1.628	1.596	1.9	1.589	1.575	0.9	1.563	1.557	0.4	1.489	1.498	-0.6	1.580	1.564	1.0
39	1.465	1.452	0.9	1.440	1.445	-0.4	1.431	1.439	-0.6	1.431	1.430	0.0	1.427	1.425	0.1	1.438	1.439	0.0
40	0.970	0.958	1.3	0.978	0.958	2.1	0.970	0.962	0.9	0.970	0.964	0.6	0.997	0.969	2.8	0.976	0.960	1.6
41	0.141	0.127	10.5*	0.128	0.123	3.8	0.137	0.127	7.4*	0.136	0.131	3.9	0.147	0.142	3.1	0.137	0.129	5.9*
42	0.461	0.439	4.7	0.443	0.431	2.7	0.446	0.439	1.5	0.452	0.448	1.0	0.487	0.472	2.9	0.456	0.444	2.6
43	0.791	0.764	3.4	0.801	0.782	2.3	0.798	0.793	0.6	0.809	0.797	1.5	0.829	0.785	5.3*	0.804	0.785	2.4
44	0.697	0.691	0.0	0.709	0.704	0.0	0.711	0.712	0.0	0.720	0.716	0.0	0.721	0.715	0.0	0.712	0.707	0.6
45	0.276	0.270	2.2	0.287	0.275	4.0	0.282	0.281	0.6	0.294	0.284	3.5	0.299	0.288	3.6	0.288	0.280	2.8

DEVIATION STATISTICS

SUM	91.29
AVERAGE	0.43
SUM OF THE SQUARES	1380.68
RMS	2.55
ICI COUNT	212.0

NOTE: (*) PERCENT DEVIATION > 5%

CYCLE 12 E 3 97.3% POWER · DATE/TIME 09/15/1995 19:30:03

PRI.P3X 3DDV · DISTRIBUTION OF DEVIATIONS BETWEEN MEASURED AND PREDICTED DETECTOR POWERS

OUTLYING DATA PLOTTED AT -25 AND +25, RESPECTIVELY

N = 212.0 MEAN = 0.4 ST. DEV. = 2.5 SKEWNESS = 0.4 PEAKEDNESS = 4.2

```
0 -25
0 -24
0 -23
0 -22
0 -21
0 -20
0 -19
0 -18
0 -17
0 -16
0 -15
0 -14
0 -13
0 -12
0 -11
0 -10
0 -9
0 -8
2 -7 **
0 -6
4 -5 ****
5 -4 *****
12 -3 *****
16 -2 *****
35 -1 *****
42 0 *****
37 1 *****
17 2 *****
16 3 *****
13 4 *****
9 5 *****
1 6 *
1 7 *
1 8 *
0 9
0 10
1 11 *
0 12
0 13
0 14
0 15
0 16
0 17
0 18
0 19
0 20
0 21
0 22
0 23
0 24
0 25
```

CYCLE 12 E 3 97.3% POWER - DATE/TIME 09/15/1995 19:30:03

PRI.P3X FCAL - ICI POWER OF 2370.2 MWT ADJUSTED TO MATCH CALORIMETRIC POWER OF 2462.3 MWT (RATIO IS 0.963)

PRI.P3X 3QPT - QUADRANT POWER TILTS FOR EACH AXIAL ICI LEVEL BASED ON TWO-WAY SYMMETRIC ICI SETS

LEVEL	QUADRANT 1	QUADRANT 2	QUADRANT 3	QUADRANT 4
5	0.9824	0.9981	1.0162	1.0033
4	0.9993	0.9934	1.0083	0.9989
3	1.0040	0.9898	1.0067	0.9995
2	0.9906	1.0040	1.0020	1.0034
1	1.0069	0.9877	1.0008	1.0045
AVERAGE	0.9966	0.9946	1.0068	1.0019

THE FOLLOWING ROTATIONAL SYMMETRIC INCORE DETECTOR SETS WERE AVAILABLE FOR TILT CALCULATIONS

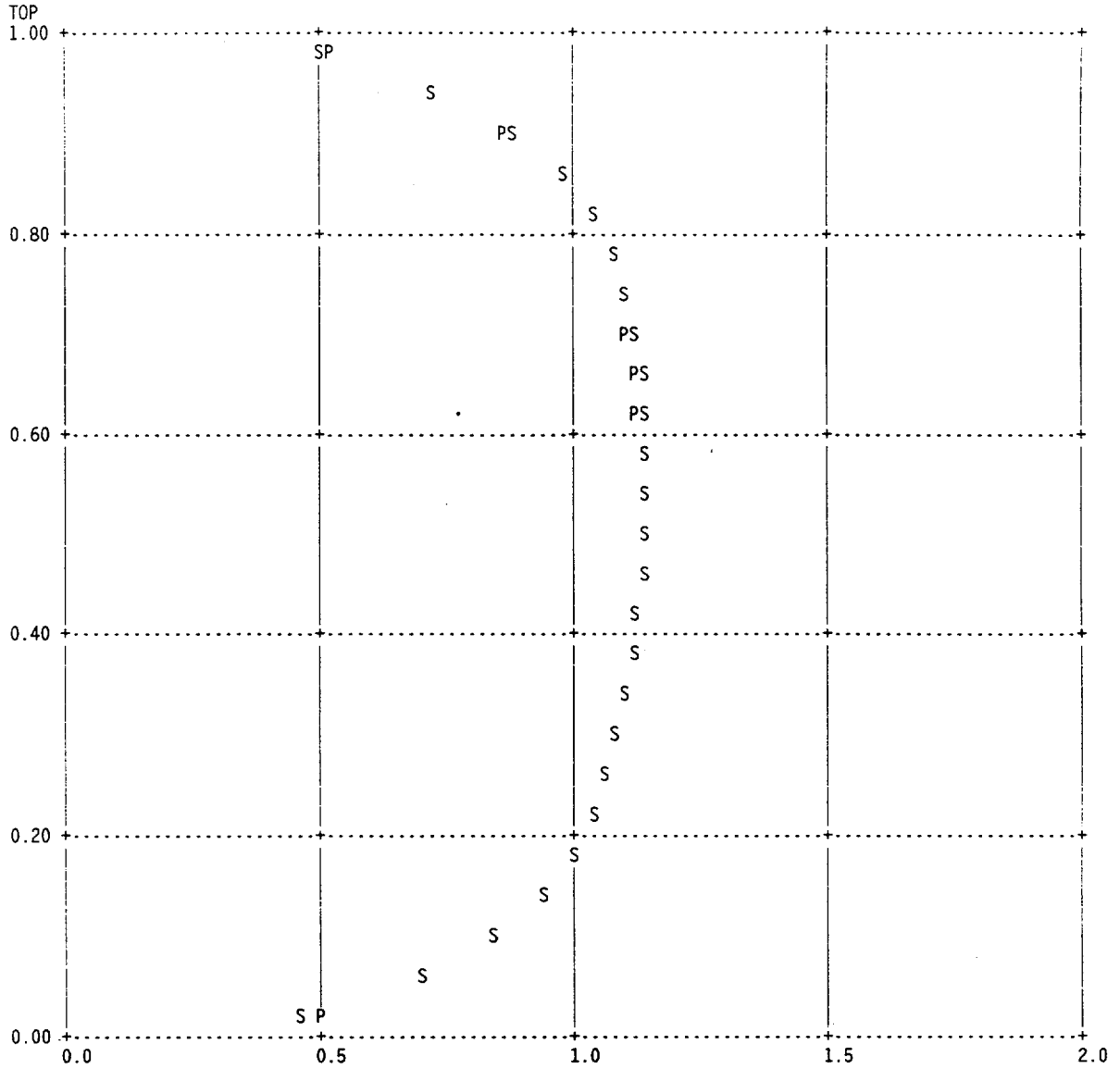
QUADRANT COMBINATIONS	POSSIBLE SYMMETRIC SETS					OPERABLE SETS BY LEVEL				
	1	2	3	4	5	1	2	3	4	5
1-2	22/14	11/ 9	3/17			3.	2.	3.	3.	3.
1-3	22/25	11/35	3/43	21/26	15/31	4.	5.	5.	5.	5.
1-4	22/32	11/36	3/30			3.	3.	3.	3.	3.
2-3	14/25	9/35	17/43			2.	2.	3.	3.	3.
2-4	14/32	9/36	17/30	19/29	6/40	5.	4.	5.	5.	5.
3-4	25/32	35/36	43/30			2.	3.	3.	3.	3.

QUADRANT POWER TILTS BASED ON INTEGRAL QUADRANT POWERS

	QUADRANT 1	QUADRANT 2	QUADRANT 3	QUADRANT 4
	0.9950	0.9999	1.0089	0.9962
QUADRANT TILT SUMMARY NI/CHANNEL	QUADRANT 1 5/A	QUADRANT 2 8/D	QUADRANT 3 6/B	QUADRANT 4 7/C
INCORE POWER FRACTION	0.9966	0.9946	1.0068	1.0019
UPPER LEVEL EXCORES	50.2441	49.8778	50.1526	50.9767
LOWER LEVEL EXCORES	50.7936	50.7936	51.6788	50.9157
NORMALIZED UPPER LEVEL EXCORES	0.9986	0.9914	0.9968	1.0132
NORMALIZED LOWER LEVEL EXCORES	0.9951	0.9951	1.0124	0.9975
NORMALIZED TOTAL EXCORES	0.9968	0.9932	1.0047	1.0053
EXC - INC QUADRANT POWERS	0.0002	0.0014	0.0021	0.0034
MAXIMUM EXC/INC DEVIATION				0.34 %
MAXIMUM INCORE QUADRANT TILT				0.68 %
MAXIMUM EXCORE QUADRANT TILT				0.53 %

THE TILT CALCULATIONS WERE PERFORMED USING THE SYMMETRIC INCORE DETECTOR TILT FORMULATION

PRI.P3X ZRPF - NORMALIZED CORE AVERAGE AXIAL POWER DISTRIBUTION (P = PIDAL-3 AND S = SIMULATE-3)



DATA LISTED FROM NODE 25 TO NODE 1

P3 -	0.534	0.728	0.878	0.983	1.050
	1.087	1.107	1.118	1.128	1.139
	1.149	1.155	1.156	1.150	1.138
	1.123	1.108	1.094	1.079	1.057
	1.018	0.952	0.850	0.704	0.516
S3 -	0.512	0.726	0.888	0.989	1.051
	1.091	1.118	1.135	1.147	1.154
	1.158	1.158	1.155	1.149	1.140
	1.128	1.112	1.094	1.071	1.042
	1.003	0.946	0.856	0.706	0.475

CYCLE 12 E 3 97.3% POWER - DATE/TIME 09/15/1995 19:30:03

PRI.P3X TSPF - PEAKING FACTORS FOR VERIFICATION OF TECHNICAL SPECIFICATION COMPLIANCE

PRI.P3X BFRA - ASSEMBLY RADIAL PEAKING FACTORS BY FUEL TYPE

ALLOWED ASSEMBLY RADIAL PEAKING FACTOR = $1.760 \cdot (1.0 + 0.3 \cdot (1.0 - 2462.3 / 2530.0)) / 1.0401 = 1.706$
 MEASURED ASSEMBLY RADIAL PEAKING FACTOR = 1.635
 LIMITING ASSEMBLY RADIAL PEAKING FACTOR RATIO = 1.043 (A/M) IN ASSEMBLY 138

FUEL TYPE	BUNDLE	ASSEMBLY MWT	TS HFP FRA	ALLOWED FRA	MEASURED FRA	ALLOWED/MEASURED
P1	42	15.70	1.76	1.71	1.300	1.312
P2	138	19.74	1.76	1.71	1.635	1.043
O1	110	18.59	1.76	1.71	1.540	1.107
O2	122	16.51	1.76	1.71	1.368	1.247
O3	136	8.78	1.76	1.71	0.727	2.345
N1	125	12.95	1.66	1.61	1.073	1.499
N2	127	13.40	1.66	1.61	1.110	1.449
N3	170	13.32	1.66	1.61	1.104	1.457
N4	107	13.52	1.66	1.61	1.121	1.436
N5	89	12.05	1.66	1.61	0.998	1.612
NS	103	2.07	1.66	1.61	0.171	9.395
NX	135	2.38	1.66	1.61	0.197	8.153
M1	178	1.66	1.57	1.52	0.137	11.081

PRI.P3X BFRT - TOTAL RADIAL PEAKING FACTORS BY FUEL TYPE

ALLOWED TOTAL RADIAL PEAKING FACTOR = $2.040 \cdot (1.0 + 0.3 \cdot (1.0 - 2462.3 / 2530.0)) / 1.0455 = 1.967$
 MEASURED TOTAL RADIAL PEAKING FACTOR = 1.818
 LIMITING TOTAL RADIAL PEAKING FACTOR RATIO = 1.082 (A/M) IN ASSEMBLY 138

FUEL TYPE	BUNDLE	PEAK PIN KW	TS HFP FRT	ALLOWED FRT	MEASURED FRT	ALLOWED/MEASURED
P1	42	98.10	2.04	1.97	1.733	1.135
P2	138	102.91	2.04	1.97	1.818	1.082
O1	110	101.11	2.04	1.97	1.786	1.101
O2	122	85.33	2.04	1.97	1.508	1.305
O3	136	58.86	2.04	1.97	1.040	1.892
N1	121	66.45	1.92	1.85	1.174	1.577
N2	155	70.99	1.92	1.85	1.254	1.476
N3	170	65.54	1.92	1.85	1.158	1.599
N4	139	70.04	1.92	1.85	1.237	1.496
N5	89	64.38	1.92	1.85	1.137	1.628
NS	103	25.98	1.92	1.85	0.459	4.033
NX	135	24.18	1.92	1.85	0.427	4.333
M1	178	21.92	1.92	1.85	0.387	4.781

PRI.P3X BKWF - LINEAR HEAT GENERATION RATE BY FUEL TYPE (KW/FT)

ALLOWED LINEAR HEAT GENERATION RATE = $15.28 \cdot 1.0000 / 1.0623 / 1.03 / 1.02 = 13.69$
 MEASURED LINEAR HEAT GENERATION RATE = 11.04
 LIMITING LINEAR HEAT GENERATION RATE RATIO = 1.240 (A/M) IN ASSEMBLY 138

FUEL TYPE	BUNDLE	MAXIMUM LHR	AXIAL PENALTY	ALLOWED LHR	MEASURED LHR	ALLOWED/MEASURED	FRACTION FROM BOTTOM OF CORE
P1	42	15.28	1.0000	13.69	10.43	1.313	0.46
P2	138	15.28	1.0000	13.69	11.04	1.240	0.50
O1	111	15.28	1.0000	13.69	10.61	1.291	0.50
O2	122	15.28	1.0000	13.69	9.04	1.515	0.50
O3	136	15.28	1.0000	13.69	6.25	2.189	0.50
N1	121	15.28	1.0000	13.69	7.02	1.951	0.50
N2	155	15.28	1.0000	13.69	7.37	1.858	0.54
N3	170	15.28	1.0000	13.69	6.77	2.022	0.50
N4	139	15.28	1.0000	13.69	7.34	1.866	0.50
N5	89	15.28	1.0000	13.69	6.72	2.036	0.50
NS	103	15.28	1.0000	13.69	2.82	4.860	0.50
NX	135	15.28	1.0000	13.69	2.58	5.303	0.54
M1	178	15.28	1.0000	13.69	2.35	5.814	0.54

PRI.P3X FALM - INCORE ALARM FACTORS BASED ON THE LHGR WITH THE MINIMUM MARGIN TO THE TECH SPEC LIMITS

LEVEL	BUNDLE	FRACTION FROM BOTTOM	ALARM FACTOR
5	126	0.82	1.3610
4	138	0.62	1.2679
3	138	0.50	1.2401
2	138	0.38	1.2674
1	169	0.18	1.3989

PRI.P3X 3APL - ALLOWABLE POWER LEVEL (LIMITED BY PEAK FUEL PIN MAXIMUM LHR)

ALLOWABLE POWER LEVEL 100.0 %
 LIMITING LOCATION IN ASSEMBLY 138
 FRACTION FROM THE BOTTOM 0.50
 V(Z) 1.1100

PRI.P3X PKWF - PEAK NODE LHGR FOR EACH ASSEMBLY (KW/FT)

RMS DEVIATION FOR THIS MAP = 1.58 %

	A	B	D	E	G	H	J	K	M	N	Q	R	T	V	X	Z
1						2.509	2.856	2.656	2.340	2.722	1.807					
						2.506	2.893	2.702	2.381	2.722	1.808					
						0.580	0.540	0.500	0.580	0.540	0.540					
						0.156	-1.285	-1.736	-1.756	-0.011	-0.063					
2				2.200	4.189	6.099	8.654	6.628	8.576	6.469	5.768	4.112	2.197			
				2.219	4.199	6.046	8.709	6.741	8.643	6.426	5.723	4.089	2.197			
				0.540	0.540	0.540	0.500	0.500	0.500	0.540	0.540	0.540	0.540			
				-0.856	-0.236	0.876	-0.631	-1.713	-0.780	0.657	0.776	0.573	0.023			
4				4.888	10.092	8.108	6.762	10.161	6.534	9.504	7.974	10.133	4.953			
				4.936	10.106	8.121	6.851	10.436	6.617	9.503	7.896	10.041	4.926			
				0.500	0.500	0.500	0.500	0.500	0.500	0.500	0.540	0.500	0.540			
				-0.988	-0.139	-0.159	-1.318	-2.699	-1.276	0.001	0.981	0.911	0.557			
5	2.220	4.980	7.754	9.430	10.821	8.836	9.305	10.422	6.729	10.664	9.083	7.910	5.025	2.255		
	2.197	4.926	7.832	9.446	10.851	8.895	9.461	10.553	6.768	10.620	9.028	7.832	4.936	2.219		
	0.540	0.500	0.500	0.500	0.500	0.500	0.500	0.500	0.540	0.500	0.540	0.540	0.540	0.540		
	1.055	1.089	-1.011	-0.171	-0.278	-0.670	-1.683	-1.251	-0.580	0.410	0.612	0.982	1.764	1.596		
7	4.180	10.428	9.103	10.856	7.262	10.528	6.695	8.256	7.860	7.339	10.921	9.562	10.411	4.272		
	4.089	10.041	9.028	10.828	7.283	10.504	6.861	8.403	7.943	7.348	10.837	9.446	10.106	4.199		
	0.500	0.460	0.500	0.500	0.500	0.500	0.540	0.540	0.540	0.540	0.500	0.500	0.500	0.540		
	2.179	3.716	0.823	0.261	-0.284	0.225	-2.485	-1.777	-1.059	-0.125	0.764	1.214	2.927	1.694		
8	1.786	5.786	8.025	10.695	7.340	6.632	8.113	9.697	6.685	9.610	6.620	7.209	10.884	8.206	6.060	2.499
	1.808	5.723	7.896	10.620	7.348	6.692	8.262	10.155	6.879	9.715	6.692	7.283	10.851	8.121	6.046	2.506
	0.740	0.540	0.500	0.500	0.540	0.540	0.500	0.420	0.540	0.500	0.540	0.500	0.500	0.500	0.540	0.540
	-1.210	1.083	1.605	0.705	-0.115	-0.902	-1.836	-4.717	-2.898	-1.093	-1.080	-1.026	0.301	1.036	0.229	-0.267
10	2.730	6.466	9.591	6.732	7.918	9.682	6.536	6.909	10.611	6.487	8.190	10.435	8.858	6.824	8.696	2.867
	2.722	6.426	9.503	6.768	7.943	9.715	6.602	7.097	10.793	6.602	8.262	10.504	8.895	6.851	8.709	2.893
	0.540	0.500	0.500	0.540	0.540	0.500	0.540	0.540	0.500	0.540	0.540	0.500	0.500	0.500	0.500	0.540
	0.287	0.611	0.916	-0.535	-0.315	-0.343	-1.012	-2.719	-1.712	-1.775	-0.883	-0.662	-0.421	-0.398	-0.151	-0.889
11	2.426	8.870	6.723	10.636	8.421	6.848	10.710	10.568	10.563	6.972	10.129	6.788	9.364	10.327	6.677	2.676
	2.381	8.643	6.617	10.553	8.403	6.879	10.793	10.688	10.688	7.097	10.155	6.861	9.461	10.436	6.741	2.702
	0.540	0.500	0.500	0.500	0.540	0.540	0.500	0.500	0.500	0.540	0.540	0.540	0.500	0.500	0.500	0.500
	1.833	2.560	1.585	0.781	0.221	-0.450	-0.774	-1.135	-1.181	-1.794	-0.256	-1.083	-1.036	-1.054	-0.966	-0.963
13	2.817	7.078	10.704	9.593	6.890	10.200	6.989	10.592	10.607	10.662	6.778	8.292	10.408	6.454	8.564	2.352
	2.702	6.741	10.436	9.461	6.861	10.155	7.097	10.688	10.688	10.793	6.879	8.403	10.562	6.623	8.643	2.381
	0.500	0.500	0.500	0.500	0.540	0.500	0.540	0.500	0.500	0.540	0.540	0.540	0.500	0.500	0.500	0.540
	4.098	4.754	2.509	1.366	0.415	0.440	-1.540	-0.906	-0.768	-1.225	-1.490	-1.331	-1.480	-2.608	-0.931	-1.256
14	2.981	9.047	7.017	9.035	10.609	8.276	6.535	10.708	7.001	6.468	9.520	7.814	6.682	9.418	6.449	2.716
	2.893	8.709	6.851	8.895	10.504	8.262	6.602	10.793	7.097	6.602	9.715	7.936	6.768	9.503	6.426	2.722
	0.500	0.500	0.500	0.500	0.500	0.540	0.540	0.500	0.540	0.540	0.540	0.540	0.540	0.500	0.500	0.540
	2.967	3.738	2.363	1.549	0.989	0.166	-1.030	-0.793	-1.377	-2.079	-2.051	-1.561	-1.280	-0.911	0.361	-0.257
16	2.582	6.253	8.337	11.040	7.335	6.686	9.675	6.803	10.062	8.106	6.424	7.246	10.559	7.860	5.710	1.792
	2.506	6.046	8.121	10.851	7.283	6.692	9.715	6.879	10.155	8.262	6.692	7.348	10.620	7.896	5.723	1.808
	0.540	0.500	0.500	0.500	0.500	0.540	0.500	0.540	0.500	0.540	0.540	0.540	0.500	0.500	0.540	0.540
	2.958	3.317	2.591	1.712	0.712	-0.089	-0.410	-1.119	-0.920	-1.925	-4.164	-1.410	-0.577	-0.460	-0.230	-0.864
17	4.523	10.404	9.612	10.904	7.367	7.913	8.352	6.782	10.403	7.189	10.825	9.012	10.051	4.084		
	4.199	10.106	9.446	10.837	7.348	7.943	8.403	6.861	10.504	7.283	10.828	9.028	10.041	4.089		
	0.540	0.500	0.500	0.500	0.540	0.500	0.540	0.540	0.500	0.500	0.500	0.500	0.500	0.540		
	7.153	2.863	1.734	0.608	0.251	-0.372	-0.606	-1.169	-0.971	-1.306	-0.023	-0.177	0.098	-0.106		
19	2.319	5.043	7.982	9.226	10.719	6.772	10.526	9.396	8.836	10.803	9.450	7.895	4.933	2.355		
	2.219	4.936	7.832	9.028	10.620	6.768	10.553	9.461	8.895	10.851	9.446	7.832	4.926	2.197		
	0.540	0.500	0.500	0.500	0.500	0.500	0.500	0.500	0.500	0.500	0.500	0.500	0.500	0.540		
	4.329	2.106	1.883	2.153	0.927	0.061	-0.259	-0.696	-0.669	-0.447	0.046	0.794	0.156	6.718		
20				4.972	10.218	7.970	9.542	6.611	10.403	6.814	8.105	10.107	4.929			
				4.926	10.041	7.896	9.503	6.617	10.436	6.851	8.121	10.106	4.936			
				0.500	0.500	0.500	0.500	0.500	0.500	0.500	0.500	0.500	0.500			
				0.941	1.730	0.929	0.408	-0.090	-0.312	-0.537	-0.203	0.012	-0.153			
22				2.203	4.121	5.747	6.441	8.649	6.717	8.695	6.005	4.172	2.205			
				2.197	4.089	5.723	6.426	8.643	6.741	8.709	6.046	4.199	2.219			
				0.540	0.540	0.540	0.500	0.500	0.500	0.500	0.540	0.540	0.540			
				0.267	0.773	0.418	0.236	0.070	-0.361	-0.159	-0.675	-0.655	-0.613			
23						1.802	2.716	2.370	2.693	2.907	2.487					
						1.808	2.722	2.381	2.702	2.893	2.506					
						0.500	0.500	0.540	0.500	0.700	0.580					
						-0.303	-0.253	-0.475	-0.324	0.470	-0.727					

PIDAL-3
SIMULATE-3
P3 PEAK LOCALE
(P3-S3)/P3*100%

PRI.P3X 2EXP - AXIALLY COLLAPSED FULL CORE EXPOSURE MAP (GWD/MTU)

RMS DEVIATION FOR THIS MAP = 1.23 %

	A	B	D	E	G	H	J	K	M	N	Q	R	T	V	X	Z
1						32.021	31.506	7.790	7.688	30.359	36.332					
						32.018	31.439	7.780	7.750	30.511	36.589					
						0.007	0.213	0.133	-0.814	-0.500	-0.706					
2				38.765	30.772	19.855	0.587	19.905	0.586	19.898	20.082	30.927	38.742			
				38.566	30.866	20.065	0.585	19.960	0.586	19.926	20.048	31.042	38.537			
				0.512	-0.304	-1.058	0.310	-0.275	-0.012	-0.137	0.172	-0.374	0.529			
4				29.714	0.678	19.835	28.262	0.768	30.329	0.738	19.532	0.673	30.261			
				29.943	0.672	19.841	28.071	0.798	30.266	0.735	19.716	0.665	30.428			
				-0.771	0.856	-0.029	0.675	-3.854	0.209	0.379	-0.944	1.205	-0.551			
5	38.610	30.440	20.556	16.282	0.874	19.287	16.155	0.839	26.901	0.843	16.988	20.105	29.966	38.733		
	38.537	30.428	20.247	16.259	0.880	19.455	16.260	0.858	26.909	0.844	17.083	20.247	29.943	38.566		
	0.188	0.039	1.504	0.137	-0.651	-0.874	-0.653	-2.198	-0.029	-0.194	-0.560	-0.709	0.077	0.431		
7	30.947	0.701	16.878	0.858	29.697	0.855	29.011	19.762	19.210	25.922	0.850	16.181	0.698	30.942		
	31.042	-0.665	17.083	0.853	29.506	0.865	28.941	19.719	19.270	25.570	0.853	16.259	0.672	30.866		
	-0.309	5.094	-1.216	0.580	0.644	-1.206	0.242	0.219	-0.315	1.356	-0.375	-0.484	3.697	0.248		
8	36.260	20.070	19.670	0.855	25.705	25.394	19.780	0.799	27.952	0.791	25.246	29.821	0.876	19.757	19.861	31.893
	36.589	20.048	19.716	0.844	25.570	25.442	19.834	0.844	27.852	0.806	25.442	29.506	0.880	19.841	20.065	32.018
	-0.906	0.111	-0.233	1.230	0.524	-0.185	-0.277	-5.619	0.356	-1.952	-0.773	1.057	-0.452	-0.424	-1.027	-0.392
10	30.670	19.805	0.751	26.948	19.127	0.796	27.766	27.082	0.847	27.991	19.661	0.849	19.299	27.986	0.590	31.103
	30.511	19.926	0.735	26.909	19.270	0.806	27.800	27.150	0.879	27.800	19.834	0.865	19.455	28.071	0.585	31.439
	0.517	-0.608	2.041	0.146	-0.751	-1.195	-0.121	-0.251	-3.763	0.684	-0.882	-1.941	-0.807	-0.305	0.851	-1.082
11	7.778	0.606	30.393	0.861	19.751	28.040	0.853	16.093	16.523	27.270	0.818	28.898	15.984	0.789	19.838	7.769
	7.750	0.585	30.266	0.858	19.719	27.852	0.879	16.238	16.238	27.150	0.844	28.941	16.260	0.798	19.960	7.780
	0.355	3.438	0.421	0.372	0.163	0.671	-3.042	-0.906	1.722	0.438	-3.179	-0.148	-1.726	-1.087	-0.617	-0.132
13	7.830	19.950	0.813	16.291	28.946	0.829	27.288	16.454	16.149	0.850	27.983	19.774	0.843	30.166	0.588	7.792
	7.780	19.960	0.798	16.260	28.941	0.844	27.150	16.238	16.238	0.879	27.852	19.719	0.858	30.266	0.585	7.750
	0.646	-0.049	1.920	0.188	0.017	-1.749	0.505	1.312	-0.556	-3.408	0.469	0.279	-1.787	-0.329	0.477	0.532
14	31.270	0.609	28.082	19.341	0.862	19.923	27.987	0.855	26.943	27.814	0.785	19.247	26.959	0.735	19.945	30.405
	31.439	0.585	28.071	19.455	0.865	19.834	27.800	0.879	27.150	27.800	0.806	19.270	26.909	0.735	19.926	30.511
	-0.541	3.914	0.038	-0.593	-0.368	0.443	0.667	-2.866	-0.769	0.052	-2.677	-0.121	0.188	-0.023	0.097	-0.350
16	32.024	20.021	19.984	0.885	29.810	25.385	0.796	28.083	0.829	19.764	25.349	25.723	0.840	19.832	20.094	36.296
	32.018	20.065	19.841	0.880	29.506	25.442	0.806	27.852	0.844	19.834	25.442	25.570	0.844	19.716	20.048	36.589
	0.018	-0.218	0.719	0.615	1.020	-0.224	-1.244	0.822	-1.729	-0.354	-0.366	0.594	-0.550	0.585	0.231	-0.808
17	30.971	0.689	16.261	0.853	25.890	19.366	20.253	28.912	0.853	29.460	0.854	17.121	0.672	30.742		
	30.866	0.672	16.259	0.853	25.570	19.270	19.719	28.941	0.865	29.506	0.853	17.083	0.665	31.042		
	0.341	2.373	0.008	0.015	1.235	0.494	2.636	-0.100	-1.400	-0.156	0.111	0.219	0.972	-0.979		
19	38.872	29.985	20.283	17.182	0.852	26.975	0.855	16.606	19.263	0.876	16.199	20.248	30.480	38.593		
	38.566	29.943	20.247	17.083	0.844	26.909	0.858	16.260	19.455	0.880	16.259	20.247	30.428	38.537		
	0.786	0.140	0.178	0.575	0.894	0.246	-0.345	2.086	-0.996	-0.468	-0.370	0.004	0.170	0.145		
20				30.483	0.683	19.891	0.747	30.339	0.799	27.900	19.756	0.679	29.899			
				30.428	0.665	19.716	0.735	30.266	0.798	28.071	19.841	0.672	29.943			
				0.181	2.666	0.878	1.619	0.241	0.170	-0.613	-0.429	0.989	-0.149			
22				38.840	30.899	20.317	19.876	0.598	20.179	0.595	20.089	30.953	38.632			
				38.537	31.042	20.048	19.926	0.586	19.960	0.585	20.065	30.866	38.566			
				0.779	-0.464	1.322	-0.248	2.023	1.086	1.661	0.123	0.281	0.171			
23						36.443	30.456	7.784	7.802	31.191	31.898					
						36.589	30.511	7.750	7.780	31.439	32.018					
						-0.401	-0.182	0.432	0.284	-0.794	-0.378					

PIDAL-3
SIMULATE-3
(P3-S3)/P3*100%

PRI.P3X BRPF - POWER FRACTIONS BY FUEL TYPE

BATCH P1 AVERAGE	1.187	MAXIMUM IS	1.300	IN ASSEMBLY	P107	IN CORE	LOCATION	42
BATCH P2 AVERAGE	1.527	MAXIMUM IS	1.635	IN ASSEMBLY	P250	IN CORE	LOCATION	138
BATCH O1 AVERAGE	1.439	MAXIMUM IS	1.540	IN ASSEMBLY	O110	IN CORE	LOCATION	110
BATCH O2 AVERAGE	1.074	MAXIMUM IS	1.368	IN ASSEMBLY	O218	IN CORE	LOCATION	122
BATCH O3 AVERAGE	0.718	MAXIMUM IS	0.727	IN ASSEMBLY	O358	IN CORE	LOCATION	136
BATCH N1 AVERAGE	1.042	MAXIMUM IS	1.073	IN ASSEMBLY	N102	IN CORE	LOCATION	125
BATCH N2 AVERAGE	0.696	MAXIMUM IS	1.110	IN ASSEMBLY	N233	IN CORE	LOCATION	127
BATCH N3 AVERAGE	0.774	MAXIMUM IS	1.104	IN ASSEMBLY	N346	IN CORE	LOCATION	170
BATCH N4 AVERAGE	0.886	MAXIMUM IS	1.121	IN ASSEMBLY	N462	IN CORE	LOCATION	107
BATCH N5 AVERAGE	0.980	MAXIMUM IS	0.998	IN ASSEMBLY	N567	IN CORE	LOCATION	89
BATCH NS AVERAGE	0.163	MAXIMUM IS	0.171	IN ASSEMBLY	NS06	IN CORE	LOCATION	103
BATCH NX AVERAGE	0.195	MAXIMUM IS	0.197	IN ASSEMBLY	N218	IN CORE	LOCATION	135
BATCH M1 AVERAGE	0.134	MAXIMUM IS	0.137	IN ASSEMBLY	M107	IN CORE	LOCATION	178
BATCH P AVERAGE	1.430							
BATCH O AVERAGE	1.148							
BATCH N AVERAGE	0.703							
BATCH M AVERAGE	0.134							

PRI.P3X BEXP - EXPOSURES BY FUEL TYPE

BATCH P1 AVERAGE	0.639	GWD/MTU	MAXIMUM IS	0.701	IN ASSEMBLY	P107	IN CORE	LOCATION	42
BATCH P2 AVERAGE	0.828	GWD/MTU	MAXIMUM IS	0.885	IN ASSEMBLY	P250	IN CORE	LOCATION	138
BATCH O1 AVERAGE	16.459	GWD/MTU	MAXIMUM IS	17.182	IN ASSEMBLY	O114	IN CORE	LOCATION	168
BATCH O2 AVERAGE	19.805	GWD/MTU	MAXIMUM IS	20.556	IN ASSEMBLY	O239	IN CORE	LOCATION	29
BATCH O3 AVERAGE	19.957	GWD/MTU	MAXIMUM IS	20.089	IN ASSEMBLY	O357	IN CORE	LOCATION	196
BATCH N1 AVERAGE	27.974	GWD/MTU	MAXIMUM IS	28.262	IN ASSEMBLY	N107	IN CORE	LOCATION	20
BATCH N2 AVERAGE	28.730	GWD/MTU	MAXIMUM IS	31.506	IN ASSEMBLY	N227	IN CORE	LOCATION	2
BATCH N3 AVERAGE	28.681	GWD/MTU	MAXIMUM IS	30.483	IN ASSEMBLY	N350	IN CORE	LOCATION	179
BATCH N4 AVERAGE	29.510	GWD/MTU	MAXIMUM IS	29.985	IN ASSEMBLY	N458	IN CORE	LOCATION	166
BATCH N5 AVERAGE	30.307	GWD/MTU	MAXIMUM IS	30.393	IN ASSEMBLY	N567	IN CORE	LOCATION	89
BATCH NS AVERAGE	7.779	GWD/MTU	MAXIMUM IS	7.830	IN ASSEMBLY	NS06	IN CORE	LOCATION	103
BATCH NX AVERAGE	31.959	GWD/MTU	MAXIMUM IS	32.024	IN ASSEMBLY	N218	IN CORE	LOCATION	135
BATCH M1 AVERAGE	37.926	GWD/MTU	MAXIMUM IS	38.872	IN ASSEMBLY	M109	IN CORE	LOCATION	165
BATCH P AVERAGE	0.774	GWD/MTU							
BATCH O AVERAGE	18.923	GWD/MTU							
BATCH N AVERAGE	26.816	GWD/MTU							
BATCH M AVERAGE	37.926	GWD/MTU							

PRI.P3X 3ICI - ICI AUGMENTED ALARM LIMITS AND SIGNALS WITH DEPLETED SENSITIVITIES

FAILED DETECTOR LEGEND
 Z = FAILED MINIMUM ICI POWER TEST (PMIN)
 > = FAILED MEASURED/PREDICTED ICI POWER TEST HIGH (PDEV)
 < = FAILED MEASURED/PREDICTED ICI POWER TEST LOW (PDEV)

FAILED	STRING	LEVEL	ALARM LIMITS (NV)	ALARM LIMITS (AMPS)	INCORE CURRENTS (NV)	INCORE CURRENTS (AMPS)	ALARM/CURRENT	KSUBS (AMPS/NV)	FRACTION OF REMAINING RHODIUM
	1	5	1.7972E+13	6.9210E-07	1.3205E+13	5.0851E-07	1.3610	3.8510E-20	0.99771
	1	4	2.3609E+13	9.0827E-07	1.8620E+13	7.1634E-07	1.2679	3.8471E-20	0.99671
	1	3	2.3016E+13	8.8544E-07	1.8559E+13	7.1400E-07	1.2401	3.8471E-20	0.99671
	1	2	2.2259E+13	8.5654E-07	1.7563E+13	6.7582E-07	1.2674	3.8481E-20	0.99696
	1	1	1.8152E+13	6.9902E-07	1.2976E+13	4.9969E-07	1.3989	3.8509E-20	0.99770
	2	5	3.3000E+13	1.2684E-06	2.4246E+13	9.3195E-07	1.3610	3.8437E-20	0.99583
	2	4	4.1064E+13	1.5758E-06	3.2387E+13	1.2428E-06	1.2679	3.8373E-20	0.99418
	2	3	4.0693E+13	1.5614E-06	3.2814E+13	1.2591E-06	1.2401	3.8370E-20	0.99410
	2	2	3.8947E+13	1.4952E-06	3.0730E+13	1.1797E-06	1.2674	3.8389E-20	0.99459
	2	1	3.2158E+13	1.2363E-06	2.2988E+13	8.8377E-07	1.3989	3.8445E-20	0.99605
	3	5	3.5694E+13	1.3714E-06	2.6226E+13	1.0076E-06	1.3610	3.8421E-20	0.99543
	3	4	4.5317E+13	1.7379E-06	3.5741E+13	1.3706E-06	1.2679	3.8349E-20	0.99356
	3	3	4.5392E+13	1.7405E-06	3.6603E+13	1.4035E-06	1.2401	3.8344E-20	0.99342
	3	2	4.3654E+13	1.6748E-06	3.4443E+13	1.3214E-06	1.2674	3.8365E-20	0.99395
	3	1	3.5459E+13	1.3627E-06	2.5347E+13	9.7411E-07	1.3989	3.8430E-20	0.99565
	4	5	6.3080E+13	2.3904E-06	4.6347E+13	1.7563E-06	1.3610	3.7895E-20	0.99181
	4	4	7.9605E+13	3.0347E-06	6.2784E+13	2.3934E-06	1.2679	3.8122E-20	0.98867
	4	3	8.1546E+13	3.1072E-06	6.5757E+13	2.5056E-06	1.2401	3.8104E-20	0.98820
	4	2	7.9676E+13	3.0382E-06	6.2865E+13	2.3972E-06	1.2674	3.8132E-20	0.98893
	4	1	6.3661E+13	2.4355E-06	4.5507E+13	1.7410E-06	1.3989	3.8258E-20	0.99219
	5	5	4.8910E+13	1.8762E-06	3.5936E+13	1.3785E-06	1.3610	3.8361E-20	0.99386
	5	4	6.4596E+13	2.4705E-06	5.0946E+13	1.9485E-06	1.2679	3.8246E-20	0.99088
	5	3	6.6355E+13	2.5364E-06	5.3507E+13	2.0453E-06	1.2401	3.8225E-20	0.99033
	5	2	6.4888E+13	2.4818E-06	5.1198E+13	1.9582E-06	1.2674	3.8247E-20	0.99092
	5	1	5.6002E+13	2.1466E-06	4.0032E+13	1.5344E-06	1.3989	3.8330E-20	0.99306
	6	5	4.4308E+13	1.7017E-06	3.2554E+13	1.2503E-06	1.3610	3.8407E-20	0.99505
	6	4	5.4230E+13	2.0772E-06	4.2771E+13	1.6382E-06	1.2679	3.8303E-20	0.99235
	6	3	5.4300E+13	2.0793E-06	4.3787E+13	1.6767E-06	1.2401	3.8292E-20	0.99207
	6	2	5.3976E+13	2.0675E-06	4.2588E+13	1.6313E-06	1.2674	3.8304E-20	0.99238
	6	1	4.4317E+13	1.7012E-06	3.1680E+13	1.2161E-06	1.3989	3.8386E-20	0.99451
	8	5	5.4491E+13	2.0891E-06	4.0036E+13	1.5349E-06	1.3610	3.8338E-20	0.99326
	8	4	6.9645E+13	2.6612E-06	5.4928E+13	2.0989E-06	1.2679	3.8211E-20	0.98999
	8	3	7.0560E+13	2.6953E-06	5.6898E+13	2.1734E-06	1.2401	3.8198E-20	0.98964
	8	2	7.0059E+13	2.6774E-06	5.5277E+13	2.1125E-06	1.2674	3.8216E-20	0.99011
	8	1	5.6305E+13	2.1580E-06	4.0249E+13	1.5427E-06	1.3989	3.8328E-20	0.99301
	9	5	6.9868E+13	2.6748E-06	5.1334E+13	1.9652E-06	1.3610	3.8283E-20	0.99183
	9	4	8.8995E+13	3.3915E-06	7.0189E+13	2.6748E-06	1.2679	3.8109E-20	0.98733
	9	3	9.0957E+13	3.4639E-06	7.3346E+13	2.7932E-06	1.2401	3.8082E-20	0.98664
	9	2	9.0115E+13	3.4341E-06	7.1102E+13	2.7096E-06	1.2674	3.8108E-20	0.98732
	9	1	7.3875E+13	2.8253E-06	5.2809E+13	2.0196E-06	1.3989	3.8243E-20	0.99082
	10	5	6.9784E+13	2.6688E-06	5.1273E+13	1.9608E-06	1.3610	3.8244E-20	0.99082
	10	4	8.8369E+13	3.3677E-06	6.9695E+13	2.6560E-06	1.2679	3.8109E-20	0.98734
	10	3	8.9336E+13	3.4031E-06	7.2039E+13	2.7442E-06	1.2401	3.8094E-20	0.98694
	10	2	8.7056E+13	3.3192E-06	6.8688E+13	2.6189E-06	1.2674	3.8127E-20	0.98780
	10	1	7.1400E+13	2.7316E-06	5.1039E+13	1.9526E-06	1.3989	3.8258E-20	0.99118
	11	5	6.6569E+13	2.5496E-06	4.8910E+13	1.8733E-06	1.3610	3.8300E-20	0.99229
	11	4	8.7551E+13	3.3375E-06	6.9051E+13	2.6322E-06	1.2679	3.8120E-20	0.98762
	11	3	9.1378E+13	3.4795E-06	7.3685E+13	2.8058E-06	1.2401	3.8078E-20	0.98652
	11	2	8.8820E+13	3.3855E-06	7.0080E+13	2.6712E-06	1.2674	3.8116E-20	0.98751
	11	1	7.6136E+13	2.9110E-06	5.4425E+13	2.0809E-06	1.3989	3.8234E-20	0.99057
	12	5	5.2117E+13	1.9988E-06	3.8292E+13	1.4686E-06	1.3610	3.8353E-20	0.99364
	12	4	6.9028E+13	2.6382E-06	5.4442E+13	2.0807E-06	1.2679	3.8219E-20	0.99018
	12	3	7.0706E+13	2.7007E-06	5.7016E+13	2.1778E-06	1.2401	3.8196E-20	0.98959
	12	2	6.9933E+13	2.6726E-06	5.5178E+13	2.1087E-06	1.2674	3.8217E-20	0.99012
	12	1	5.8720E+13	2.2500E-06	4.1975E+13	1.6084E-06	1.3989	3.8317E-20	0.99271
	13	5	1.0092E+13	3.8904E-07	7.4150E+12	2.8584E-07	1.3610	3.8549E-20	0.99873
	13	4	1.1878E+13	4.5771E-07	9.3681E+12	3.6099E-07	1.2679	3.8534E-20	0.99834
	13	3	1.1661E+13	4.4934E-07	9.4032E+12	3.6234E-07	1.2401	3.8533E-20	0.99833
	13	2	1.1497E+13	4.4304E-07	9.0710E+12	3.4956E-07	1.2674	3.8536E-20	0.99840
	13	1	9.2373E+12	3.5614E-07	6.6032E+12	2.5458E-07	1.3989	3.8554E-20	0.99887
	14	5	6.5263E+13	2.4721E-06	4.7950E+13	1.8164E-06	1.3610	3.7880E-20	0.99141
	14	4	8.1635E+13	3.1110E-06	6.4384E+13	2.4536E-06	1.2679	3.8109E-20	0.98832
	14	3	8.1609E+13	3.1095E-06	6.5808E+13	2.5075E-06	1.2401	3.8103E-20	0.98817
Z	14	2	1.0000E+16	0.0000E+00	0.0000E+00	0.0000E+00	1.2674	3.8299E-20	0.99326
	14	1	6.7807E+13	2.5928E-06	4.8471E+13	1.8535E-06	1.3989	3.8238E-20	0.99168
	15	5	6.5518E+13	2.5071E-06	4.8138E+13	1.8420E-06	1.3610	3.8265E-20	0.99138
	15	4	8.1115E+13	3.0943E-06	6.3974E+13	2.4404E-06	1.2679	3.8147E-20	0.98832
	15	3	8.1678E+13	3.1150E-06	6.5864E+13	2.5119E-06	1.2401	3.8138E-20	0.98807
	15	2	7.9598E+13	3.0382E-06	6.2804E+13	2.3972E-06	1.2674	3.8169E-20	0.98890
	15	1	6.7184E+13	2.5716E-06	4.8026E+13	1.8383E-06	1.3989	3.8277E-20	0.99169

FAILED	STRING	LEVEL	ALARM LIMITS (NV) (AMPS)		INCORE CURRENTS (NV) (AMPS)		ALARM/ CURRENT	KSUBS (AMPS/NV)	FRACTION OF REMAINING RHODIUM	
		16	5	5.9243E+13	2.2698E-06	4.3527E+13	1.6677E-06	1.3610	3.8314E-20	0.99264
		16	4	7.1495E+13	2.7317E-06	5.6387E+13	2.1545E-06	1.2679	3.8209E-20	0.98992
		16	3	7.2400E+13	2.7652E-06	5.8382E+13	2.2298E-06	1.2401	3.8193E-20	0.98951
		16	2	7.0235E+13	2.6843E-06	5.5416E+13	2.1180E-06	1.2674	3.8219E-20	0.99018
		16	1	5.8023E+13	2.2237E-06	4.1477E+13	1.5896E-06	1.3989	3.8324E-20	0.99289
		17	5	3.5344E+13	1.3580E-06	2.5968E+13	9.9775E-07	1.3610	3.8422E-20	0.99544
		17	4	4.5098E+13	1.7296E-06	3.5568E+13	1.3641E-06	1.2679	3.8353E-20	0.99365
		17	3	4.5404E+13	1.7410E-06	3.6613E+13	1.4039E-06	1.2401	3.8345E-20	0.99345
		17	2	4.4254E+13	1.6976E-06	3.4917E+13	1.3394E-06	1.2674	3.8360E-20	0.99384
		17	1	3.6271E+13	1.3938E-06	2.5928E+13	9.9633E-07	1.3989	3.8427E-20	0.99557
		18	5	5.8825E+13	2.2534E-06	4.3220E+13	1.6556E-06	1.3610	3.8306E-20	0.99244
		18	4	7.2082E+13	2.7539E-06	5.6850E+13	2.1720E-06	1.2679	3.8205E-20	0.98982
		18	3	7.2149E+13	2.7557E-06	5.8179E+13	2.2222E-06	1.2401	3.8195E-20	0.98956
		18	2	7.0634E+13	2.6994E-06	5.5731E+13	2.1298E-06	1.2674	3.8217E-20	0.99012
		18	1	6.0784E+13	2.3286E-06	4.3450E+13	1.6646E-06	1.3989	3.8309E-20	0.99252
		19	5	5.8658E+13	2.2465E-06	4.3098E+13	1.6506E-06	1.3610	3.8299E-20	0.99225
		19	4	6.9649E+13	2.6616E-06	5.4932E+13	2.0992E-06	1.2679	3.8215E-20	0.99007
		19	3	6.9675E+13	2.6622E-06	5.6185E+13	2.1467E-06	1.2401	3.8209E-20	0.98991
		19	2	6.7063E+13	2.5644E-06	5.2914E+13	2.0233E-06	1.2674	3.8238E-20	0.99067
		19	1	5.7480E+13	2.2030E-06	4.1089E+13	1.5748E-06	1.3989	3.8326E-20	0.99296
		20	5	5.2197E+13	2.0012E-06	3.8351E+13	1.4703E-06	1.3610	3.8339E-20	0.99329
		20	4	6.6052E+13	2.5257E-06	5.2095E+13	1.9920E-06	1.2679	3.8237E-20	0.99065
Z		20	3	1.0000E+16	0.0000E+00	0.0000E+00	0.0000E+00	1.2401	3.8545E-20	0.99864
		20	2	6.5229E+13	2.4949E-06	5.1466E+13	1.9685E-06	1.2674	3.8248E-20	0.99093
		20	1	5.4717E+13	2.0978E-06	3.9114E+13	1.4996E-06	1.3989	3.8338E-20	0.99327
		21	5	6.0836E+13	2.3292E-06	4.4698E+13	1.7113E-06	1.3610	3.8286E-20	0.99191
		21	4	7.2621E+13	2.7738E-06	5.7275E+13	2.1876E-06	1.2679	3.8195E-20	0.98956
		21	3	7.2920E+13	2.7846E-06	5.8801E+13	2.2454E-06	1.2401	3.8186E-20	0.98934
		21	2	7.0404E+13	2.6906E-06	5.5549E+13	2.1229E-06	1.2674	3.8216E-20	0.99012
		21	1	6.0621E+13	2.3224E-06	4.3334E+13	1.6601E-06	1.3989	3.8310E-20	0.99254
		22	5	6.4272E+13	2.4595E-06	4.7222E+13	1.8071E-06	1.3610	3.8267E-20	0.99144
		22	4	8.4109E+13	3.2072E-06	6.6336E+13	2.5295E-06	1.2679	3.8131E-20	0.98791
		22	3	8.5068E+13	3.2428E-06	6.8597E+13	2.6149E-06	1.2401	3.8120E-20	0.98763
		22	2	8.2202E+13	3.1348E-06	6.4858E+13	2.4734E-06	1.2674	3.8135E-20	0.98800
		22	1	7.3062E+13	2.7947E-06	5.2227E+13	1.9977E-06	1.3989	3.8251E-20	0.99100
		23	5	3.9403E+13	1.5130E-06	2.8950E+13	1.1117E-06	1.3610	3.8399E-20	0.99485
		23	4	5.0533E+13	1.9364E-06	3.9855E+13	1.5272E-06	1.2679	3.8319E-20	0.99277
		23	3	5.2249E+13	2.0013E-06	4.2132E+13	1.6138E-06	1.2401	3.8304E-20	0.99238
		23	2	5.0483E+13	1.9349E-06	3.9832E+13	1.5266E-06	1.2674	3.8327E-20	0.99297
		23	1	4.0412E+13	1.5521E-06	2.8888E+13	1.1095E-06	1.3989	3.8407E-20	0.99505
		24	5	6.0493E+13	2.3164E-06	4.4446E+13	1.7019E-06	1.3610	3.8292E-20	0.99207
		24	4	7.4087E+13	2.8294E-06	5.8432E+13	2.2315E-06	1.2679	3.8190E-20	0.98944
		24	3	7.4852E+13	2.8578E-06	6.0359E+13	2.3045E-06	1.2401	3.8180E-20	0.98916
		24	2	7.2044E+13	2.7529E-06	5.6843E+13	2.1721E-06	1.2674	3.8211E-20	0.98998
		24	1	6.2085E+13	2.3781E-06	4.4381E+13	1.7000E-06	1.3989	3.8304E-20	0.99238
		25	5	6.8519E+13	2.6205E-06	5.0343E+13	1.9254E-06	1.3610	3.8246E-20	0.99087
		25	4	8.5314E+13	3.2525E-06	6.7286E+13	2.5652E-06	1.2679	3.8124E-20	0.98771
		25	3	8.6071E+13	3.2802E-06	6.9406E+13	2.6451E-06	1.2401	3.8111E-20	0.98737
		25	2	8.3471E+13	3.1843E-06	6.5860E+13	2.5124E-06	1.2674	3.8148E-20	0.98835
		25	1	1.0000E+16	0.0000E+00	0.0000E+00	0.0000E+00	1.3989	3.8285E-20	0.99188
		26	5	6.0324E+13	2.3096E-06	4.4322E+13	1.6969E-06	1.3610	3.8286E-20	0.99192
		26	4	7.2678E+13	2.7762E-06	5.7320E+13	2.1895E-06	1.2679	3.8198E-20	0.98964
		26	3	7.3015E+13	2.7885E-06	5.8878E+13	2.2486E-06	1.2401	3.8190E-20	0.98943
		26	2	7.0377E+13	2.6898E-06	5.5528E+13	2.1223E-06	1.2674	3.8220E-20	0.99020
		26	1	6.1389E+13	2.3516E-06	4.3883E+13	1.6810E-06	1.3989	3.8306E-20	0.99244
		27	5	6.7967E+13	2.5992E-06	4.9938E+13	1.9097E-06	1.3610	3.8242E-20	0.99079
		27	4	8.2958E+13	3.1634E-06	6.5428E+13	2.4950E-06	1.2679	3.8133E-20	0.98795
		27	3	8.4023E+13	3.2031E-06	6.7754E+13	2.5829E-06	1.2401	3.8121E-20	0.98765
		27	2	8.1440E+13	3.1076E-06	6.4257E+13	2.4519E-06	1.2674	3.8158E-20	0.98860
		27	1	6.9498E+13	2.6593E-06	4.9680E+13	1.9010E-06	1.3989	3.8265E-20	0.99138
		28	5	5.1555E+13	1.9765E-06	3.7879E+13	1.4522E-06	1.3610	3.8337E-20	0.99325
		28	4	6.5273E+13	2.4962E-06	5.1480E+13	1.9687E-06	1.2679	3.8243E-20	0.99080
		28	3	6.6545E+13	2.5437E-06	5.3661E+13	2.0512E-06	1.2401	3.8226E-20	0.99036
		28	2	6.5777E+13	2.5156E-06	5.1899E+13	1.9849E-06	1.2674	3.8245E-20	0.99086
		28	1	5.5948E+13	2.1446E-06	3.9994E+13	1.5331E-06	1.3989	3.8333E-20	0.99312
		29	5	5.7716E+13	2.2108E-06	4.2406E+13	1.6243E-06	1.3610	3.8304E-20	0.99238
		29	4	6.9360E+13	2.6505E-06	5.4703E+13	2.0904E-06	1.2679	3.8214E-20	0.99005
		29	3	6.8894E+13	2.6326E-06	5.5555E+13	2.1229E-06	1.2401	3.8212E-20	0.99000
		29	2	6.6959E+13	2.5604E-06	5.2831E+13	2.0202E-06	1.2674	3.8238E-20	0.99067
		29	1	5.7665E+13	2.2101E-06	4.1221E+13	1.5798E-06	1.3989	3.8326E-20	0.99295
		30	5	3.5231E+13	1.3537E-06	2.5885E+13	9.9462E-07	1.3610	3.8424E-20	0.99550
		30	4	4.4805E+13	1.7185E-06	3.5337E+13	1.3554E-06	1.2679	3.8355E-20	0.99369
		30	3	4.5282E+13	1.7364E-06	3.6514E+13	1.4002E-06	1.2401	3.8345E-20	0.99346
		30	2	4.4022E+13	1.6888E-06	3.4734E+13	1.3325E-06	1.2674	3.8363E-20	0.99391
		30	1	3.6409E+13	1.3991E-06	2.6027E+13	1.0001E-06	1.3989	3.8427E-20	0.99557

FAILED	STRING	LEVEL	ALARM LIMITS		INCORE CURRENTS		ALARM/ CURRENT	KSUBS (AMPS/NV)	FRACTION OF REMAINING RHODIUM
			(NV)	(AMPS)	(NV)	(AMPS)			
	31	5	6.6109E+13	2.5295E-06	4.8573E+13	1.8585E-06	1.3610	3.8262E-20	0.99130
	31	4	8.1849E+13	3.1221E-06	6.4553E+13	2.4624E-06	1.2679	3.8145E-20	0.98826
	31	3	8.2247E+13	3.1364E-06	6.6322E+13	2.5291E-06	1.2401	3.8134E-20	0.98799
	31	2	8.0731E+13	3.0809E-06	6.3697E+13	2.4309E-06	1.2674	3.8163E-20	0.98872
	31	1	6.7288E+13	2.5755E-06	4.8100E+13	1.8411E-06	1.3989	3.8275E-20	0.99164
	32	5	6.8324E+13	2.6131E-06	5.0200E+13	1.9199E-06	1.3610	3.8245E-20	0.99086
	32	4	8.4088E+13	3.2064E-06	6.6319E+13	2.5288E-06	1.2679	3.8131E-20	0.98790
	32	3	8.4905E+13	3.2365E-06	6.8466E+13	2.6099E-06	1.2401	3.8120E-20	0.98761
	32	2	8.3835E+13	3.1979E-06	6.6147E+13	2.5232E-06	1.2674	3.8145E-20	0.98825
	32	1	7.1462E+13	2.7338E-06	5.1084E+13	1.9542E-06	1.3989	3.8256E-20	0.99113
	33	5	5.4216E+13	2.0782E-06	3.9834E+13	1.5269E-06	1.3610	3.8332E-20	0.99310
	33	4	6.5343E+13	2.4988E-06	5.1535E+13	1.9708E-06	1.2679	3.8241E-20	0.99075
	33	3	6.4860E+13	2.4800E-06	5.2302E+13	1.9998E-06	1.2401	3.8236E-20	0.99063
	33	2	6.3251E+13	2.4200E-06	4.9906E+13	1.9094E-06	1.2674	3.8260E-20	0.99124
	33	1	5.4470E+13	2.0884E-06	3.8937E+13	1.4929E-06	1.3989	3.8340E-20	0.99332
	34	5	2.2060E+13	8.4916E-07	1.6208E+13	6.2390E-07	1.3610	3.8493E-20	0.99729
	34	4	2.7480E+13	1.0566E-06	2.1673E+13	8.3333E-07	1.2679	3.8449E-20	0.99615
	34	3	2.8113E+13	1.0807E-06	2.2670E+13	8.7143E-07	1.2401	3.8441E-20	0.99592
	34	2	2.6022E+13	1.0007E-06	2.0531E+13	7.8959E-07	1.2674	3.8458E-20	0.99636
	34	1	2.0899E+13	8.0459E-07	1.4939E+13	5.7515E-07	1.3989	3.8500E-20	0.99745
	35	5	6.9205E+13	2.6497E-06	5.0847E+13	1.9468E-06	1.3610	3.8288E-20	0.99196
	35	4	8.9163E+13	3.3980E-06	7.0322E+13	2.6799E-06	1.2679	3.8110E-20	0.98735
	35	3	9.1273E+13	3.4757E-06	7.3601E+13	2.8028E-06	1.2401	3.8081E-20	0.98660
	35	2	8.9222E+13	3.4007E-06	7.0397E+13	2.6832E-06	1.2674	3.8115E-20	0.98750
	35	1	7.3842E+13	2.8240E-06	5.2785E+13	2.0187E-06	1.3989	3.8244E-20	0.99082
	36	5	6.8802E+13	2.6344E-06	5.0551E+13	1.9355E-06	1.3610	3.8289E-20	0.99200
	36	4	8.8781E+13	3.3837E-06	7.0020E+13	2.6686E-06	1.2679	3.8112E-20	0.98742
	36	3	9.0711E+13	3.4547E-06	7.3147E+13	2.7858E-06	1.2401	3.8085E-20	0.98671
	36	2	8.9817E+13	3.4231E-06	7.0867E+13	2.7009E-06	1.2674	3.8112E-20	0.98740
	36	1	7.4868E+13	2.8629E-06	5.3518E+13	2.0465E-06	1.3989	3.8240E-20	0.99072
	37	5	5.9971E+13	2.2988E-06	4.4062E+13	1.6890E-06	1.3610	3.8332E-20	0.99310
	37	4	7.5238E+13	2.8732E-06	5.9340E+13	2.2661E-06	1.2679	3.8189E-20	0.98939
	37	3	7.8069E+13	2.9787E-06	6.2953E+13	2.4019E-06	1.2401	3.8154E-20	0.98850
	37	2	7.6639E+13	2.9263E-06	6.0469E+13	2.3089E-06	1.2674	3.8183E-20	0.98925
	37	1	6.5310E+13	2.5004E-06	4.6686E+13	1.7874E-06	1.3989	3.8285E-20	0.99190
	38	5	6.7204E+13	2.5722E-06	4.9377E+13	1.8899E-06	1.3610	3.8274E-20	0.99162
	38	4	8.6840E+13	3.3105E-06	6.8490E+13	2.6110E-06	1.2679	3.8122E-20	0.98767
	38	3	8.9357E+13	3.4041E-06	7.2056E+13	2.7450E-06	1.2401	3.8095E-20	0.98697
	38	2	8.9201E+13	3.3999E-06	7.0380E+13	2.6826E-06	1.2674	3.8116E-20	0.98750
	38	1	7.5612E+13	2.8912E-06	5.4051E+13	2.0667E-06	1.3989	3.8237E-20	0.99065
	39	5	6.1776E+13	2.3627E-06	4.5389E+13	1.7359E-06	1.3610	3.8245E-20	0.99187
	39	4	7.7753E+13	2.9647E-06	6.1323E+13	2.3382E-06	1.2679	3.8129E-20	0.98886
	39	3	7.8861E+13	3.0059E-06	6.3592E+13	2.4239E-06	1.2401	3.8117E-20	0.98853
	39	2	7.7664E+13	2.9623E-06	6.1278E+13	2.3373E-06	1.2674	3.8142E-20	0.98918
	39	1	6.6400E+13	2.5393E-06	4.7465E+13	1.8152E-06	1.3989	3.8243E-20	0.99180
	40	5	4.4082E+13	1.6932E-06	3.2388E+13	1.2441E-06	1.3610	3.8411E-20	0.99514
	40	4	5.4465E+13	2.0862E-06	4.2956E+13	1.6453E-06	1.2679	3.8303E-20	0.99236
	40	3	5.5270E+13	2.1161E-06	4.4568E+13	1.7064E-06	1.2401	3.8288E-20	0.99196
	40	2	5.4612E+13	2.0917E-06	4.3090E+13	1.6504E-06	1.2674	3.8301E-20	0.99231
	40	1	4.5057E+13	1.7294E-06	3.2208E+13	1.2363E-06	1.3989	3.8383E-20	0.99443
	41	5	9.2561E+12	3.5687E-07	6.8007E+12	2.6220E-07	1.3610	3.8555E-20	0.99889
	41	4	1.1140E+13	4.2932E-07	8.7860E+12	3.3860E-07	1.2679	3.8538E-20	0.99845
	41	3	1.1444E+13	4.4099E-07	9.2282E+12	3.5561E-07	1.2401	3.8535E-20	0.99836
	41	2	1.0527E+13	4.0572E-07	8.3058E+12	3.2012E-07	1.2674	3.8542E-20	0.99854
	41	1	9.4945E+12	3.6604E-07	6.7870E+12	2.6166E-07	1.3989	3.8553E-20	0.99884
	42	5	2.5207E+13	9.7011E-07	1.8520E+13	7.1277E-07	1.3610	3.8485E-20	0.99708
	42	4	3.0262E+13	1.1631E-06	2.3867E+13	9.1735E-07	1.2679	3.8435E-20	0.99578
	42	3	3.0352E+13	1.1664E-06	2.4475E+13	9.4054E-07	1.2401	3.8428E-20	0.99560
	42	2	2.9588E+13	1.1373E-06	2.3345E+13	8.9734E-07	1.2674	3.8438E-20	0.99585
	42	1	2.5253E+13	9.7169E-07	1.8052E+13	6.9460E-07	1.3989	3.8478E-20	0.99689
	43	5	3.6560E+13	1.4045E-06	2.6862E+13	1.0319E-06	1.3610	3.8416E-20	0.99528
	43	4	4.5212E+13	1.7340E-06	3.5658E+13	1.3676E-06	1.2679	3.8352E-20	0.99362
	43	3	4.5231E+13	1.7344E-06	3.6473E+13	1.3986E-06	1.2401	3.8345E-20	0.99345
	43	2	4.4492E+13	1.7068E-06	3.5104E+13	1.3466E-06	1.2674	3.8361E-20	0.99387
	43	1	3.6585E+13	1.4058E-06	2.6153E+13	1.0049E-06	1.3989	3.8426E-20	0.99554
	45	5	1.6275E+13	6.2686E-07	1.1958E+13	4.6058E-07	1.3610	3.8518E-20	0.99792
	45	4	2.0554E+13	7.9106E-07	1.6211E+13	6.2390E-07	1.2679	3.8487E-20	0.99712
	45	3	2.0042E+13	7.7135E-07	1.6161E+13	6.2200E-07	1.2401	3.8487E-20	0.99712
	45	2	1.9898E+13	7.6592E-07	1.5700E+13	6.0432E-07	1.2674	3.8492E-20	0.99726
	45	1	1.5838E+13	6.1007E-07	1.1321E+13	4.3610E-07	1.3989	3.8520E-20	0.99799

PRI.P3X FSUM - SUMMARY OF CORE INFORMATION

TOTAL CORE POWER	2462.3 MWT
EXPOSURE BLOCK ENERGY	655995.9 MWHRS
CORE AVERAGE EXPOSURE	18066.7 MWD/MTU
CYCLE AVERAGE EXPOSURE	546.1 MWD/MTU
CYCLE EFPD	17.6 DAYS
TOTAL CORE WEIGHT	81492.840 KGU
P3 AXIAL OFFSET (L-U/L+U)	-0.011
S3 AXIAL OFFSET (L-U/L+U)	-0.016

PRI.P3X FASI - EXCORE MONITORING SYSTEM OPERATOR INFORMATION

NI/CHANNEL	QUADRANT 1 5/A	QUADRANT 2 8/D	QUADRANT 3 6/B	QUADRANT 4 7/C
AXIAL SHAPE INDICES	-0.007	-0.018	-0.026	-0.011
EXCORE POWER RATIO	0.005	0.009	0.015	-0.001
SHAPE ANNEALING FACTORS	2.177	2.317	2.365	2.075
CONSTANT B	-0.019	-0.039	-0.061	-0.010
AVERAGE AXIAL SHAPE INDEX				-0.015
APL - ALLOWABLE POWER LEVEL				100.0 %
POWER USED TO DETERMINE APL				97.3 %

PRI.P3X TS06A - TECHNICAL SPECIFICATION CORE REACTIVITY BALANCE

REFERENCE DATA

CYCLE EXPOSURE THROUGH STEP E - 3	546.1 MWD/MTU
CALORIMETRIC REACTOR POWER	97.3 %
MEASURED BORON CONCENTRATION	1092.0 PPM
GROUP 4 CONTROL ROD POSITION	131.1 INCHES WITHDRAWN

TECHNICAL DATA BOOK INFORMATION AT REFERENCE CONDITIONS

PREDICTED HFP ARO BORON CONCENTRATION	1116.2 PPM
RECIP. BORON AT 100.0% POWER	123.3 PPM/% DRHO
RECIP. BORON AT 97.3% POWER	123.2 PPM/% DRHO
EQUAL. XENON AT 100.0% POWER	2.466 % DRHO
EQUAL. XENON AT 97.3% POWER	2.446 % DRHO
POWER DEFECT AT 100.0% POWER	1.440 % DRHO
POWER DEFECT AT 97.3% POWER	1.399 % DRHO
CONTROL ROD WORTH AT 131.1 INCHES	0.005 % DRHO

REACTIVITY BALANCE CALCULATIONS

DIFFERENCE IN REACTIVITY DUE TO XENON	0.020 % DRHO
DIFFERENCE IN REACTIVITY DUE TO POWER DEFECT	0.041 % DRHO
SUM OF XENON AND POWER DEFECT REACTIVITY	0.061 % DRHO
	7.5 PPM
WORTH OF CONTROL RODS	0.6 PPM
NET BORON DIFFERENCE	6.9 PPM
PREDICTED BORON CONCENTRATION AT 97.3 % POWER	1123.2 PPM
BORON ANOMALY	-31.2 PPM
REACTIVITY ANOMALY	-0.253 % DRHO

NOTE: NEGATIVE ANOMALY - MEASURED BORON < PREDICTED
 POSITIVE ANOMALY - MEASURED BORON > PREDICTED

PRI.P3X TS06B - TECHNICAL SPECIFICATION CORE SURVEILLANCE SUMMARY

A PLANT SNAPSHOT DATE: 09/15/1995 19:30:03

B OPERABLE INCORE DETECTORS	QUADRANT 1	QUADRANT 2	QUADRANT 3	QUADRANT 4	
LEVEL 5	10	11	11	11	
4	10	11	11	11	
3	9	11	11	11	
2	10	10	11	11	
1	10	11	10	11	
TOTAL	49	54	54	55	212

C APL - ALLOWABLE POWER LEVEL 100.0 %
 POWER USED TO DETERMINE APL 97.3 %

D QUADRANT POWER TILT NI/CHANNEL	QUADRANT 1 5/A	QUADRANT 2 8/D	QUADRANT 3 6/B	QUADRANT 4 7/C
INCORE % POWER TILT	-0.335	-0.539	0.681	0.191
EXCORE % POWER TILT	-0.316	-0.678	0.467	0.527
ABSOLUTE % DEVIATION ABS(INC - EXC)	0.019	0.139	0.214	0.336

E INCORE AXIAL OFFSET				
EXCORE ASI	-0.007	-0.018	-0.026	-0.011
ABSOLUTE DEVIATION ABS(INC - EXC)	0.003	0.007	0.015	0.001

F PEAKING FACTORS	ALLOWED	MEASURED	ALLOWED/ MEASURED
FRA - ASSEMBLY RADIAL PEAKING FACTOR	1.706	1.635	1.043
FRT - TOTAL RADIAL PEAKING FACTOR	1.967	1.818	1.082
FQ - TOTAL PEAKING FACTOR	2.657	2.143	1.240

G QUALIFIED CORE EXIT THERMOCOUPLE TEMPERATURES

DETECTOR	CURVE FIT	MEASURED
2	570.4	572.5
5	593.1	594.0
9	616.8	615.4
10	615.3	614.3
11	616.1	620.5
16	589.5	587.2
19	588.8	587.7
21	590.5	591.1
23	580.7	581.0
25	613.0	613.1
27	613.3	612.0
30	574.3	575.3
31	609.6	611.4
33	585.4	583.2
35	616.6	614.8
36	616.7	617.1

QUALIFIED CORE EXIT THERMOCOUPLES OPERABLE 16

PRI.P3X 2CET - CURVE FIT CET TEMPERATURES (F)

	A	B	D	E	G	H	J	K	M	N	Q	R	T	V	X	Z
1						5.430 0.194	5.474 0.279	5.414 0.163	5.411 0.158	5.452 0.238	5.399 0.135					
2				5.398 0.132	5.528 0.383	5.704 0.720	5.897 1.088	5.780 0.866	5.896 1.086	5.743 0.795	5.666 0.648	5.520 0.368	5.397 0.130			
4				5.564 0.453	5.988 1.261	5.924 1.140	5.851 1.001	6.071 1.419	5.834 0.968	6.041 1.362	5.931 1.153	5.984 1.254	5.561 0.447			
5		5.398 0.133	5.566 0.457	5.833 0.967	6.060 1.399	6.174 1.614	6.031 1.342	6.068 1.414	6.137 1.544	5.897 1.089	6.145 1.559	6.043 1.367	5.832 0.966	5.568 0.460	5.399 0.134	
7		5.526 0.379	6.008 1.300	6.054 1.388	6.168 1.603	5.901 1.096	6.153 1.574	5.901 1.095	5.990 1.265	5.978 1.243	5.894 1.082	6.161 1.590	6.064 1.405	6.007 1.298	5.531 0.389	
8	5.400 0.136	5.670 0.656	5.939 1.168	6.155 1.579	5.900 1.094	5.868 1.033	5.980 1.246	6.099 1.472	5.881 1.057	6.090 1.454	5.864 1.026	5.895 1.085	6.176 1.617	5.929 1.149	5.700 0.712	5.429 0.193
10	5.454 0.240	5.745 0.798	6.052 1.383	5.904 1.103	5.987 1.259	6.097 1.467	5.888 1.072	5.903 1.099	6.141 1.551	5.884 1.064	5.981 1.248	6.147 1.563	6.032 1.345	5.855 1.009	5.899 1.092	5.474 0.280
11	5.414 0.163	5.914 1.120	5.849 0.998	6.156 1.580	6.003 1.290	5.891 1.078	6.147 1.562	6.134 1.539	6.133 1.537	5.905 1.104	6.118 1.508	5.905 1.103	6.075 1.426	6.087 1.450	5.785 0.875	5.414 0.164
13	5.418 0.171	5.807 0.917	6.110 1.493	6.091 1.456	5.914 1.121	6.130 1.531	5.905 1.105	6.135 1.540	6.133 1.537	6.143 1.555	5.884 1.064	5.992 1.269	6.140 1.549	5.833 0.966	5.897 1.089	5.412 0.159
14	5.479 0.288	5.917 1.126	5.868 1.032	6.044 1.368	6.160 1.587	5.990 1.265	5.889 1.073	6.148 1.564	5.908 1.110	5.885 1.066	6.085 1.446	5.977 1.241	5.897 1.088	6.039 1.358	5.743 0.795	5.452 0.238
16	5.431 0.197	5.708 0.727	5.934 1.159	6.185 1.635	5.904 1.102	5.870 1.038	6.096 1.467	5.890 1.075	6.126 1.522	5.982 1.249	5.854 1.006	5.892 1.080	6.143 1.555	5.925 1.142	5.665 0.645	5.399 0.134
17		5.537 0.400	5.999 1.282	6.067 1.411	6.166 1.599	5.900 1.094	5.986 1.258	6.000 1.284	5.910 1.113	6.151 1.570	5.898 1.090	6.167 1.600	6.046 1.371	5.983 1.252	5.520 0.369	
19		5.400 0.136	5.568 0.459	5.838 0.977	6.058 1.395	6.156 1.580	5.905 1.104	6.151 1.570	6.081 1.438	6.035 1.351	6.176 1.617	6.062 1.402	5.838 0.976	5.563 0.450	5.400 0.137	
20				5.566 0.456	5.994 1.272	5.934 1.160	6.050 1.380	5.844 0.988	6.097 1.468	5.859 1.016	5.925 1.142	5.989 1.264	5.565 0.455			
22				5.398 0.132	5.523 0.373	5.669 0.654	5.748 0.804	5.906 1.106	5.791 0.886	5.904 1.102	5.699 0.712	5.528 0.382	5.398 0.133			
23						5.400 0.136	5.454 0.241	5.413 0.161	5.416 0.167	5.478 0.288	5.430 0.194					CET TEMP (X100) PIDAL-3 2D RPF

THE ORIGINAL PRODUCTION RUN DATE 09/15/1995 19:30:03

APPENDIX B

SUGGESTED SER REVISION

2.0 BACKGROUND

Palisades is a first-generation Combustion Engineering (CE) pressurized water reactor (PWR) with a unique core design consisting of 204 fuel bundles and 45 cruciform control blades. The core power distribution is monitored by self-powered rhodium incore detectors in a maximum of 45 instrumented fuel assemblies. Each detector location contains five equally spaced rhodium detectors (40cm in length) with centers at 10, 30, 50, 70, and 90 percent of the active fuel height. Currently, only 36 of 45 incore locations are being used, since 2 locations are reserved for use by the reactor vessel level monitoring system and the other 7 are no longer needed with low leakage core designs.

The rhodium detectors are of a standard design for CE type incore monitoring systems. These rhodium detectors produce a current directly proportional to the incident neutron flux at each detector location by a neutron-beta reaction. This current is passed to the Palisades plant computer (PPC) and converted from an analog to a digital signal. The PPC performs the background and depletion sensitivity corrections, and provides all the necessary plant data to the PIDAL-3 incore analysis system.

The incore detector signals (amps) measured by the PPC are corrected for background noise and depletion sensitivity (amps/nv), and converted to flux (nv). The integral powers over each axial detector segment are then determined by the application of signal-to-power conversion ratios (W-primes). The W-primes are supplied by SIMULATE-3, an advanced three-dimensional two-group diffusion theory nodal code, as part of the incore monitoring system. The PPC provides SIMULATE-3 with all the necessary plant data, and SIMULATE-3 provides PIDAL-3 with all the necessary theoretical data.

The assembly powers for uninstrumented locations are inferred using coupling coefficients to adjacent instrumented neighbors. This process allows the determination of a measured or inferred radial core power distribution at each of the five axial detector levels. A detailed axial power shape is then inferred using a five mode Fourier curve fit to the five level power integral for each assembly.

The incore analysis program is executed to determine the measured reactor core power distribution. Based on this analysis the following TS surveillances may be performed:

<u>TS Section</u>	<u>Specific Surveillance Item</u>
3.1.1.e	Monitoring axial power shape within limits
3.11.1.a	Incore detector operability
3.11.1.b	Calculation of incore alarms for the incore monitoring system
3.11.2.a	Calculation of target axial offset (AO) and allowable power level (APL)
3.11.2.a-c	Excure system calibration for LHGR monitoring
3.11.2.b	Excure system calibration for ASI monitoring
3.11.2.c	Excure system calibration for quadrant power tilt (T _Q) monitoring
3.23.1	Monitoring LHGR within limits
3.23.2	Monitoring radial peaking factors within limits
3.23.3	Monitoring T _Q within limits

Technical Specification 3.1.1.e establishes limits on the core average axial power shape to ensure that the axial power profiles assumed in the development of the primary coolant inlet temperature Limiting Condition for Operation (LCO) bound the measured axial profiles. The axial power shape, referred to as the axial offset (AO) or the axial shape index (ASI), is defined in TS 1.0 as the power in the lower half of the core minus the power in the upper half of the core divided by the sum of the powers in the lower half and upper half of the core. The excure system continuously monitors the ASI and is calibrated to the incore analysis program measured core average AO.

Technical Specification 3.11.1.a requires the determination of the operability of sufficient incore instruments (ICI) to allow the incore analysis program to perform the required TS surveillances and the generation of the PPC incore alarm set points. Currently, at least 50 percent of the 180 individual detectors presently used must be operable including at least two incores per axial level per core quadrant.

Technical Specification 3.11.1.b requires the generation of PPC high alarm set points in order to protect the core from high local power densities by continuously comparing the directly measured ICI signals to the alarm set points.

The alarm limits, one for each of the five axial detector levels, are calculated by the incore analysis program and are equivalent to the minimum margin to the LHGR TS limit as measured for each detector level.

Technical Specification 3.11.2 requires the calculation of the target AO and the allowable power level (APL), along with the verification that the excore monitoring system is calibrated for monitoring the LHGR, the ASI, and the quadrant power tilt (T_Q). The target AO is derived from the core average AO measured by the incore analysis program and provides the basis for calibrating the excore detectors ASI monitoring function. The measured power distribution also provides the target or baseline quadrant power tilts which are used to calibrate the excore quadrant power tilt monitoring function. The APL is calculated based on the limiting measured LHGR and ensures that the core LHGR limits are protected within a given band of the AO.

The TS 3.23.1 LHGR limits ensure that the peak cladding temperature (PCT) will not exceed 2200 °F in the event of a loss-of-coolant accident (LOCA). The LHGR (and the related three-dimensional nuclear pin peaking factor F_Q) is continuously monitored by either the PPC incore high alarm set points or by the excore monitoring system axial shape index (ASI) and allowable power limit (APL) alarms. In order to calculate the incore alarm set points and to calibrate the excore monitoring system, the incore analysis program must calculate the local LHGR by applying local peaking factors (LPF) or pin-to-box (PTB) factors to the measured/inferred three-dimensional nodal power distribution. These LPFs are also supplied by SIMULATE-3 as part of the incore monitoring system. The calculated local peak pin powers are converted to local linear heat rates for comparison with the TS limits.

The TS 3.23.2 radial peaking factor limits ensure that the assumptions used in the analyses for establishing margin to DNB, LHGR and for the thermal margin/low-pressure (TM/LP) and the variable high power RPS trip set points remain valid. This requires verification of the two radial peaking factors defined by TS 1.1:

F_R^A The assembly radial peaking factor is the maximum ratio of the individual fuel assembly power to the core average assembly power integrated over the total core height, including tilt

F_R^T The total radial peaking factor is the maximum ratio of the individual fuel pin power to the core average pin power integrated over the total core height, including tilt.

The assembly radial peaking factor is determined directly from the two-dimensional assembly radial power distribution resulting from the axially collapsed three-dimensional measured/inferred nodal power distribution. The total radial peaking factor is determined by multiplying the three-dimensional measured/inferred nodal power distribution to the three-dimensional LPFs and the ratio of the average number of pins/assembly to the number of pins in the assembly, then collapsing it axially to two dimensions.

Technical Specification 3.23.3 requires verification of the quadrant power tilt defined by TS 1.1 to ensure that the design safety margins are maintained:

T_Q The quadrant power tilt is the maximum positive ratio of the power generated in any quadrant minus the average quadrant power, to the average quadrant power.

Operation is not restricted with tilts up to 5 percent. Larger tilts, not to exceed 10 percent, require verification of radial peaking factor limits and/or reduction to less than 85 percent of rated power. Tilts exceeding 10 percent require reduction to less than 50 percent power and verification of radial peaking factor limits and tilts greater than 15 percent require shutdown to hot standby conditions within 12 hours.

The TS verification that the excore system is calibrated is performed by comparing the measured core average AO and quadrant power tilts to the corresponding values recorded by the four power range (safety) excore detectors. If any excore reading differs from the corresponding incore measured value by more than the allowable margin, that channel is declared inoperable and is recalibrated based on the incore measurements. Each time the TS requirements are performed, a complete set of detector alarm limits are created. Presently, these alarm limits are loaded into the PPC at least once every 7 days for use until the next required update.

3.0 EVALUATION

3.1 Methodology

B.2

General

The PIDAL-3 program always models the reactor power distribution on a full-core basis with quarter core symmetry. The incore data collection procedure, including the background and depletion corrections is equivalent to the previous monitoring programs. The incore detector signal-to-power conversion using SIMULATE-3 is equivalent to the CECORLIB program used to generate the W-prime and LPF library for CECOR (Ref. 8). The axial power distribution interpolation technique, including the use of theoretical axial boundary conditions derived using the NRC-approved SIMULATE-3 nodal model (Ref. 9), is similar to the previous monitoring programs. Fuel and control rod exposure calculations, and the TS analysis procedure are equivalent to the previous monitoring programs.

The significant differences between the PIDAL-3 methodology and the original PIDAL methodology are:

- 1) Theoretical Nodal Power Distribution
- 2) Incore Detector Signal-to-Power Conversion
- 3) Local Peaking Factors and Pin Ratio
- 4) Full Core Theoretical Coupling Coefficients

Theoretical Nodal Power Distribution

The original PIDAL program used XTG to determine the theoretical nodal powers on a quarter core basis. This limited PIDAL's ability to measure radial tilts since the XTG model was limited to quarter core. The PIDAL-3 program uses SIMULATE-3 to determine the theoretical nodal powers on a full core basis. This allows PIDAL-3 to accurately measure radial tilts since the SIMULATE-3 model is full core and will accept individual dropped control rods.

Incore Detector Signal-to-Power Conversion

The original PIDAL program used PDQ to determine the theoretical W-primes on a quarter core basis. This limited PIDAL's ability to measure radial tilts since the PDQ model was limited to quarter core and to group 4 control rod insertion only.

The PIDAL-3 program uses SIMULATE-3 to determine the theoretical W-primes on a full core basis at any power. This allows PIDAL-3 to accurately measure radial tilts at any power since the SIMULATE-3 model is full core and will accept individual dropped control rods.

Local Peaking Factors and Pin Ratio

The original PIDAL program used PDQ to determine the theoretical LPFs on a quarter core basis. This limited PIDAL's ability to measure radial tilts since the PDQ model was limited to quarter core and to group 4 control rod insertion only. The original PIDAL program did not account for different numbers of fuel pins/assembly. This caused PIDAL to over-measure pin powers in assemblies with more pins than the average and under-measure pin powers in assemblies with less than the average.

The PIDAL-3 program uses SIMULATE-3 to determine the theoretical LPFs on a full core basis at any power. This allows PIDAL-3 to accurately measure radial tilts at any power since the SIMULATE-3 model is full core and will accept individual dropped control rods. The PIDAL-3 program accounts for different numbers of fuel pins/assembly and hence, accurately measures the peak pin to the average pin of the core (Ref. 11).

Full Core Theoretical Coupling Coefficients

The original PIDAL program determined the full core power distribution based on XTG quarter core coupling integrated with measured powers and expanded to full core coupling. This limited PIDAL's ability to measure radial tilts since the XTG model was limited to quarter core.

The PIDAL-3 program determines the full core power distribution based on SIMULATE-3 full core coupling integrated with measured powers. This allows PIDAL-3 to accurately measure radial tilts since the SIMULATE-3 model is full core.

3.2 Uncertainty Analysis

General

As defined in the TS and discussed in Section 2.0, the peaking factors of interest for Palisades are F_Q , F_R^A , and F_R^T . Three separate components for the uncertainty associated with determination of the above peaking factors are considered as follows:

- 1) The box measurement component is defined as the uncertainty associated with measuring segment powers in the detector locations.
- 2) The nodal synthesis component is the uncertainty associated with using the radial and axial power distribution synthesis techniques employed by PIDAL-3 to calculate a nodal power. Specifically, the uncertainties associated with the radial coupling to the uninstrumented locations and the axial curve fitting used to obtain an axial power shape from the five discrete detector powers.
- 3) The pin-to-box component is the uncertainty associated with using the SIMULATE-3 LPFs to represent the pin power distribution within each assembly.

To adequately address the above uncertainties, it is necessary to mathematically re-define the individual peaking factors in terms of these components. Since the current fuel vendor for Palisades is Siemens Power Corporation (SPC), CPC chose to utilize the SPC breakdown as described in their St. Lucie-1 uncertainty analysis (Ref. 10).

In the uncertainty analysis of the PIDAL-3 statistical model (Ref. 12), CPC has separated the above factors into individual components which can be investigated and quantified independently. These components are statistically recombined into the appropriate uncertainty values for the TS surveillance requirements.

The specific form of the peaking factors used by CPC is as follows:

$$F(q) = F(s) * F(r) * F(z) * F(L)$$

$$F(rT) = F(sa) * F(r) * F(L)$$

$$F(rA) = F(sa) * F(r)$$

where:

$F(s)$ = Relative power associated with a single detector measurement.

$F(sa)$ = Relative power associated with the average of the detector measurements within a single assembly.

$F(r)$ = Ratio of the assembly relative power to the relative power of the detector measurements within that assembly.

$F(z)$ = Ratio of the peak planar power in an assembly to the assembly average power.

$F(L)$ = Peak local pin power within an assembly relative to the assembly average power.

CPC uses standard forms for the sample means (\bar{x}), standard deviations (s), and root-mean-square (rms) differences. Based on the mean, the standard deviation, and the sample size, the 95/95 tolerance limit (bias plus-or-minus the reliability factor) was determined for each component, assuming that the percent difference (error) between calculated values and measured data are normal distributions. The individual variances are defined in standard terms and are combined statistically by assuming that the individual uncertainty components are independent.